THE UNIVERSITY OF CHICAGO

THEORETICAL APPROACHES TO ENVIRONMENTAL FEEDBACKS AND COMMUNITY COEXISTENCE

A DISSERTATION SUBMITTED TO
THE FACULTY OF THE DIVISION OF THE BIOLOGICAL SCIENCES
AND THE PRITZKER SCHOOL OF MEDICINE
IN CANDIDACY FOR THE DEGREE OF
DOCTOR OF PHILOSOPHY

DEPARTMENT OF ECOLOGY AND EVOLUTION

BY
ZACHARY R. MILLER

CHICAGO, ILLINOIS
AUGUST 2022

TABLE OF CONTENTS

LIST OF FIGURES

ACKNOWLEDGMENTS

This dissertation collects five years of research by one author, but reflects the influence and contributions of many people over more than two decades. Stefano Allesina, my thesis advisor, has shaped me as a scientist more than any other individual. Over long days at the whiteboard and early mornings around cups of coffee, Stefano has given his time and wisdom generously, and always modeled a passionate, adventurous, and never-too-serious approach to research. I owe him a deep debt of thanks for sharing his unfailingly creative ideas – including the seeds that grew into this dissertation – and his sharp insights that illuminated hard problems. It is a debt I can only hope to repay by one day inspiring and encouraging students as Stefano has for me.

Stefano has also cultivated a laboratory like no other. From the first day, the Allesina Lab has been a welcoming, stimulating, dynamic, and thoroughly enjoyable place to work and learn. I have been lucky to share it with many brilliant colleagues, including Matt Michalska-Smith, Theo Gibbs, José Capitán, Paula Lemos-Costa, Abby Skwara, Pablo Lechón-Alonso, and Katja Della Libera. A few others deserve special mention. Jacopo Grilli shared his clear and thoughtful approach to problem-solving, which he exemplified on problems including the first incarnation of the models developed in this dissertation. Daniel Maynard showed me what a complete scientist looks like, as he churned out ideas and papers and still found time to pick up new skills and mull over big questions during his time in the lab. He also found time to mentor me patiently and with good humor. And I would like to thank Carlos Serván, who is one of the most gifted mathematical thinkers I have ever met, and who deeply shaped the way I look at mathematical problems. Carlos has been a great teacher and an even greater friend, who helped me not only build my analytical skills, but to have a lot of fun in the process.

Beyond the Allesina Lab, I have appreciated the chance to work with kind and talented people throughout the Darwinian Sciences cluster. My dissertation committee – Joy

Bergelson, Mercedes Pascual, and John Novembre – helped guide me through five years of intellectual and professional growth. Many other teachers, including Matthias Steinrücken, Greg Dwyer, Sarah Cobey, Tim Wootton, and Marcus Kronforst, helped me become a more well-rounded scientist, and always made me feel welcome. And my work would be impossible without the support of the Ecology and Evolution department staff, including Bonnie Brown, Mike Guerra, and especially Audrey Aronowsky, all of whom were unfailingly friendly and patient with any issue.

At the University of Chicago, I have also found an incredible student community. The friendship of my PhD cohort – Katie Dixon, Natasha Ershova, and Carlos Calzada – supported me especially through the first years of the program. I am thankful to count as friends, collaborators, and mentors Daniel Smith, Maryn Carlson, Keven Dooley, John Park, Rahul Subramanian, Marcos Costa Vieira, Kiseok Lee, Nadya Ali, and many others.

Going back in time, two undergraduate advisors at Yale, Oswald Schmitz and David Vasseur, profoundly shaped my scientific perspective and interests. These two were wonderful teachers and patient mentors who helped guide me toward graduate school, and helped me build confidence and independence as a scientific thinker. They also lead vibrant research groups with many students and postdocs who encouraged me. Chief among these was Colin Donihue, who offered mentorship and friendship and helped set me on a path to all the research I have done since.

At Yale, I also found an incomparable group of friends: Carmen Baskauf, Josh Chang, Charlotte Finegold, Aidan Kaplan, Benjamin Klempay, Layla Treuhaft-Ali, and Amanda Crego-Emley. These truly wonderful people have helped me grow not only as a student and teacher, but as a person. And it is the greatest stroke of fortune I will ever know that Amanda has become my best friend and the love of my life. Her kindness and love have made every day of my PhD a joy, whether they were days of breakthroughs or roadblocks. Amanda always reminds me what really matters in life.

Finally, I thank my family for a lifetime of love and support. I am lucky to have a large family, with many aunts, uncles, and cousins who all deserve thanks. My brother, Mason, shared in the schemes and adventures of our childhood, and always helped me imagine I could be the scientist I've become. My parents, Gary and Sheila, worked tirelessly so I could pursue my passions. They also modeled the love of reading, learning, and the natural world that led me to scientific research. And my grandmother, Beverly, helped raise me as something like a third parent. My "Grammy days" were filled with open-ended concoctions, aimless drives through the countryside, and her deep love for all of nature's "critters". I didn't know it then, but a young ecologist could ask for no better training.

ABSTRACT

Distinct biological species can coexist in the same ecosystem by occupying distinct niches. However, the niches available in a given environment – which reflect the range of environmental conditions and limiting factors that are present – are not necessarily a fixed property of the system. Environmental conditions can be shaped, and possibly diversified, by the resident community, through modifications that range from chemical excretion to physical remodeling to biotic control of local environmental microbiomes. To varying degrees, all species modify their local environment, driving changes that can feed back to affect the set of available niches and ultimately the composition and coexistence of the community. Here, we study minimal mathematical models for these kinds of modifications in the context of community coexistence. We review some existing empirical and theoretical approaches to understanding environmental feedbacks, highlighting the essential similarities in the dynamics of several system-specific examples. We then extend and carefully examine one prominent model for plant-soil feedbacks, a broad class of environmental feedbacks that operate in plant communities. We show that this widely-used model cannot account for the coexistence of more than two plant species. We go on to develop a simple, nested modeling framework for environmental feedbacks based on the classic metapopulation paradigm. We show that this model can account for the coexistence of an arbitrary number of species, and we derive analytical characterizations of when and how species coexist in ecosystems with environmental feedbacks.

CHAPTER 1

INTRODUCTION

A classic question in ecology asks, *Why are there so many kinds of animals* [112]? A classic answer is that species partition variation in the environment, allowing different biological types to coexist by occupying distinct ecological niches. While modern notions of the niche and niche partitioning were not developed until the mid-twentieth century, the basic idea that environmental variation explains biological variation was central even at ecology's inception more than a century earlier. In work that laid the foundations for all of biogeography, and much of the rest of ecology, Alexander von Humboldt pioneered the use of rigorous, quantitative approaches to map the variation of biotic communities across space and geophysical gradients [171, 117]. Around the same time, the lesser-known George Sinclair undertook one of the first manipulative experiments in ecology, systematically measuring the growth of grasses in various soils to dissect the mechanisms that led distinct soils to foster distinct plant communities in natural landscapes [220, 98]. Later researchers, whether arguing for the primacy of abiotic controls on species distributions and coexistence [12, 256, 37], or the importance of interspecific competition for niches [152, 193, 52], largely maintained an emphasis on interpreting biological diversity within the constraints set by environmental variation.

Alongside this link from environmental to biotic pattern, ecologists have always recognized a causal arrow pointing in the opposite direction. While primarily thinking of soils as determinants of plant yield, Sinclair, drawing on centuries of agricultural folk knowledge, also discussed the capacity of different plants to exhaust or rejuvenate soils [220]. In fact, all organisms change their local environment in some way – through the depletion of resources, the excretion of wastes, the modification of physical structures. This old observation implies that species do not simply occupy niches carved out by geology, chemistry, and climate. Instead, organisms have the capacity to shape and even create niches through their interac-

tions with the environment [120, 175]. Because such interactions are bidirectional, they may give rise to complex feedbacks between biotic communities and the landscapes they inhabit.

Despite this recognition, ecological research from Sinclair's time up to the present has typically focused much more on abiotic conditions as drivers of biotic community composition, rather than the reverse. The principal exception is consumer-resource theory, which provides a mathematical framework for species interactions mediated by exploitative competition for resources [244, 46, 44]. In this picture, species do not interact with one another directly, but all deplete a set of shared resources, which they depend on for sustenance and growth. Consumer-resource theory boasts some of the most sophistical analytical development and widespread application in ecology. However, consumer-resource models depict a limited kind of environmental feedback. Species are assumed to modify the environment only by consuming resources, and resources are strictly beneficial to consumers. As we will see below, and as one might already imagine, the ways in which species can affect their environment, and vice versa, are much more diverse and nuanced. Standard consumer-resource models also do not capture two important features of many environmental feedbacks [96]: the modifications made by species are often localized in space and persistent in time. While both aspects have been addressed to some degree in extensions of the usual consumer-resource framework, such as spatially explicit models with variation in resource supply [244, 180, 2, 83], and models that include explicit nutrient cycling [62, 90, 182], these directions remain underdeveloped. Developing them further is no easy task, because these models tend to quickly become cumbersome and analytically intractable.

A final limitation of classical consumer-resource theory brings us back to the question of why there are so many species. G. Evelyn Hutchinson puzzled over this question at a time when ecologists were rapidly refining the limits of coexistence permitted by niche partitioning. The competitive exclusion principle [71, 93] and various quantitative generalizations [150, 159] implied that the number of coexisting species in an ecosystem should be limited by

the number of distinct niches – and ultimately by the amount of environmental heterogeneity available for species to partition. But in many ecosystems, there is not enough apparent variation to support the rich biodiversity that we observe. Hutchinson exemplified this inconsistency with his *paradox of the plankton*: How could many species of phytoplankton coexist in an essentially uniform environment with little abiotic variation and very few distinct resources [113]? This paradox is apparently irreconcilable within standard consumer-resource theory, which only permits species to draw down the availability of a fixed number of resources. However, a more general vision of feedbacks between community and environment allows that species might modify their surroundings in a way that generates variation above and beyond what is present in the abiotic landscape. Thus, environmental feedbacks might offer a sort of generic bootstrap to many-species coexistence – a possibility that has been recognized in number of specific ecological contexts, but rarely treated systematically.

Of course, this is not to say that environmental feedbacks are *the* answer to Hutchinson's question, or that there is any unique answer. Indeed, the intervening decades of ecological research have established many possible or partial resolutions. Hutchinson himself suggested several, including temporal fluctuations in environmental conditions, or biotic relationships such as symbiosis or predation that could multiply the possibilities for coexistence. But the generation of environmental heterogeneity, the raw material for niche partitioning and coexistence, by biotic processes represents a mechanism of considerable generality and potential importance.

This thesis is concerned with the mathematical theory of such processes, and especially the question of when they are able to support the coexistence of many species. We examine both existing theoretical models and some newly proposed. In developing new theory, we aim to strike a productive balance between the complexity needed to capture potentially intricate and indirect environmental feedbacks, and the simplicity and generality that make it possible to analyze the models, draw meaningful conclusions, and, with luck, recognize principles that

apply across ecosystems. In this respect, our theory fills a gap between existing approaches. Environmental feedbacks of the kind considered here fall under the very broad umbrella of contemporary niche theory, a framework for understanding species coexistence in terms of species' impacts and requirements in a shared environment [44, 163, 130]. While contemporary niche theory encompasses general forms of environmental modification in principle, its development and applications have typically focused on consumer-resource dynamics, with the limitations already discussed (but see, for example, [137, 248, 130]). Additionally, the graphical analysis at the heart of contemporary niche theory can be challenging generalize to ecosystems with many species and complex environments. The models we consider in later chapters can be viewed as specific instances of a general niche model [163, 157], emphasizing features not captured by the usual specializations, although we leave behind the frame of contemporary niche theory for our analysis and instead draw on mathematical tools from various sources within and outside of ecology.

More progress has been made on understanding environmental feedbacks and community coexistence in the context of specific ecosystems, or specific kinds of feedbacks. The essential dynamics have been recognized a number of times independently, leading to the development of several distinct strands of theory. We briefly review four such strands here. These examples illustrate the range of biological processes or mechanisms that might underlie environmental feedbacks, as well as the unifying features they share. We also survey the diversity of existing theoretical approaches, each with certain strengths or limitations. A central aim of this thesis is to bridge these independent lines of inquiry by developing and analyzing minimal models that capture the core features of these dynamics.

Our first example comes from microbial communities, where the transfer of nutrients between cells, known as cross-feeding, plays a critical role in mediating interspecific interactions and coexistence [262, 79]. An explosion of research into these processes has demonstrated that microbes do not simply deplete resources, as in classical consumer-resource models, but

also recycle them and, through internal biochemical reactions, transform them to generate forms not present in the abiotic resource environment. By generating novel variation in the ecosystem, cross-feeding creates new niches and facilitates coexistence. For example, recent experiments have demonstrated how feedbacks due to cross-feeding can allow the emergence and persistence of complex communities supplied with a single external resource – a situation that should lead to the competitive exclusion of all but one species in the conventional view [202, 79, 61]. Quantitative theory for microbial cross-feeding has advanced rapidly by extending standard consumer-resource models to include resource recycling, yielding mathematical stability criteria [40, 41, 73] and testable predictions for community-scale patterns and dynamics [79, 156, 146]. However, cross-feeding theory remains in its infancy, with many open questions in both the specification and analysis of its models [146, 73]. Additionally, theoretical work in this area continues to focus heavily on consumable resources, while other forms of chemical excretion and uptake, such as pH modification [196, 9] and production or degradation of toxins [126, 194], are widespread and can drive microbial community dynamics.

While cross-feeding represents a direct extension of consumer-resource dynamics, the literatures on ecosystem engineering and niche construction have highlighted quite distinct environmental modification processes [120, 175]. These concepts emphasize the importance of environmental feedbacks for creating novel habitats and ecological niches, often focusing on modifications that shape the physical environment, such as tunneling by earthworms or the building of structures like nests, reefs, or dams [96, 119]. Research on ecosystem engineers demonstrates their role in generating habitat heterogeneity and thereby promoting species diversity [260, 20, 201]. Such studies usually focuses on the modifications made by exceptionally impactful species, which shape the environment for many others, and often function as keystone species. Beavers, which create habitat for a range of plants, insects, and other organisms through their construction of dams, are a prototypical example [260, 20].

Reciprocal relationships between different "engineers" have been much less studied (but see [111]). As a result, this field has developed less in the way of mathematical theory for species coexistence, with more theoretical emphasis on the evolutionary consequences of environmental feedbacks [138, 175, 39], and with quantitative models centered on the population dynamics of focal engineer species [86, 259, 59, 197].

At something of an opposite extreme, research in plant communities has shown an important role for more passive and diffuse environmental modification in maintaining the coexistence of very diverse communities. Many plants attract or cultivate a specialized community in their immediate surroundings, including microbial pathogens or mutualists in the soil beneath them, or seed- and sap-feeding insects on and around them. The presence of this associated biota can impact the survival of plants germinating nearby, or at the same site even after the death of the occupant. Known as Janzen-Connell effects [118, 54] or plant-soil feedbacks [31, 28], these processes create heterogeneity in the biotic background of a landscape, which can promote the coexistence of multiple species even in the absence of abiotic variation [31, 30, 237, 250]. In particular, the theory of these processes emphasizes the role of specialized pathogens and predators that disadvantage conspecifics of a focal plant. Across a landscape, this kind of "modification" creates negative frequency-dependent feedbacks, which ensure that there are always patches of habitat less hospitable to each species, thereby maintaining diversity in the landscape and community. Both mathematical theory [31, 28] and experimental evidence [188, 135, 155] support this picture, with theory closely guiding empirical research in this area. Plant-soil feedback theory is overwhelmingly grounded in a simple modeling framework that generates tractable criteria for species coexistence, but which encompasses only two plant species [31]. The Janzen-Connell view of these feedbacks emphasizes a spatial component, which has made analytical theory more difficult to develop. However, there is a need for theoretical predictions that can help disentangle the importance of feedback effects and other drivers of coexistence in experimental

and observational data [16, 211, 49].

The preceding example illustrates that it can be useful to take a broad view of what constitutes the "environment" for a focal community, to include biotic factors such pathogens or microbial mutualists. Contemporary niche theory adopts the same position, allowing the conceptual unification of processes such as resource and predator partitioning. Our final example pushes this view of environmental variation even further, to include the immune status of hosts for set of a pathogens. Pathogens modify their hosts by inducing specific immunity following infection. Like the legacy effects of plants in soil, or the creation of meadows by beavers, this immunity changes the suitability of a host for colonization by the same or related pathogens in the future. Strain theory in disease ecology explains how the resulting heterogeneity in host populations can mediate pathogen competition and coexistence [11, 85, 80]. Because adaptive immunity typically disadvantages strains that have been previously encountered, this kind of modification gives rise to negative frequency-dependent feedbacks essentially identical the dynamics of plant-soil feedbacks. Sophisticated modeling frameworks have been developed for multi-strain pathogen dynamics, building on the robust theory of compartmental models in epidemiology [76, 133]. This area of research has grappled productively with the central challenge of modeling the high-dimensional state space that results from combinatorial nature of immune history, although significant difficulties remain [257], such as understanding and incorporating path-dependent immune memory [176].

These four examples span a tremendous range of taxa, physical scales, and specific mechanisms. They hint at the ubiquity of environmental feedbacks across ecosystems. In each system considered here, modification by the focal community generates heterogeneity in the environment, and when these processes are organized in the right way, they can create the conditions for the coexistence of many species. Tractable – and sufficiently general – models for environmental feedbacks can help clarify precisely what we mean by "the right way". They can also foster a more unified understanding of feedback dynamics. As we have seen,

existing approaches reflect the diversity of their study systems: Microbial cross-feeding and immune-mediated pathogen competition have inspired sophisticated theory for large numbers of species or strains, but these models are somewhat restricted to particular feedback mechanisms. Ecosystem engineering theory takes a broader view of mechanism, but usually treats environmental heterogeneity as produced by one species and experienced by others, neglecting more complex indirect interactions between species. Feedback research in plant communities encompasses multiple mechanisms in highly diverse ecosystems, but lacks formal theory that can explicitly handle this diversity.

Each of these areas of research has a produced important insights, but we argue that a more general and systematic approach is needed to facilitate the transfer of knowledge between them, and to help draw out generic principles from system specific details. The remaining chapters take several steps toward such an approach. In the second chapter, we examine the canonical model at the heart of plant-soil feedback research. We extend this model to include an arbitrary number of plant species, and show that the extended model cannot support robust species coexistence. This surprising case study highlights two important lessons: There is an important role to play for tractable models that can guide the design and analysis of feedback experiments, but models for community coexistence must account for the species diversity of natural systems in order to offer useful guidance. Motivated by these lessons, in the third chapter we develop a novel modeling framework for environmental feedbacks among many species. We begin by considering a minimal model for community dynamics in the presence of fixed, abiotic heterogeneity, and then show how to incorporate feedbacks that shape this heterogeneity over time. Our framework treats environmental heterogeneity as distributed across space – building on the classic metapopulation paradigm to provide a minimal implementation of spatial structure – but is otherwise agnostic to the mechanisms underlying environmental modification and feedbacks. We analyze the feedback model in several special cases, and in the fourth chapter we look closely at this model in the

limit where environmental feedbacks occur much faster than population dynamics. Finally, in the fifth chapter we discuss conclusions suggested by these models, potential implications and applications, and important questions left open.

CHAPTER 2

NO ROBUST MULTISPECIES COEXISTENCE IN A CANONICAL MODEL OF PLANT-SOIL FEEDBACKS

2.1 Introduction

It has become well understood that reciprocal interactions between plants and the soil biota, collectively termed plant-soil feedbacks (PSFs), play an important role in structuring the composition and dynamics of plant communities. PSFs operate alongside other factors, including abiotic drivers [23] and above-ground trophic interactions [251], but are thought to be a key mechanism generating negative frequency-dependent feedbacks that promote coexistence and maintain plant diversity [135, 250, 30]. The existence of PSFs has long been known [252, 26], but our understanding of their importance – particularly in relation to patterns of coexistence – has developed rapidly in recent years [129, 188, 155, 55]. Broad interest in PSFs was ignited by the development of simple mathematical models that illustrated the potential of PSFs to mediate plant coexistence [31, 28, 124]. These models have played a crucial guiding role for a wide range of empirical studies, as well [135, 186, 136].

The first, and still most widely known and used, model for PSFs was introduced by Bever and colleagues in the 1990s [25, 31, 24]. In this framework, often referred to simply as the Bever model, each plant species is assumed to promote the growth of a specific soil component (i.e. associated bacteria, fungi, invertebrates, considered collectively) in the vicinity of individual plants. In turn, the fitness of each plant species is determined by the relative frequency of different soil components. Starting from minimal assumptions, Bever *et al.* [31] derived a set of differential equations to capture these dynamics. PSFs can be either

Originally published as: Miller, Zachary R., Pablo Lechón-Alonso, and Stefano Allesina. "No robust multispecies coexistence in a canonical model of plant–soil feedbacks." *Ecology Letters* (2022).

positive (fitness of a plant species is higher in soil conditioned by conspecifics, compared to heterospecific soil) or negative (a plant species experiences lower relative fitness in its own soil). Bever *et al.* introduced a single quantity to summarize whether community-wide PSFs are positive or negative, and showed that this value characterizes the dynamical behavior of the model. In the original Bever model of two plant species, positive PSFs lead to priority effects, and consequently the exclusion of one species, while negative PSFs result in neutral oscillations. It is thus widely suggested that negative PSFs help sustain coexistence in real-world plant communities [135, 250], perhaps with spatial asynchrony playing a role in stabilizing the cyclic dynamics [28, 198].

Subsequent studies have generalized PSF models to include, for example, more realistic functional forms [247, 65], more explicit representations of the soil community [29], spatial structure [168, 65, 233], or additional processes such as direct competitive interactions between plants [28]. However, the original Bever model remains an important touchstone for the theory of PSFs [124, 125, 1] and informs empirical research through the interaction coefficient, I_s, derived by Bever *et al.*, which is commonly measured and used to draw conclusions about coexistence in experimental studies. Despite the ubiquity of this model, and the fruitful interplay of theory and experiment in the PSF literature, extensions to communities with more than two or three species have appeared only rarely and recently [but see 136, 64, 154]. While PSF models motivate hypotheses and conclusions about species-rich natural communities, there is much still unknown about the behavior of these models with natural levels of diversity [250].

Here, we extend the Bever model to include any number of plant species, and show that the model is equivalent to a special form of the replicator equation studied in evolutionary game theory [105]. In particular, this model corresponds to the class of bimatrix games, where there are two players (here, plants and soil components) which interact with asymmetric strategies and payoffs. The replicator dynamics of bimatrix games are well-studied,

allowing us to characterize many properties of the Bever model with n plant species. Surprisingly, using this equivalence, we show that coexistence of more than two species in this model is never robust.

2.2 Results

2.2.1 Generalizing a classic PSF model

Inspired by emerging empirical evidence for the important role of PSFs in plant community dynamics and coexistence [252, 26], Bever *et al.* [31] introduced a simple mathematical model to investigate their behavior. In this model, two plant species, 1 and 2, grow exponentially with growth rates determined by the state of the soil biota in the system. These effects of soil on plants are specified by parameters α_{ij}, the growth rate of plant species i in soil type j. There is a soil component corresponding to each plant species, which grows exponentially in the presence of its associated plant at a rate β_i. Bever *et al.* set an important precedent by considering the dynamics of *relative* abundances in such a system; starting from dynamics of the form

$$\begin{cases} \frac{dx_i}{dt} &= x_i \left(\frac{\alpha_{ii}\, y_i + \alpha_{ij}\, y_j}{y_i + y_j} \right) , \quad i,j = 1,2 \\ \frac{dy_i}{dt} &= y_i \left(\frac{\beta_i\, x_i}{x_i + x_j} \right) \end{cases} \tag{2.1}$$

for the *absolute* abundances of plants (x_i) and soil components (y_i), one derives dynamics for the relative abundances (frequencies), $p_i = x_i \,/\, \sum_j x_j$ and $q_i = y_i \,/\, \sum_j y_j$. Using the facts $p_i = 1 - p_j$ and $q_i = 1 - q_j$, these can be written as:

$$\begin{cases} \frac{dp_i}{dt} & = p_i\, p_j \left((\alpha_{ii} - \alpha_{ji})\, q_i + (\alpha_{ij} - \alpha_{jj})\, q_j \right) , \quad i, j = 1, 2 \\ \frac{dq_i}{dt} & = q_i\, q_j (\beta_i\, p_i - \beta_j\, p_j) \, . \end{cases} \tag{2.2}$$

This model may admit a coexistence equilibrium where

$$\begin{cases} p_i^\star & = \frac{\beta_j}{\beta_i + \beta_j} \, , \quad i, j = 1, 2 \\ q_i^\star & = \frac{\alpha_{jj} - \alpha_{ji}}{\alpha_{ii} - \alpha_{ij} + \alpha_{jj} - \alpha_{ji}} \, . \end{cases} \tag{2.3}$$

A central finding of the analysis by Bever *et al.* was that the denominator of $q_i^\star$, which they termed the "interaction coefficient", I_s ($= \alpha_{ii} - \alpha_{ij} + \alpha_{jj} - \alpha_{ji}$), controls the model dynamics: When $I_s > 0$, which represents a community with positive feedbacks, the equilibrium in Eq. 2.3 is unstable, and the two species cannot coexist. On the other hand, when $I_s < 0$, the equilibrium is neutrally stable, and the dynamics cycle around it, providing a form of non-equilibrium coexistence. In fact, these conclusions also depend on the existence of a feasible equilibrium (i.e. positive equilibrium values), which further requires that $\alpha_{ii} < \alpha_{ji}$ for both $i, j = 1, 2$, in order for the model to exhibit coexistence [31, 124].

This coexistence is fragile. Plant and soil frequencies oscillate neutrally, similar to the textbook example of Lotka-Volterra predator-prey dynamics. Any stochasticity, external forcing, or temporal variation in the model parameters can destroy these finely balanced oscillations and cause one species to go extinct [198]. However, coupled with mechanisms that buffer the system from extinctions, such as migration between desynchronized patches or the presence of a seed bank, the negative feedbacks in this model might produce sustained coexistence [28, 198].

Of course, most natural plant communities feature more than two coexisting species,

and it is precisely in the most diverse communities that mechanisms of coexistence hold the greatest interest [250]. While it is not immediately clear how to generalize Eq. 2.2 to more than two species, Eq. 2.1 is naturally extended by maintaining the assumption that the overall growth rate for any plant is a weighted average of its growth rate in each soil type:

$$\begin{cases} \frac{dx_i}{dt} & = x_i \left(\sum_j \alpha_{ij} \, q_j \right) , \quad i = 1, \dots n \\ \frac{dy_i}{dt} & = y_i \left(\beta_i \, p_i \right) . \end{cases} \tag{2.4}$$

From Eq. 2.4, one can derive the n-species analogue of Eq. 2.2,

$$\begin{cases} \frac{dp_i}{dt} & = p_i \left(\sum_j \alpha_{ij} \, q_j - \sum_{j,k} \alpha_{jk} \, p_j \, q_k \right) , \quad i = 1, \dots n \\ \frac{dq_i}{dt} & = q_i \left(\beta_i \, p_i - \sum_j \beta_j \, p_j \, q_j \right) \end{cases} \tag{2.5}$$

giving the dynamics for species and soil component frequencies (Fig. 2.1). Eq. 2.5 is conveniently expressed in matrix form as

$$\begin{cases} \frac{d\boldsymbol{p}}{dt} & = D(\boldsymbol{p}) \left(A\boldsymbol{q} - (\boldsymbol{p}^T A \boldsymbol{q}) \mathbf{1} \right) \\ \frac{d\boldsymbol{q}}{dt} & = D(\boldsymbol{q}) \left(B\boldsymbol{p} - (\boldsymbol{q}^T B \boldsymbol{p}) \mathbf{1} \right) \end{cases} \tag{2.6}$$

where vectors are indicated in boldface (e.g. $\boldsymbol{p}$ is the vector of plant species frequencies $(p_1, p_2, \dots p_n)^T$ and $\mathbf{1}$ is a vector of n ones) and $D(\boldsymbol{z})$ is the diagonal matrix with vector $\boldsymbol{z}$ on the diagonal. We have introduced the matrices $A = (\alpha_{ij})$ and $B = D(\beta_1, \beta_2, \dots \beta_n)$, specifying soil effects on plants and plant effects on soil, respectively. Because $\boldsymbol{p}$ and $\boldsymbol{q}$ are vectors of frequencies, they must sum to one: $\mathbf{1}^T \boldsymbol{p} = \mathbf{1}^T \boldsymbol{q} = 1$. Using these constraints, one

can easily show that the Bever model (Eq. 2.2) is a special case of Eqs. 2.5 and 2.6 when $n = 2$.

This model (Eq. 2.5) is a direct multispecies generalization of the classic Bever model [31]; it requires precisely the same assumptions as the original, and includes the same biological processes. Other extensions of the Bever model have been introduced, including versions that incorporate plant-plant competition and self-regulation [28] or modified soil dynamics [64, 154]. Contrasting the predictions of these models can illuminate the connections between particular biological processes (model assumptions) and resulting community dynamics, a point we return to in the Discussion. However, it is also important to recognize that different biological assumptions can give rise to identical dynamics; for example, we show in the Supplemental Methods that the model introduced by Bever in 2003, which includes more realistic plant dynamics and interactions, reduces to our Eq. 2.5 when plants are competitively equivalent.

2.2.2 Equivalence to bimatrix game dynamics

Systems that take the form of Eq. 2.6 are well-known and well-studied in evolutionary game theory. Our generalization of the Bever model is a special case of the *replicator equation*, corresponding to the class of *bimatrix games* [235, 103, 105, 56]. Bimatrix games arise in diverse contexts, such as animal behavior [235, 212], evolutionary theory [105, 56], and economics [70], where they model games with asymmetric players, meaning that each player (here, the plant community and the soil) has a distinct set of strategies (plants species and soil components, respectively) and payoffs (realized growth rates).

Much is known about bimatrix game dynamics, and we can draw on this body of knowledge to characterize the behavior of the Bever model with n species. Essential mathematical background and details are presented in the Supplemental Methods; for a detailed introduction to bimatrix games, see Hofbauer and Sigmund [105].

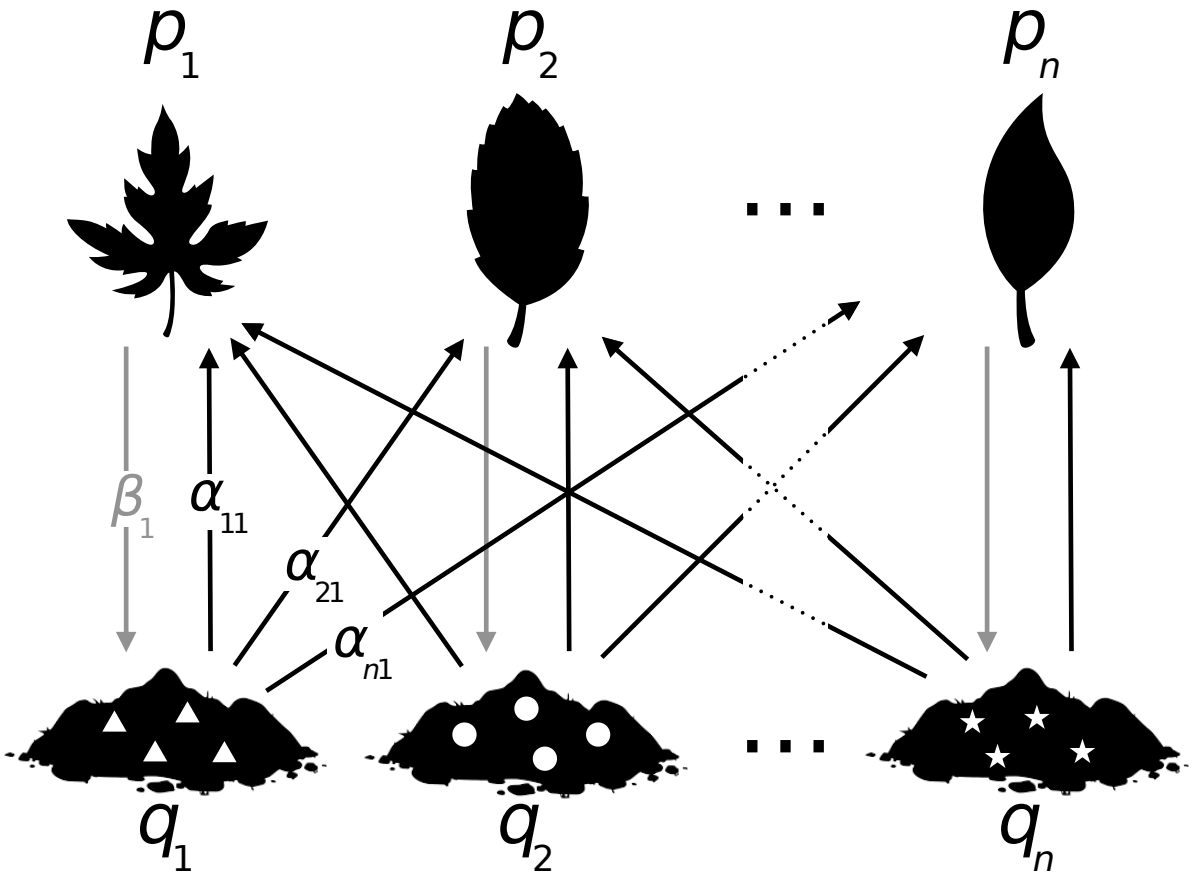

Figure 2.1: The model described by Eqs. 2.5-2.6 is shown here graphically. Plant species (top) promote the growth of their respective soil components (bottom) at a rate β_i (gray arrows). In turn, growth of each plant is governed by the mix of soil components present in the system, with the effect of soil component j on species i quantified by the parameter α_{ij} (black arrows). This model is a straightforward extension of the model proposed by Bever *et al.* [31] to an arbitrary number of species. Note only selected parameter labels are shown for clarity.

Under the mild condition that matrix A is invertible, Eq. 2.6 admits a unique coexistence equilibrium given by $\boldsymbol{p}^\star = k_p\, B^{-1}\mathbf{1}$ and $\boldsymbol{q}^\star = k_q\, A^{-1}\mathbf{1}$, where $k_p = 1/(\mathbf{1}^T B^{-1}\mathbf{1})$ and $k_q = 1/(\mathbf{1}^T A^{-1}\mathbf{1})$ are constants of proportionality that ensure the equilibrium frequencies sum to one for both plants and soil. Because B is a diagonal matrix, and all β_i are assumed positive, the equilibrium plant frequencies, $\boldsymbol{p}^\star$, are always positive, as well. Thus, feasibility of the equilibrium hinges on the soil frequencies, $\boldsymbol{q}^\star$, which are all positive if the elements of $A^{-1}\mathbf{1}$ all share the same sign.

As we have seen, when the community consists of two plant species, the coexistence equilibrium, if feasible, can be either unstable or neutrally stable. The same is true for the n-species extension (and, more generally, for any bimatrix game dynamics; see [67, 212, 105]). This can be established using straightforward local stability analysis, after accounting for the relative abundance constraints, which imply $p_n = 1 - \sum_{i=1}^{n-1} p_i$ and $q_n = 1 - \sum_{i=1}^{n-1} q_i$. Using these substitutions, Eq. 2.5 can be written as a system of $2n-2$ (rather than $2n$) equations, and the community matrix for this reduced model has a very simple form (see Supplemental Methods). In particular, the community matrix has all zero diagonal elements, which implies that the eigenvalues of this matrix sum to zero. These eigenvalues govern the stability of the coexistence equilibrium, and this property leaves two qualitatively distinct possibilities: either the eigenvalues have a mix of positive and negative real parts (in which case the equilibrium is unstable), or the eigenvalues all have zero real part (in which case the equilibrium is neutrally stable). Already, we can see that the model never exhibits stable equilibrium coexistence, regardless of the number of species.

In fact, these conclusions apply to a much broader class of models that are structurally similar to the Bever model. Consider any PSF dynamics that can be written in the form

$$\begin{cases} \frac{dx_i}{dt} &= x_i\, f_i(\boldsymbol{q}) \\ \frac{dy_i}{dt} &= y_i\, g_i(\boldsymbol{p})\,. \end{cases} \tag{2.7}$$

Such a model has a bipartite structure, meaning that the per capita growth rate of each plant species is an arbitrary function, f_i, of the soil frequencies, with no dependence on the plant abundances or frequencies, and vice versa. The corresponding dynamics for plant and soil frequencies may possess one or more coexistence equilibria. At any of these equilibrium points, the community matrix, which governs its stability, necessarily takes the same form as for the Bever model, with all zero diagonal elements. As such, these equilibria must be either unstable or neutrally stable. This is a robust consequence of the strictly bipartite structure of Eq. 2.7.

Another notable property of bimatrix game dynamics is that the vector field defined by the model equations is divergence-free or incompressible (see [105] for a proof). The divergence theorem from vector calculus [14] then dictates that Eq. 2.6 cannot have any attractors – that is, regions of the phase space that "pull in" trajectories – with multiple species. This rules out coexistence in a stable limit cycle or other non-equilibrium attractors (e.g. chaotic attractors). Thus, only the relatively fragile coexistence afforded by neutral oscillations is possible, as in the two-species model.

Based on the local stability properties of the coexistence equilibrium, Bever *et al.* concluded that such neutral cycles arise for two species when $\alpha_{11} < \alpha_{21}$ and $\alpha_{22} < \alpha_{12}$. The equivalence between their model and a bimatrix game with two strategies allows us to give a fuller picture of these cycles. Namely, we can identify a constant of motion for the two-species dynamics:

$$H = (\alpha_{12} - \alpha_{22}) \log q_1 + (\alpha_{21} - \alpha_{11}) \log q_2 + \beta_2 \log p_1 + \beta_1 \log p_2. \tag{2.8}$$

Using the chain rule and time derivatives in Eq. 2.2, it is easy to show that $\frac{dH}{dt} = 0$ for any plant and soil frequencies (see Supplemental Methods). The level curves of H form closed orbits around the equilibrium when the equilibrium is neutrally stable. Thus, H implicitly defines the trajectories of the model, and can be used to determine characteristics such as the amplitude of oscillations arising from particular initial frequencies [254].

Because neutral cycles provide the only possible form of coexistence in this model, a key question becomes whether and when neutral cycles with n plant species can arise. Do the "negative feedback" conditions identified by Bever *et al.* generalize in richer communities? Indeed, they do; however, for more than two species, these conditions are very severe. The model in Eq. 2.6 supports oscillations with n plant species – for any n – if matrices A and B satisfy a precise relationship (see Supplemental Methods for details). In particular, the model parameters must satisfy the conditions $\alpha_{ij} = \gamma_i + \delta_j$ for some constants γ_i, δ_i in $i = 1, \ldots, n$ (when $i \neq j$), and $\alpha_{ii} = \gamma_i + \delta_i - c\beta_i$ (where c is a positive constant that must be the same for all species i). In the language of bimatrix games, such systems are called *rescaled zero-sum games* [103, 105]. It is a long-standing conjecture in evolutionary game theory that these parameterizations are the *only* cases where n-species coexistence can occur [103, 104].

Ecologically, these conditions mean there is a fixed effect of each soil type and plant species identity, and the growth rate of plant i in soil type j is the additive combination of these two, with no interaction effects. The only exception is for plants growing in their own soil type, which must experience a fitness cost ($\gamma_i + \delta_i - \alpha_{ii}$) exactly proportional to the rate at which they promote growth of their soil type (β_i). These conditions clearly extend the intuitive notion that each plant must have a disadvantage in its corresponding soil type to allow for coexistence. But the parameters of the model are constrained so strongly that we never expect to observe cycles with more than two plant species in practice. When $n > 2$, a great deal of fine-tuning is necessary to satisfy the rescaled zero-sum game condition; the

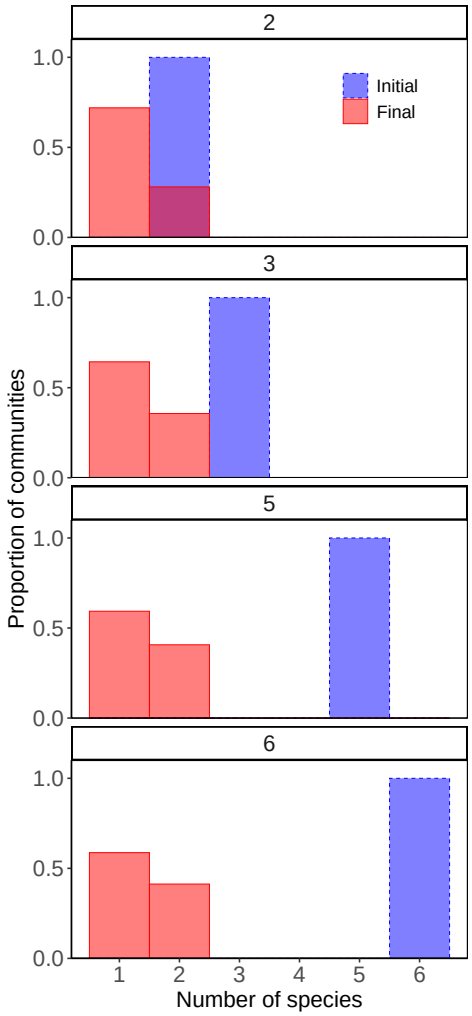

Figure 2.2: Final community sizes with varying initial richness. We show the distribution of final richness (number of species, in red) for 5000 communities governed by the n-species Bever model, initialized with 2, 3, 5, or 6 plant species. Parameters α_{ij} and β_i were sampled independently from a standard uniform distribution, $U(0, 1)$. For each random parameterization at each level of initial richness, we integrated the dynamics of Eq. 2.6 until the system reached a periodic orbit or until only one species remained. In agreement with the conjecture that coexistence of more than two species is vanishingly unlikely, we found that regardless of the number of species initially present, every community collapsed to a subset with one or two surviving species.

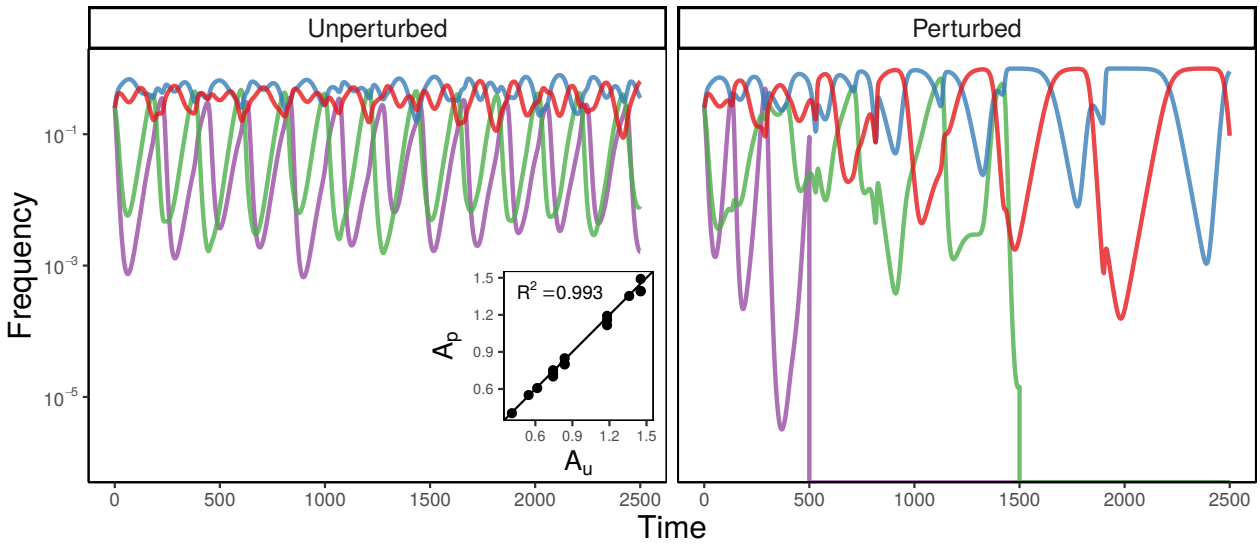

Figure 2.3: Coexistence of three or more species is not robust. It is possible to obtain neutrally stable oscillations with any number of plant species if the model parameters constitute a rescaled zero-sum game (see text for conditions). Here, for example, we show sustained oscillations with 4 plant species (soil frequencies not shown) using fine-tuned parameters, A_u (left). However, if we randomly perturb A_u by a small amount to obtain new parameters, A_p, the dynamics quickly collapse to a two-species subset (right). Any slight perturbation is enough to disrupt coexistence; for this example, the parameters A_u and A_p are highly correlated (inset) and differ in value by less than 3% on average.

probability that random parameters will be suitable is infinitesimally small. We confirm this numerically with simulations shown in Fig. 2.2. Although n-species cycles are clearly possible (as in Fig. 2.3), when parameters are drawn independently at random communities always collapse to one or two species, regardless of the initial richness.

Parameter combinations permitting many-species oscillations are not only rare, they are also extremely sensitive to small changes to the parameter values. The rescaled zero-sum condition imposes many exact equality constraints on the matrix A (e.g. $\alpha_{ij} - \alpha_{ik} = \alpha_{lj} - \alpha_{lk}$ for all i, j, k, and l). Even if biological mechanisms exist to generate the requisite qualitative patterns, inevitable quantitative variation in real-world communities will disrupt coexistence (Fig. 2.3). Coexistence of $n > 2$ plant species – even in the weak sense of neutral cycles – is not robust to small changes in the model parameters.

Interestingly, the two-species model is not subject to the same fragility. It can be shown

(see Supplemental Methods) that all 2×2 bimatrix games take the same general form as a rescaled zero-sum game, although the constant c may be positive or negative, depending on the parameters. When I_s, the interaction coefficient identified by Bever *et al.*, is negative, c is positive, ensuring (neutral) stability. This condition amounts to an inequality constraint, rather than an equality constraint, and so it *is* generally robust to small variations in model parameters. As we can now see, the case $n = 2$ is unique in this regard.

2.3 Discussion

The Bever model has played a central role in motivating PSF research, and continues to guide both theory and experiment in this fast-growing field [30, 122, 125, 1]. Here, we extend the Bever model to include any number of plant species, and highlight its equivalence to bimatrix game dynamics. Taking advantage of the well-developed theory for these dynamics, we are able to characterize the behavior of this generalized Bever model in detail.

Our central finding is that there can be no robust coexistence of plant species in this model. Regardless of the number of species, n, the model never exhibits equilibrium coexistence or other attractors. Coexistence can be attained through neutral oscillations, but these dynamics lack any restoring force, meaning diversity would quickly be eroded by stochasticity or exogenous forcing. In this respect, the generalized model behaves similarly to the classic two-species system. However, unlike the two-species model, oscillations with $n > 2$ species can only occur under very restricted parameter combinations. These parameterizations are vanishingly unlikely to arise by chance and highly sensitive to small deviations. Thus, coexistence of more than two species is neither dynamically nor structurally stable.

This result may seem surprising, because a significant body of experimental evidence indicates that PSFs can and do play an important role in mediating the coexistence of more than two species in natural communities [135, 188, 155, 30]. Apparently, the picture suggested by the two-species Bever model generalizes in nature, but not in the model framework itself.

We note that this framework was introduced as an intentional simplification to illustrate the potential role of PSFs in mediating coexistence, not to accurately model the biological details of PSFs. Indeed, the model has been wildly successful in spurring research into PSFs. Alongside extensive empirical study of these processes, other modeling approaches have emerged, accounting for more biological realism [e.g., 247, 66, 29], or with the demonstrated capacity to produce multispecies coexistence [e.g., 34, 64, 164]. Some of these are minor modifications of the Bever model framework; others build on distinct foundations [124, 125]. Our results suggest that these various avenues are worth pursuing further.

Our findings also help clarify important aspects of coexistence across modeling approaches. For example, Eppinga *et al.* [64] and Mack *et al.* [154] recently introduced a multispecies PSF model which can exhibit stable coexistence. Their model is inspired by the Bever model framework, but departs from it in two ways: by introducing more realistic soil dynamics, including a carrying capacity for soil communities, and by applying a separation of timescales, under the assumption that soil dynamics are very rapid compared to plant dynamics. Our analysis indicates that the second feature is unable to account for stabilization. Regardless of the relative rates of plant and soil dynamics, the coexistence equilibrium of the generalized Bever model is never attractive (see also Figs. 2.5 and 2.6). This is a fundamental feature of the model structure, not a result of particular parameter choices. When oscillations do exist in the Bever model, they are always neutral, meaning that their amplitude is fixed by the initial conditions of the system, and cannot diminish through the dynamics. These observations make clear that the crucial factor driving coexistence in the model of Eppinga, Mack, and colleagues is self-regulation within soil communities, not rapid soil dynamics.

Indeed, our analysis suggests that the internal dynamics of plant or soil communities must interact with PSFs to maintain diversity in natural systems. We have shown that PSF models that are structurally similar to the Bever model – in which plant dynamics depend

only on soil frequencies, and soil dynamics depend only on plant frequencies – are incapable of exhibiting stable coexistence of any number of species. Multispecies coexistence becomes possible when plants [28, 198], soils [64, 154], or both experience an independent source of self-regulation, which might arise from resource competition, physical limits to density, or some other mechanism. PSFs are likely to matter most for the maintenance of diversity when they interact with these internal plant or soil dynamics in non-trivial ways. In the case of combined plant competition-feedback models [28], for example, we have already seen that no robust coexistence is possible when plants are competitively equivalent and experience "mean-field" interactions. On the other hand, when plant competition is dominated by strong intraspecific interactions, all plant species would coexist even in the absence of PSFs. Thus, PSFs can only contribute to the maintenance of diversity in such models by modifying competitive outcomes [28, 198, 122] – that is, by interacting with the structure of the plant-plant competitive network.

These conclusions have practical implications for the study of PSFs in real-world communities. The predictions of the Bever model are commonly used to guide the design and analysis of PSF experiments, especially in drawing conclusions about coexistence. Our analysis cautions that direct application of this model in multispecies communities might lead to incorrect inference. For example, attempts to parameterize the Bever model for three species using empirical data have produced predictions of non-coexistence in plant communities that coexist experimentally [136]. In many other studies, the interaction coefficient, I_s, is calculated for species pairs and used to assess whole-community coexistence [135, 68, 185, 233, 134, 225, 21, 195, 55]. However, we have seen that whole-community coexistence is virtually impossible within the generalized model, and there is no guarantee that the pairwise coexistence conditions for this model will agree with n-species coexistence conditions in other frameworks (but see [155, 64]). For example, $I_s < 0$ for all species pairs is neither necessary nor sufficient to produce coexistence in a metapopulation-based model

for PSFs [164].

Theory suggests that when PSFs do play a role in maintaining robust coexistence, interactions between plants and soil will necessarily be only part of the picture. On this point, we echo calls that have emerged in the empirical literature for more closely integrated study of PSFs and other processes, such as plant competition [42, 140] and more detailed soil biology [29, 102]. Our results strongly suggest that pairwise PSF measurements are insufficient to characterize plant coexistence and require contextualization alongside these other ecosystem processes.

Fundamentally, our analysis demonstrates that PSFs as envisioned in the classic Bever model cannot produce robust n-species coexistence in isolation. Our results also indicate basic structural features that are necessary for PSF models to support multispecies coexistence. Significantly, we find not only the absence of stabilization in the Bever model, but generic *instability*. This suggests that, in diverse communities, other processes must exert a sufficiently strong influence on the community dynamics to overcome the baseline instability. We illustrate this idea in the Supplemental Methods, where we examine the effect of adding negative frequency-dependence in the classic Bever model. Any amount of frequency-dependence stabilizes neutral oscillations, but when these effects are weak, they cannot turn unstable equilibria into stable ones. The result is that the augmented model can only support multispecies coexistence when the rescaled zero-sum game condition is met, and, as we have shown, this condition is never robust to small parameter variations.

In this example, we consider negative frequency-dependence, rather than density-dependence (as in [28]), because it is difficult to compare the strengths of processes that mix units of frequency and density. This difficulty hints at a central limitation of classic PSF models, which are derived by projecting dynamics for plant and soil *abundances* onto the space of *frequencies*. [136, 198, 64, 125]. The projected dynamics can mask unbiological outcomes in the original model (e.g. relative abundances oscillate around equilibrium while absolute

abundances shrink to zero or explode to infinity). Indeed, the absolute abundance model (Eq. 2.4) used to derive our n-species frequency dynamics (Eqs. 2.5-2.6) does not generally possess any fixed point, which is a basic requirement for species coexistence [114, 115]. The same is true for the model introduced by Eppinga *et al.* [64] and Mack *et al.* [154], even though this model exhibits stable dynamics for plant and soil frequencies. It is usually seen as desirable to study PSFs in the space of species frequencies, both because this facilitates connections to data, and because frequencies are considered appropriate units for analyzing processes that stabilize coexistence ([4, 64], but see [122, 125]). But models that introduce frequencies through a natural constraint, such as competition for finite space, will likely produce more realistic and straightforwardly interpretable dynamics.

From a broader theoretical perspective, the qualitative change in model behavior that we observe as the number of species increases from two to three or more is a striking phenomenon, but not an unprecedented one. Ecologists have repeatedly found that intuitions from two-species models can generalize (or fail to generalize) to more diverse communities in surprising ways [230, 222, 19]. Our analysis provides another illustration of the fact that "more is different" [10] in ecology, and highlights the importance of developing theory for species-rich communities.

2.4 Supplemental methods

2.4.1 Model derivation

As described in the Main Text, we begin with the system

$$\begin{cases} \frac{dx_i}{dt} &= x_i \left(\sum_j \alpha_{ij} \, q_j \right) , \quad i = 1, \dots n \\ \frac{dy_i}{dt} &= y_i \left(\beta_i \, p_i \right) \end{cases} \tag{2.9}$$

governing the time-evolution of plant abundances x_i and soil components y_i, where $p_i = x_i / \sum_j x_j$, $q_i = y_i / \sum_j y_j$, and Greek letters denote nonnegative parameters. These equations capture the assumptions outlined by Bever *et al.* [31] for two species and extend them straightforwardly to any n species. Following the approach of Bever *et al.* for two species [31] and consistent with other generalizations of this model (e.g., [135, 64]), we derive dynamics for frequencies by applying the chain rule:

$$\begin{aligned}
\frac{dp_i}{dt} &= \frac{d}{dt}\frac{x_i}{\sum x_j} \\
&= \frac{1}{\sum_j x_j}\frac{dx_i}{dt} - \frac{x_i}{(\sum_j x_j)^2}\sum_j \frac{dx_j}{dt} \\
&= \frac{x_i}{\sum_j x_j}\left(\sum_j \alpha_{ij}\, q_j\right) - \frac{x_i}{\sum_j x_j}\left(\sum_j \frac{x_j}{\sum_k x_k}\sum_l \alpha_{jl}\, q_l\right) \\
&= p_i\left(\sum_j \alpha_{ij}\, q_j - \sum_{j,k} \alpha_{jk} p_j q_k\right) .
\end{aligned} \tag{2.10}$$

This last expression is identical to the first line of Eq. 2.5 in the Main Text. The dynamics for q_i can be derived in exactly the same way (using the definitions $\beta_{ii} = \beta_i$ and $\beta_{ij} = 0$). The two terms of each per capita growth rate in Eq. 2.5 have natural interpretations in the language and notation of linear algebra: $\sum_j \alpha_{ij}\, q_j$ is the ith component of the matrix-vector product $A\boldsymbol{q}$ and $\sum_{j,k} \alpha_{jk} p_j q_k$ is the bilinear form $\boldsymbol{p}^T A \boldsymbol{q}$. Here, A (and B) is an $n \times n$ matrix and $\boldsymbol{p}$ and $\boldsymbol{q}$ are vectors of length n, as described in the Main Text. We can re-write Eq. 2.5 as

$$\begin{aligned}
\frac{dp_i}{dt} &= p_i\left((A\boldsymbol{q})_i - \boldsymbol{p}^T A \boldsymbol{q}\right) \\
\frac{dq_i}{dt} &= q_i\left((B\boldsymbol{p})_i - \boldsymbol{q}^T B \boldsymbol{p}\right)
\end{aligned} \tag{2.11}$$

or even more compactly as

$$\begin{cases} \frac{d\boldsymbol{p}}{dt} &= D(\boldsymbol{p})\left(A\boldsymbol{q} - (\boldsymbol{p}^T A\boldsymbol{q})\mathbf{1}\right) \\ \frac{d\boldsymbol{q}}{dt} &= D(\boldsymbol{q})\left(B\boldsymbol{p} - (\boldsymbol{q}^T B\boldsymbol{p})\mathbf{1}\right) \end{cases} \tag{2.12}$$

which is Eq. 2.6 in the Main Text.

An alternative derivation of these dynamics (Eqs. 2.5 and 2.6) takes the model introduced by Bever [28] as a starting point. Using our notation, this model can be written as

$$\begin{cases} \frac{dx_i}{dt} &= x_i\left(r_i + \sum_j \alpha_{ij}\, q_j - \sum_j c_{ij} x_j\right), \quad i = 1, \ldots n \\ \frac{dy_i}{dt} &= y_i\left(\beta_i\, p_i\right) \end{cases} \tag{2.13}$$

where all variables have the same meaning as before. In this model, plants experience competitive Lotka-Volterra dynamics alongside frequency-dependent soil effects. The parameters r_i are intrinsic growth rates for plants, and the c_{ij} quantify the competitive effect of plant j on plant i, as in the usual Lotka-Volterra model. We note that in this context, the soil effects on plants, α_{ij} may be positive or negative, as they modify the baseline plant growth rates, set by r_i. The dynamics of soil communities are exactly as before.

One can write the dynamics for plant frequencies under this model as:

$$\frac{dp_i}{dt} = p_i\left(r_i + \sum_j \alpha_{ij}\, q_j - \sum_j c_{ij} x_j - \sum_j p_j\left[r_j + \sum_k \alpha_{jk}\, q_k - \sum_k c_{jk} x_k\right]\right), \quad i = 1, \ldots n \tag{2.14}$$

following a calculation similar to Eq. 2.10. As other researchers have noted [28, 64], if $r_i = r$ and $c_{ij} = c$ for all i and j, indicating a situation where all plants are demographically and

competitively equal, then Eq. 2.14 reduces to

$$\frac{dp_i}{dt} = p_i \left(\sum_j \alpha_{ij}\, q_j - \sum_j p_j \sum_k \alpha_{jk}\, q_k \right) , \quad i = 1, \ldots n \tag{2.15}$$

which is identical to the dynamics for plant frequencies shown in Eq. 2.5 of the Main Text. Thus, under the simplifying assumption of "mean-field" plant interactions, the two models yield equivalent dynamics for plant and soil frequencies. We will show at the end of this section that the potential difference in signs (i.e. α_{ij} must be nonnegative in the first model formulation, but may take any sign here) has no effect on the dynamics.

The system described by Eq. 2.12, however obtained, is identical to standard bimatrix replicator dynamics [103, 105]. Bimatrix games have two strategy sets (here, the p_i and q_i), and interactions take place only between strategies from opposite sets. The growth rate terms we considered above now have interpretations as payoffs or fitnesses: $\sum_j \alpha_{ij}\, q_j = (A\boldsymbol{q})_i$ is the payoff for strategy i (an average of payoffs playing against each strategy of the other "player", weighted by the frequency of each strategy, q_j) and $\sum_{j,k} \alpha_{jk} p_j q_k = \boldsymbol{p}^T A \boldsymbol{q}$ is the average payoff across the population of strategies. A general bimatrix game may have any B; our model assumptions lead to the special case where B is diagonal. We note that one could easily and plausibly consider an extension of the Bever model where each plant species has some effect on (up to) all n of the soil components. Then, our PSF model would be map exactly onto the full space of bimatrix game dynamics (rather than just a subset). However, all of the results we consider hold for arbitrary bimatrix games, meaning the same conclusions about the dynamics of Eqs. 2.5-2.6 would apply to this extended model, as well.

We note two useful properties of Eqs. 2.5-2.6, as they will be important for the analysis that follows. First, we have the constraint $\sum_i p_i = \sum_i q_i = 1$ at every point in time. Second, the dynamics are completely unchanged by adding a constant to any *column* of the parameter

matrices A or B. The first fact is a direct consequence of our definition for p_i and q_i; the second can easily be shown. Suppose we have added a constant w to each element in the lth column of A. Then

$$\begin{aligned}\frac{dp_i}{dt} &= p_i \left(\sum_j \alpha_{ij}\, q_j + w\, q_l - \sum_{j,k} \alpha_{jk}\, p_j\, q_k - \sum_j w\, p_j\, q_l \right) \\ &= p_i \left(\sum_j \alpha_{ij}\, q_j + w\, q_l - \sum_{j,k} \alpha_{jk}\, p_j\, q_k - w\, q_l \right) \\ &= p_i \left(\sum_j \alpha_{ij}\, q_j - \sum_{j,k} \alpha_{jk}\, p_j\, q_k \right)\end{aligned} \tag{2.16}$$

which is precisely the differential equation we obtained prior to adding w. Clearly the trajectories of both systems (with and without the column shift) must be identical. The same considerations apply for the matrix B. Intuitively, this property reflects the fact that we are always subtracting the average payoff, and so any change to the payoffs that benefits (or harms) each species equally is "invisible" to the dynamics.

In the remaining sections, we outline the main behaviors of Eqs. 2.5-2.6, especially with regard to coexistence. We closely follow the treatment by Hofbauer and Sigmund [105], and urge interested readers to consult this excellent introduction (see especially chapters 10 and 11). Here, we reproduce or sketch the essential details needed to justify the results in the Main Text.

2.4.2 Coexistence equilibrium

Written in matrix form, it is easy to see that the model admits a unique fixed point where all species are present at non-zero frequency. This fixed point, $(\boldsymbol{p}^\star, \boldsymbol{q}^\star)$, must take the form $(k_p B^{-1}\mathbf{1}, k_q A^{-1}\mathbf{1})$ for some undetermined constants k_p and k_q. Substituting this ansatz

into the growth rates in Eq. 6 and equating them to zero, we have

$$A\boldsymbol{q}^\star - ((\boldsymbol{p}^\star)^T A\boldsymbol{q}^\star)\mathbf{1} = k_q AA^{-1}\mathbf{1} - (k_p k_q \mathbf{1}^T (B^{-1})^T AA^{-1}\mathbf{1})\mathbf{1} = k_q(1 - k_p \mathbf{1}^T (B^{-1})^T \mathbf{1})\mathbf{1} = 0$$
$$B\boldsymbol{p}^\star - ((\boldsymbol{q}^\star)^T B\boldsymbol{p}^\star)\mathbf{1} = k_p BB^{-1}\mathbf{1} - (k_p k_q \mathbf{1}^T (A^{-1})^T BB^{-1}\mathbf{1})\mathbf{1} = k_p(1 - k_q \mathbf{1}^T (A^{-1})^T \mathbf{1})\mathbf{1} = 0 \tag{2.17}$$

From the final two equations, it is clear that $k_p = \frac{1}{\mathbf{1}^T (B^{-1})^T \mathbf{1}} = \frac{1}{\mathbf{1}^T B^{-1}\mathbf{1}}$ and $k_q = \frac{1}{\mathbf{1}^T (A^{-1})^T \mathbf{1}} = \frac{1}{\mathbf{1}^T A^{-1}\mathbf{1}}$.

These rescaling factors make intuitive sense, as they ensure that $\sum_i p_i^\star = \sum_i q_i^\star = 1$, consistent with their definition as frequencies.

Describing these equilibrium frequencies in terms of the parameters is a difficult problem that has received significant attention elsewhere [64, 154, 205, 213, 190, 204]. In particular, one is usually interested in identifying whether all of the frequencies are nonnegative (such a fixed point is said to be feasible). The existence of a feasible fixed point is a requirement for the model to exhibit permanence, meaning that no species go extinct or grow to infinity. Throughout our analysis, we assume the existence of a feasible fixed point; considering the question of feasibility simultaneously would only make coexistence less likely in each case. We present some additional details regarding feasibility in the section *Equilibrium feasibility*, below.

2.4.3 Local stability analysis

Perturbations around the coexistence equilibrium are constrained to respect the conditions $\sum_i p_i = \sum_i q_i = 1$. For this reason, it is convenient to remove these constraints before performing a local stability analysis. As in the two species case [31], this can be done by eliminating the nth species and soil component, which leaves us with a $2n-2$ dimensional system with no special constraints.

We use $p_n = 1 - \sum_{i=1}^{n-1} p_i \equiv f(\boldsymbol{p})$ and $q_n = 1 - \sum_{i=1}^{n-1} q_i \equiv g(\boldsymbol{q})$ and write these frequencies as functions of the others. The reduced dynamics are given by

$$\begin{cases} \frac{dp_i}{dt} & = p_i\Big(\sum_j^{n-1} \alpha_{ij}\, q_j + \alpha_{in} g(\boldsymbol{q}) - \sum_{j,k}^{n-1} \alpha_{jk}\, p_j\, q_k - f(\boldsymbol{p}) \sum_j^{n-1} \alpha_{nj} q_j - \\ & \qquad g(\boldsymbol{q}) \sum_j^{n-1} \alpha_{jn} p_j - \alpha_{nn} f(\boldsymbol{p}) g(\boldsymbol{q}) \Big) \\ \frac{dq_i}{dt} & = q_i \left(\beta_i\, p_i - \sum_j^{n-1} \beta_j\, p_j\, q_j - \beta_n f(\boldsymbol{p}) g(\boldsymbol{q}) \right) , \quad i = 1, \ldots n-1 \end{cases} \tag{2.18}$$

Although these equations appear more complex, it is now straightforward to analyze the local stability of the coexistence equilibrium.

The elements of the community matrix (the Jacobian evaluated at the coexistence equilibrium) are easily computed from Eq. 2.18. First we consider the plant dynamics differentiated with respect to the plant frequencies. In these calculations, all frequencies are evaluated at their equilibrium values.

$$\begin{aligned} \frac{\partial}{\partial p_j} \frac{dp_i}{dt} &= p_i \left(- \sum_k^{n-1} \alpha_{jk}\, q_k + \sum_k^{n-1} \alpha_{nk} q_k - \alpha_{jn} g(\boldsymbol{q}) + \alpha_{nn} g(\boldsymbol{q}) \right) \\ &= p_i \left(- \sum_k^{n} \alpha_{jk}\, q_k + \sum_k^{n} \alpha_{nk} q_k \right) \\ &= 0 \end{aligned} \tag{2.19}$$

Here, we have used the fact that $A\boldsymbol{q}^\star \propto \mathbf{1}$. Notice that, because the factors in parentheses in Eq. 2.18 are zero at equilibrium, these community matrix calculations are valid even for $i = j$.

The other elements are computed similarly:

$$\begin{aligned}\frac{\partial}{\partial q_j}\frac{dq_i}{dt} &= q_i\left(-\beta_i q_i + \beta_n f(\boldsymbol{p})\right)\\ &= 0\end{aligned} \tag{2.20}$$

$$\begin{aligned}\frac{\partial}{\partial q_j}\frac{dp_i}{dt} &= p_i\left(\alpha_{ij} - \alpha_{in} - \sum_k^{n-1}\alpha_{kj}\,p_k - \alpha_{nj}\,f(\boldsymbol{p}) + \sum_k^{n-1}\alpha_{kn}p_k + \alpha_{nn}f(\boldsymbol{p})\right)\\ &= p_i(\alpha_{ij} - \alpha_{in})\end{aligned} \tag{2.21}$$

$$\frac{\partial}{\partial p_j}\frac{dq_i}{dt} = \begin{cases} q_i\,\beta_i\,, & i = j \\ 0\,, & i \neq j \end{cases} \tag{2.22}$$

From these calculations, it is apparent that the trace of the community matrix, given by $\sum_i^{n-1}\frac{\partial}{\partial p_i}\frac{dp_i}{dt} + \sum_j^{n-1}\frac{\partial}{\partial q_j}\frac{dq_j}{dt}$, is zero. The trace of a square matrix is equal to the sum of its eigenvalues [109], so the eigenvalues of the community matrix must include either (i) a mix of positive and negative real parts or (ii) only purely imaginary values. In the first case, the coexistence equilibrium is locally unstable, because at least one eigenvalue has positive real part. In the second case, the coexistence equilibrium is neutrally or marginally stable. These two possibilities exclude asymptotically stable equilibria. In this respect, the behavior of the two-species model is the generic behavior of the generalized n-species model.

2.4.4 Zero divergence implies no attractors

We can extend this picture beyond a local neighborhood of the coexistence equilibrium by considering the divergence of the vector field associated with Eqs. 2.5-2.6. The divergence, defined by $\sum_i \frac{\partial}{\partial p_i}\frac{dp_i}{dt} + \sum_i \frac{\partial}{\partial q_i}\frac{dq_i}{dt}$, measures the outgoing flux around a given point. It can

be shown [see 67, 105] that up to a change in velocity (i.e., rescaling time by a positive factor), the vector field corresponding to any bimatrix game dynamics has zero divergence everywhere in the interior of the positive orthant (i.e., where $p_i, q_i > 0$ for all i).

The divergence theorem [14] equates the integral of the divergence of a vector field over some n-dimensional region to the net flux over the boundary of the region. For a vector field with zero divergence, this implies that every closed surface has zero net flux. As a consequence, such *divergence-free* vector fields cannot have attractors, or subsets of the phase space toward which trajectories of the corresponding dynamical system tend to evolve. If an attractor existed, one could define a surface enclosing it sufficiently tightly, and the net flux over this surface would be negative (as trajectories enter, but do not exit, this region). But this would present a contradiction, and so we conclude that there can be no attractors, such as limit cycles, for the dynamics.

For our model, these facts mean that attractors can only exist on the boundary of the phase space. Because each boundary face for the n-dimensional system is another bimatrix replicator system on $n-2$ dimensions, the same logic applies, and the only possible attractors are points where a single species (and corresponding soil component) is present [105]. States with multiple species present are never attractive. This leaves neutrally-stable oscillations as the only potential form of species coexistence.

2.4.5 Rescaled zero-sum games are neutrally stable

In the context of bimatrix games, a zero-sum game is one where $A = -B^T$. A rescaled zero-sum game is one where there exist constants γ_i, δ_j, and $c > 0$ such that $a_{ij} - \delta_j = -cb_{ji} + \gamma_i$ for all i and j (here, we understand $A = (a_{ij}), B = (b_{ij})$) [105]. Any rescaled zero-sum game can be turned into a zero-sum game by adding constants (in particular, δ_j and $-\gamma_j$) to each column of A and B, and then multiplying B by a positive constant $1/c$. As such, the dynamics of a rescaled zero-sum game and its corresponding zero-sum game are the same

up to a rescaling of time.

If a rescaled zero-sum game has a feasible coexistence equilibrium, this equilibrium is neutrally stable. We can see this by considering the associated community matrix. First, we assume without loss of generality that $A = -cB^T$ (otherwise, we shift columns to obtain this form, without altering the dynamics in the process) Now we add the column-constant matrix $\frac{1}{c}\boldsymbol{b}_n\mathbf{1}^T$ to A and $c\boldsymbol{a}_n\mathbf{1}^T$ to B, where $\boldsymbol{a}_n$ ($\boldsymbol{b}_n$) denotes the nth column of A (B). Again, the dynamics, including both equilibrium values and stability properties, are unchanged by this operation. From Eqs. 2.19-2.22, we see that the community matrix, J, of the resulting system is given by

$$\begin{pmatrix} 0 & D(\boldsymbol{p}^\star)(\bar{A} + \frac{1}{c}\boldsymbol{b}_n\mathbf{1}^T - \mathbf{1}\boldsymbol{a}_n^T) \\ D(\boldsymbol{q}^\star)(\bar{B} + c\boldsymbol{a}_n\mathbf{1}^T - \mathbf{1}\boldsymbol{b}_n^T) & 0 \end{pmatrix} \tag{2.23}$$

where $\bar{A}$ ($\bar{B}$) denotes the $(n-1)\times(n-1)$ submatrix of A (B) obtained by dropping the nth row and column. Finally, we consider the similarity transform $P^{-1}JP$, defined by the change of basis matrix

$$P = \begin{pmatrix} \sqrt{c}D(\boldsymbol{p}^\star)^{1/2} & 0 \\ 0 & D(\boldsymbol{q}^\star)^{1/2} \end{pmatrix}. \tag{2.24}$$

The resulting matrix, J', which shares the same eigenvalues as J [109], is given by

$$\begin{pmatrix} 0 & \sqrt{c}D(\boldsymbol{p}^\star)^{1/2}(\bar{A} + \frac{1}{c}\boldsymbol{b}_n\mathbf{1}^T - \mathbf{1}\boldsymbol{a}_n^T)D(\boldsymbol{q}^\star)^{1/2} \\ \sqrt{c}D(\boldsymbol{q}^\star)^{1/2}(-\bar{A}^T + \boldsymbol{a}_n\mathbf{1}^T - \frac{1}{c}\mathbf{1}\boldsymbol{b}_n^T)D(\boldsymbol{p}^\star)^{1/2} & 0 \end{pmatrix} \tag{2.25}$$

which is a skew-symmetric matrix. Every eigenvalue of a skew-symmetric matrix must have zero real part [109]. Thus, the eigenvalues of J, the community matrix, have zero real part, and the coexistence equilibrium of our original system is neutrally stable.

Here, we have outlined a proof that applies to all rescaled zero-sum games. When B is a diagonal matrix, as in our model of PSFs, the condition for A and B to constitute a rescaled zero-sum game reduces to the condition given in the Main Text.

Rescaled zero-sum games are the only bimatrix games known to produce neutrally stable oscillations. It is a long-standing conjecture that no other bimatrix games have this property [103, 105, 104].

2.4.6 Two-species bimatrix games

For $n > 2$, the rescaled zero-sum game condition is very stringent – it places exacting equality constraints on the elements of A and B. However, for $n = 2$, every bimatrix game satisfies $a_{ij} - \delta_j = -cb_{ji} + \gamma_i$ for some c potentially positive (in which case we have a rescaled zero-sum game) or negative (in which case the game is called a *partnership game*, and the coexistence equilibrium is unstable) [105]. Thus, neutral oscillations arise whenever $c > 0$.

To see that this is true, we first suppose that A and B have the form

$$A = \begin{pmatrix} 0 & a_1 \\ a_2 & 0 \end{pmatrix} \qquad B = \begin{pmatrix} 0 & b_1 \\ b_2 & 0 \end{pmatrix} . \tag{2.26}$$

If this is not the case, we can use constant column shifts to arrive at this form (e.g., in general, $a_1 = a_{12} - a_{22}$). Now consider the constants $c = -\frac{a_1+a_2}{b_1+b_2}$ and $\gamma_1 = -\delta_1 = a_1 + cb_2$ and $\gamma_2 = \delta_2 = 0$. Examining the equation $a_{ij} - \delta_j - \gamma_i = -cb_{ji}$ for each i and j, one verifies

$$\begin{aligned} 0 - \gamma_1 - \delta_1 &= 0 \\ a_1 - \gamma_1 - \delta_2 &= -cb_2 \\ a_2 - \gamma_2 - \delta_1 = -c(b_1 + b_2 - b_2) &= -cb_1 \\ 0 &= 0 \end{aligned} \tag{2.27}$$

and so the parameters A and B always constitute a rescaled zero-sum or partnership game. In the particular case of our model, $a_1+a_2 = -\alpha_{11}+\alpha_{21}+\alpha_{12}-\alpha_{22} = -I_s$ and $b_1+b_2 = -\beta_1-\beta_2$. c is positive (as needed for cycles) when these signs disagree; since $b_1 + b_2 = -\beta_1 - \beta_2$ is always negative, $a_1 + a_2$ must be positive, meaning $I_s < 0$, as found by Bever *et al.* [31].

2.4.7 Constants of motion

When A and B satisfy the rescaled zero-sum game condition, the function

$$H(\boldsymbol{p}, \boldsymbol{q}) = \sum_i p_i^\star \log p_i + c \sum_j q_j^\star \log q_j \tag{2.28}$$

is a constant of motion for the dynamics [105]. As above, we suppose that $A = -cB^T$, and shift the columns of each matrix as needed if this is not the case. Then consider the time derivative

$$
\begin{aligned}
\frac{dH}{dt} &= \sum_i p_i^\star \frac{1}{p_i}\frac{dp_i}{dt} + c\sum_j q_j^\star \frac{1}{q_i}\frac{dq_i}{dt} \\
&= \sum_i p_i^\star \left(\sum_j \alpha_{ij}\, q_j - \sum_{j,k} \alpha_{jk}\, p_j\, q_k \right) + c\sum_j q_j^\star \left(\beta_i\, p_i - \sum_j \beta_j\, p_j\, q_j \right) \\
&= \sum_{i,j} \alpha_{ij}\, p_i^\star\, q_j - \sum_{j,k} \alpha_{jk}\, p_j\, q_k + c\sum_i \beta_i\, q_i^\star\, p_i - c\sum_j \beta_j\, p_j\, q_j \\
&= \sum_{i,j} \alpha_{ij}\, (p_i^\star - p_i)\, q_j + c\sum_i \beta_i\, (q_i^\star - q_i)\, p_i
\end{aligned}
$$

Now, because $A = -cB^T$, we have

$$
\begin{aligned}
&= c\sum_i \beta_i\, (-(p_i^\star - p_i)\, q_i + (q_i^\star - q_i)\, p_i) \\
&= c\sum_i \beta_i\, (-p_i^\star\, q_i + q_i^\star\, p_i)
\end{aligned}
$$

and because $q_i^\star = p_i^\star = \frac{Z}{\beta_i}$, with Z the normalizing constant,

$$
\begin{aligned}
&= c\, Z \sum_i (-q_i + p_i) \\
&= 0
\end{aligned}
\tag{2.29}
$$

In the last line, we use the fact that both sets of frequencies always sum to one.

Each orbit remains in the level set defined by the initial conditions, $(\boldsymbol{p}_0, \boldsymbol{q}_0)$:

$$
H(\boldsymbol{p}_0, \boldsymbol{q}_0) = \sum_i p_i^\star \log p_i + c\sum_j q_j^\star \log q_j \tag{2.30}
$$

For the two-species model studied by Bever *et al.* [31], these level sets precisely define the

trajectories in the (p, q) phase plane.

2.4.8 Equilibrium feasibility

Throughout this study, we focus primarily on the stability properties of the generalized Bever model. However, as mentioned above, coexistence also requires the existence of a feasible equilibrium – that is, an equilibrium where all frequencies are nonnegative. In the context of this model, feasibility is determined solely by the matrix A. If all elements of $A^{-1}\mathbf{1}$ share the same sign, the coexistence equilibrium is feasible. For even moderately large n, feasibility of the coexistence equilibrium is very unlikely if the parameters α_{ij} are iid random variables. However, the probability of feasibility has little bearing on the prospects for coexistence in this model. Even assuming the existence of a feasible equilibrium, our results show that robust coexistence of more than two species is impossible. To confirm that this is the case, we repeat the simulations shown in Fig. 2.2 (Main Text), but now rejecting parameter combinations that do not yield a feasible coexistence equilibrium. The results are show in Fig. 2.4. Conditioning on feasibility increases the probability that randomly parameterized two-species communities oscillate neutrally from $\frac{1}{4}$ to $\frac{1}{2}$, but has little effect on the results observed for $n > 3$. In particular, coexistence of more than two species is never observed, regardless of feasibility.

It is interesting to note that the rescaled zero-sum game condition, which ensures neutral stability of a fixed point, also ensures feasibility. This is easy to verify using the transformation explained in the section *Rescaled zero-sum games are neutrally stable*, above. Using column shifts applied to A and B, one obtains a new system where both matrices are diagonal with constant signs. In other words, one finds a system of the form $A = -cB^T$ with the same dynamics (and so the same equilibria) as the original. Because B is a diagonal matrix, and we assume $\beta_i > 0$ for all i, both $\boldsymbol{p}^\star$ and $\boldsymbol{q}^\star$ will be feasible. However, we note that this property does not alter any of the conclusions of the Main Text. While the rescaled

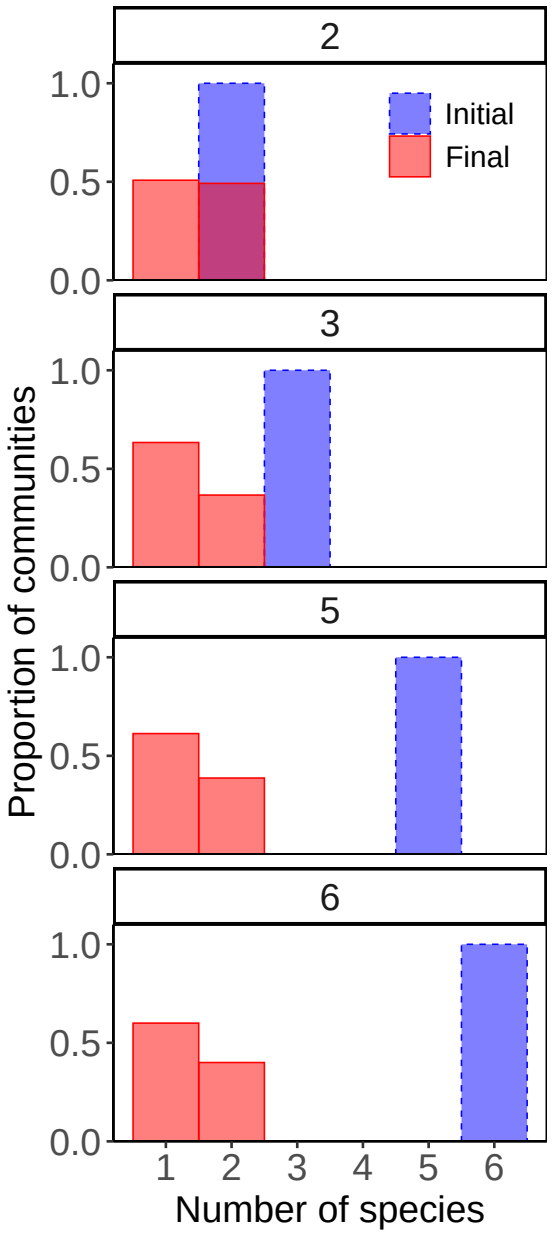

Figure 2.4: Final community sizes with varying initial richness, conditioned on feasible coexistence equilibrium. As in Fig. 2.2 (Main Text), except that parameter combinations yielding unfeasible equilibria were discarded. We continued sampling until 5000 feasible parameter sets were obtained for each level of initial richness. Conditioning on feasibility increases the probability that an initial community of two species coexists in a neutral cycle, but has negligible effect on the results for richer communities. In particular, coexistence of more than two species is never observed.

zero-sum game condition guarantees a weak form of coexistence (i.e. the existince of neutral oscillations), this behavior is extremely fragile; small changes in the model parameters will cause all but two species to go extinct.

2.4.9 Varying relative timescales

To clearly demonstrate that varying the relative timescales of plant and soil dynamics does not affect the qualitative character of the dynamics, we include two representative simulations below (Figs. 2.5 and 2.6).

In each case, we sampled model parameters uniformly at random and then simulated the dynamics starting with identical initial conditions but with soil parameters given by $\epsilon\boldsymbol{\beta}$ for different values of ϵ. As ϵ becomes large, the dynamics of soil components become rapid relative to the dynamics of plants. We show that varying these timescales across two orders of magnitude has no qualitative effect on the dynamics – an unstable equilibrium remains unstable (Fig. 2.5) and a neutrally stable equilibrium remains neutrally stable (Fig. 2.6).

2.4.10 Adding frequency dependence

To illustrate the robustness of our main findings, we consider an extension of the Bever model to include direct intraspecific plant competition. Building on Eq. 2.9, we add a negative frequency-dependent term for each plant species:

$$\frac{dx_i}{dt} = x_i \left(\sum_j \alpha_{ij} q_j - c_i p_i \right) \tag{2.31}$$

Here, c_i specifies the strength of intraspecific competition. Soil dynamics remain exactly as in Eq. 2.9.

This model is conceptually close to the combined plant competition-feedback model in-

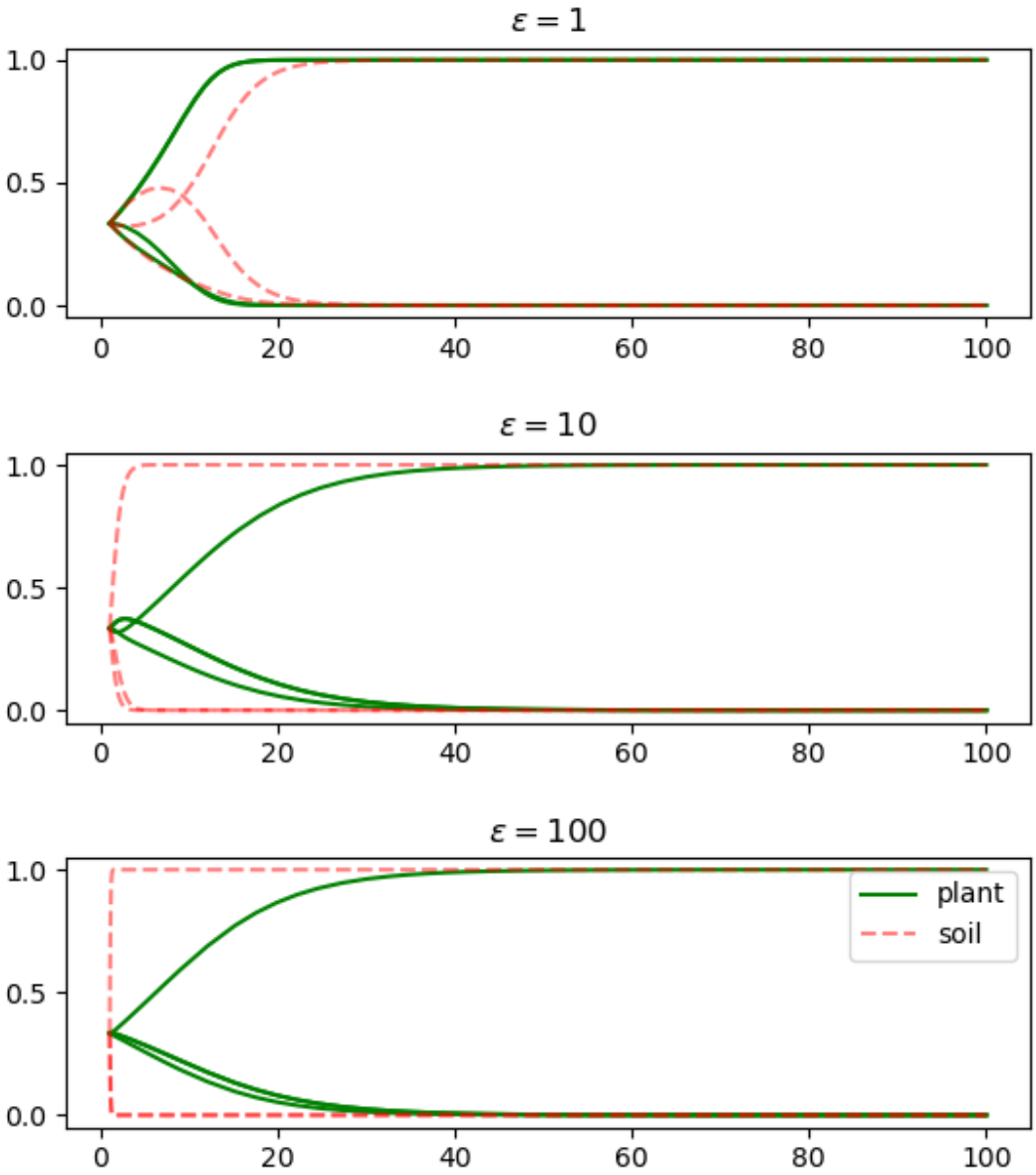

Figure 2.5: See text for simulation details. Time is shown on the x-axis, and frequencies are shown on the y-axis. Here, $n = 3$ (species identities are unlabeled). As ϵ varies across two orders of magnitude, the qualitative outcome of the dynamics is unchanged: One species excludes the other two. Only the rate of exclusion changes.

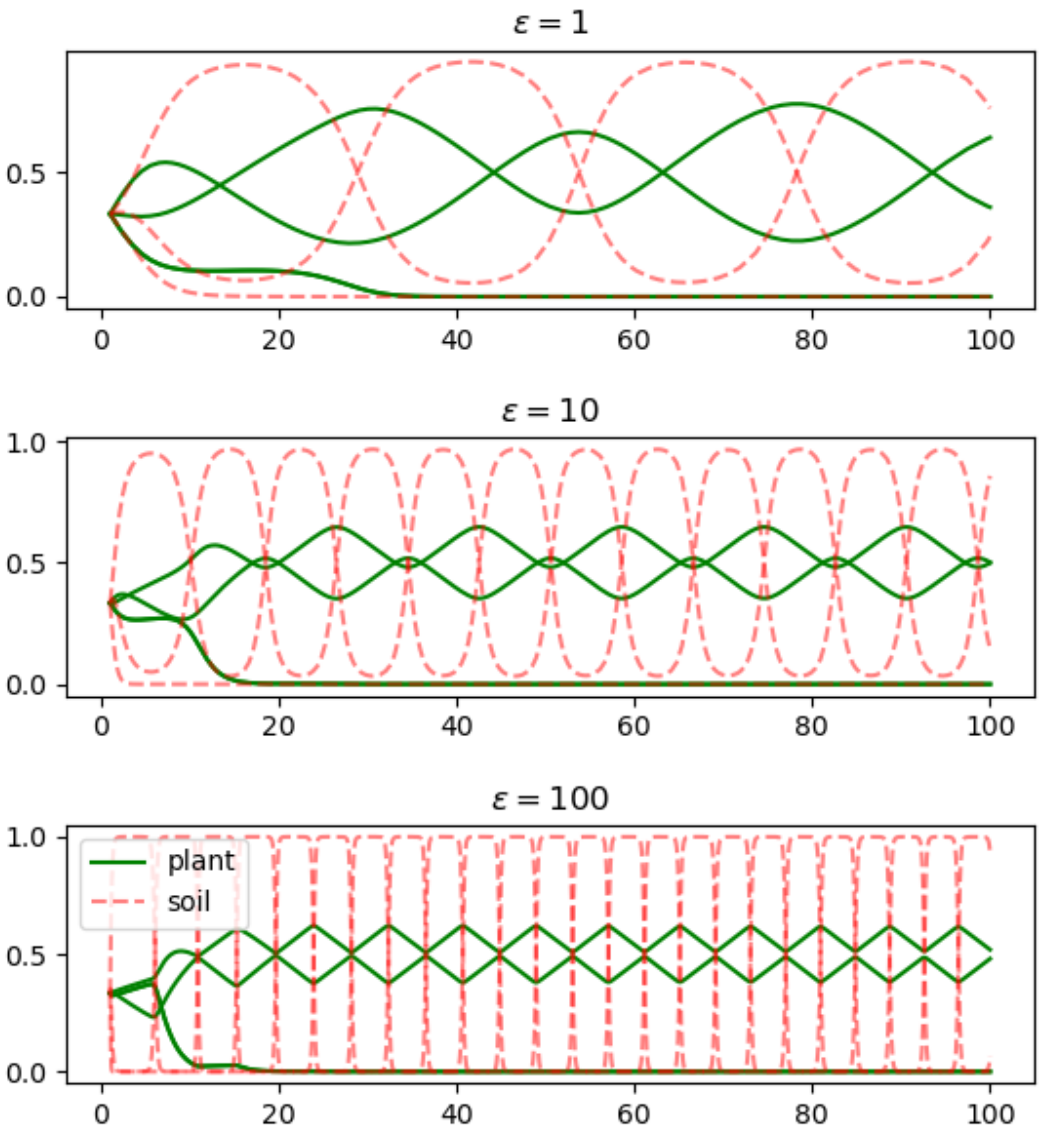

Figure 2.6: See text for simulation details. Time is shown on the x-axis, and frequencies are shown on the y-axis. Here, $n = 3$ (species identities are unlabeled). As ϵ varies across two orders of magnitude, the qualitative outcome of the dynamics is unchanged: One species is excluded and the two surviving species oscillate neutrally. The frequency and amplitude of the oscillations change with ϵ, but we note that these properties will also depend on rate at which the third species is excluded.

troduced by Bever [28]. Unlike Bever, we consider only intraspecific plant interactions for simplicity. Additionally, while Bever took plant-plant interactions to be density-dependent, as in the Lotka-Volterra competition model, we assume frequency-dependent effects. As explained in the Main Text, this choice is motivated by consistency with the frequency-dependent nature of PSFs in this model.

The frequency dynamics associated with this model are given by

$$\begin{cases} \frac{dp_i}{dt} & = p_i \left(\sum_j \alpha_{ij}\, q_j - c_i\, p_i - \sum_j p_j (\sum_k \alpha_{jk}\, q_k - c_j\, p_j) \right) , \quad i = 1, \dots n \\ \frac{dq_i}{dt} & = q_i \left(\beta_i\, p_i - \sum_j \beta_j\, p_j\, q_j \right) . \end{cases} \tag{2.32}$$

To consider small deviations from the canonical Bever model, we focus on the case where the negative frequency-dependence is weak relative to PSFs (i.e. c_i parameters are much smaller than α_{ij} parameters). At the opposite extreme ($c_i \gg \alpha_{ij}$), it is easy to see that all plant species will coexist, with no meaningful role for PSFs. We also assume that frequency-dependence is equal for all plant species (i.e. $c_i = c$), for simplicity.

Now we study the stability properties of equilibria in this extended model. After some algebraic manipulations to remove the zero-sum constraints (as in the section *Local stability analysis*), we find that the community matrix for the coexistence equilibrium takes the form

$$J' = \begin{pmatrix} -cI & M_1 \\ M_2 & 0 \end{pmatrix} \tag{2.33}$$

where

$$J = \begin{pmatrix} 0 & M_1 \\ M_2 & 0 \end{pmatrix} \tag{2.34}$$

is the community matrix for the corresponding Bever model (i.e. the model with $c = 0$). We have already shown that the eigenvalues of J must be of mixed signs or all purely imaginary.

Let us denote those eigenvalues by λ_i. The eigenvalues of our extended matrix, which we call λ_i', can be related to the λ_i in a straightforward way. We first notice that the eigenvectors of J' are closely related to the eigenvectors of J, which we write as $(\boldsymbol{u}_i, \boldsymbol{v}_i)^T$. The eigenvector equations for J' take the form

$$\begin{pmatrix} -cI & M_1 \\ M_2 & 0 \end{pmatrix} \begin{pmatrix} \boldsymbol{u}_i \\ k_i \boldsymbol{v}_i \end{pmatrix} = \lambda_i' \begin{pmatrix} \boldsymbol{u}_i \\ k_i \boldsymbol{v}_i \end{pmatrix} \tag{2.35}$$

with k_i an undetermined constant. This system implies the relations $k_i\, \lambda_i' = \lambda_i$ and $\frac{\lambda_i'+c}{k_i} = \lambda_i$. Solving these equations for λ_i' gives

$$\lambda_i' = \frac{-c \pm \sqrt{c^2 + 4\lambda_i^2}}{2} \tag{2.36}$$

and finally, for small c, the approximation

$$\lambda_i' \approx \lambda_i - \frac{c}{2}\,. \tag{2.37}$$

This analysis shows that there is a tight relationship between the stability properties of the Bever model and the extension with weak frequency-dependent self-regulation. If the underlying Bever model has an unstable coexistence equilibrium, where the eigenvalues λ_i have mixed signs, then the extended model will have an unstable equilibrium as well. The slight shift by $\frac{c}{2}$ is not enough to push the positive real parts of these eigenvalues across zero, by assumption. The correspondence when all of the λ_i are purely imaginary is more interesting. In this case, the eigenvalues of the extended model, λ_i', will all have a small negative real part. This shift induces a qualitative change in the model dynamics: a neutrally stable equilibrium in the underlying Bever model becomes an asymptotically stable equilibrium in the model with frequency-dependence. Each of these cases is illustrated in Fig. 2.7.

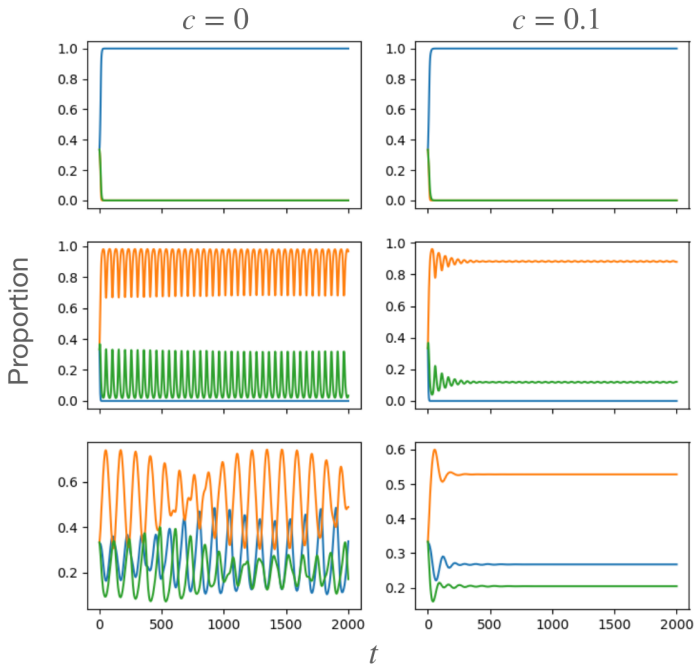

Figure 2.7: Representative dynamics for the extended Bever model with negative plant frequency-dependence. When the Bever model (left column) possess an unstable coexistence equilibrium, so will the extended model (right) with weak self-regulation (top row). On the other hand, when the Bever model possesses a neutrally stable equilibrium, the extended model will have a corresponding *stable* equilibrium, with the same number of species. We show an example where one of three species goes extinct and the other two cycle in Bever model, or stably coexist in the extended model (middle row). We also see that when the Bever model possess an n-species cycle (here $n = 3$), the extended model will have a stable equilibrium with all n species. Such cases are only possible when the matrices A and B satisfy the rescaled zero-sum game condition, described in the Main Text and above.

Very weak frequency-dependence can only produce such a qualitative change when the underlying model is structurally unstable – i.e. when the real parts of the λ_i are exactly zero. We have shown that this is only the case when the Bever model parameters meet the rescaled zero-sum game condition. Thus, even though the extended model can support stable coexistence, this outcome is subject to the same stringent conditions as are n-species oscillations in the Bever model. In particular, these parameterizations are never realized at random, and are not robust to small perturbations of the parameters.

This simple example demonstrates that the lack of robust n-species coexistence in the Bever model can be disentangled from the biologically unrealistic prediction of neutral oscillations. The generic behavior of the Bever model with more than two plant species is instability, and other ecological processes must be sufficiently strong to overcome this instability; very small modifications of the dynamics will not do.

2.4.11 Numerical simulations

To complement our analytical findings, we investigated the dynamics of many randomly parameterized communities using numerical simulations. In particular, we integrated Eq. 2.12 with 2, 3, 5, or 6 initial plant species and corresponding soil components (see Figs. 2.2 and 2.4). For each case, we sampled 5000 parameter sets at random and integrated the dynamics in Python using SciPy's (version 1.7.1) solve_ivp function with the "BDF" method. We sampled non-singular payoff matrices A and B with each non-zero element drawn independently from the uniform distribution U(0, 1). For every choice of parameters, we integrated the system until a subset with ≤ 2 species was reached (which occurred in all cases). Code for reproducing all numerical simulations is available at `https://github.com/pablolich/plant_soil_feedback`.

CHAPTER 3

HABITAT HETEROGENEITY, ENVIRONMENTAL FEEDBACKS, AND SPECIES COEXISTENCE ACROSS TIMESCALES

3.1 Introduction

Environmental heterogeneity provides the raw material for niche partitioning in ecological communities. When the environment varies from place to place, differences in the ways species respond to local conditions can facilitate their coexistence at the landscape scale, even when local coexistence is impossible [47, 7]. This connection between environmental heterogeneity and the maintenance of species diversity has deep roots in ecology [12, 151, 256], and has been well-studied both theoretically [108, 48, 116, 47] and empirically [209, 219, 51, 177].

However, this picture becomes more complex when species themselves shape their environment. Feedbacks between the biotic community and landscape conditions across space can enhance or reduce environmental heterogeneity over time [57, 260, 181]. Prominent examples include plant-soil feedbacks [31, 155, 250] and related Janzen-Connell effects [118, 54], wherein plants directly or indirectly shape the local densities of soil microbes or natural enemies such as seed predators, generating a dynamic landscape of legacy effects. These processes are thought to play an important role in maintaining the diversity of many natural plant communities, but they may also lead to positive feedbacks that drive monodominance [258, 250].

Here, we introduce a flexible modeling framework for community dynamics in heterogeneous landscapes with and without feedbacks that change environmental conditions through time. We build on the classical metapopulation paradigm [144] and related patch models, which provide a minimalist approach to studying ecosystems with distinct local and

global scales [48, 116, 7]. The simplicity of this framework allows us to capture and analyze essential features of complex environmental feedbacks. While a range of conceptual and quantitative models [203, 31, 86, 111, 197, 170] have shed light on such processes – and particularly on when they might help or hinder coexistence – they remain challenging to incorporate in tractable mathematical frameworks. One central obstacle is the high species diversity in many natural systems, although accounting for this diversity is crucial to understanding real-world coexistence [167]. Additionally, many studies – and even sub-fields of ecology – focus on a single source of heterogeneity, making it hard to draw general conclusions that cut across system specifics. In particular, fixed or "exogenous" heterogeneity and biotically-generated or "endogenous" heterogeneity have often been approached from very different perspectives [32, 223]. Our models and analysis help overcome these challenges by providing coexistence criteria that extend naturally to communities of arbitrary size, and by building endogenous environmental feedbacks directly into a core model for landscapes with exogenous heterogeneity.

We develop a general approach that is agnostic to the specific sources of environmental heterogeneity and allows us to consider feedbacks on a wide range of timescales. We show that our framework includes a recent model for rapid habitat modification [164] as a limiting case. To delineate the full spectrum of possible dynamics, we focus especially on the the opposite extreme of feedbacks that shape the landscape over very long times. In doing so, we identify essential features of coexistence maintained by exogenous and endogenous heterogeneity. Across the two extremes of very fast and very slow feedbacks, coexistence maintained by endogenous heterogeneity can be characterized by the same simple analytical conditions. Over long times, these limiting cases behave similarly to one another, and qualitatively differently from systems with exogenous heterogeneity, even though slow feedbacks are difficult to distinguish from exogenous heterogeneity on short timescales. Our results help explain how environmental feedbacks emerge and play out over different timescales,

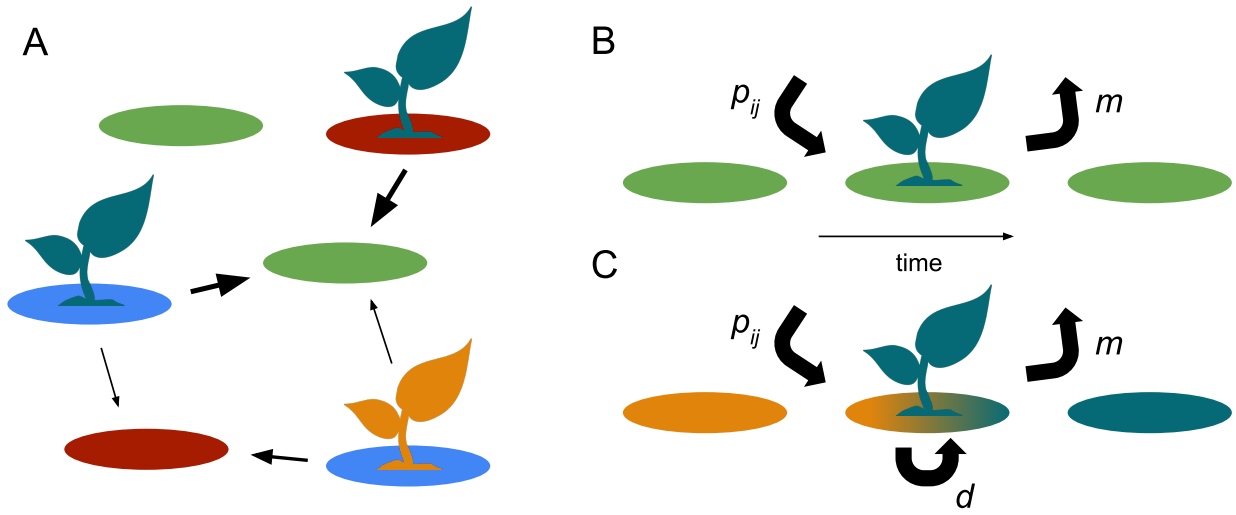

Figure 3.1: Metapopulation models with exogenous and endogenous patch heterogeneity. (A) We model an ecosystem where species disperse between patches with varying local conditions. The environmental conditions within a patch, summarized by the patch type or state, influence the rates at which different species can colonize and establish. We consider models where variation in patch conditions is (B) a fixed property of the landscape (Eq. 3.2), or (C) shaped by the biotic community over time (Eq. 3.5). Here, colors indicate patch types/states and species identities. When heterogeneity is endogenous (C) each patch state is identified with a species in the community, reflecting environmental modifications (occurring at a rate d) due to that species' presence.

and the modeling framework we introduce offers a platform for comparing exogenous and endogenous heterogeneity on equal footing. Finally, we discuss how and under what conditions our models can be parameterized from observational data, and other implications for the analysis of community dynamics in natural communities.

3.2 Exogenous heterogeneity

We consider a landscape composed of many local patches, which can be classified into ℓ discrete types. The type of a patch summarizes its internal conditions as they are relevant to a focal community of n species inhabiting the landscape. For example, in the context of a plant community, patches might be classified by soil type or topography. The rate at which each species can establish in a patch depends on the patch type, and may differ between

species, reflecting interspecific differences in niche requirements. Following conventional models, we assume there is global dispersal between all patches, and that each patch can be occupied by at most a single species at any time. Denoting the proportion of all patches that are of type j and occupied by species i at time t by $X_{ij}(t)$, and the proportion of all patches that are of type j and vacant by $y_j(t)$, we can model the dynamics of these proportions across a sufficiently large landscape by:

$$\begin{aligned} \frac{dX_{ij}(t)}{dt} &= -m_{ij}X_{ij}(t) + p_{ij}y_j(t)\sum_{k=1}^{\ell} X_{ik}(t) \\ \frac{dy_j(t)}{dt} &= \sum_{i=1}^{n} m_{ij}X_{ij}(t) - y_j(t)\sum_{i=1}^{n} p_{ij}\sum_{k=1}^{\ell} X_{ik}(t) \end{aligned} \tag{3.1}$$

The parameters $p_{ij} \geq 0$ and $m_{ij} > 0$ specify the rates at which species i establishes or goes locally extinct in patches of type j, respectively. As in classic metapopulation models, the dynamics represent the net action of these two processes: colonization of empty patches by propagules or dispersers from occupied patches, and local extinctions at a constant rate per patch. The summations over patch type (index k) reflect the fact that empty patches of type j may be colonized by propagules of species i dispersed from patches of any type. Summations over species identity (index i) reflect the fact that the type is a fixed property of each patch, so a patch of type j always returns to the y_j class when vacated. This also implies that the total proportion of patches of type j, which we denote by $w_j = y_j(t) + \sum_i X_{ij}(t)$, is constant through time for every j.

In principle, we can allow local extinction rates to depend on both species identity and patch type; however, in this study we focus primarily on the simplest case where $m_{ij} = m$. Thus, the effects of landscape heterogeneity are realized through rates of establishment, not local persistence. The suitability of this assumption will depend on the community of interest, but environmental heterogeneity is thought to act more strongly on establishment than

persistence in many relevant systems, typically because smaller populations or immature individuals are more sensitive to patch conditions [84, 132, 153, 17]. We are also assuming that there are no significant differences in local extinction rates between species, reflecting a community of demographically similar species, or a community where patch extinctions are primarily driven by external disturbance.

Under this equal m assumption, we can greatly simplify the dynamics by tracking only the proportion of patches – regardless of type – occupied by species i at time t. We denote these proportions by $x_i = \sum_j X_{ij}$. Instead of $\ell(n+1)$ equations, there are now $n+\ell$, given by:

$$\begin{aligned} \frac{dx_i(t)}{dt} &= -mx_i(t) + x_i(t)\sum_{j=1}^{\ell} p_{ij}y_j(t) \\ \frac{dy_j(t)}{dt} &= m\big(w_j - y_j(t)\big) - y_j(t)\sum_{i=1}^{n} p_{ij}x_i(t)\,. \end{aligned} \tag{3.2}$$

The w_j, which must sum to one, are now seen as parameters that describe the heterogeneity of the landscape.

These dynamics take precisely the same mathematical form as a consumer-resource model with external inflow of abiotic resources [243, 40, 157]. In this parallel, each species plays the role of a consumer, and each patch type is interpreted as a resource with inflow rate proportional to w_j. Both "consumers" and "resources" experience density-independent mortality at a rate m, and p_{ij} are analogous to consumption rates.

Consumer-resource systems of the form in Eq. 3.2 have been studied extensively, allowing us to immediately draw conclusions about multispecies dynamics in heterogeneous metapopulations by translating results from the consumer-resource setting. For example, it is well-known that the number of coexisting consumers is at most equal to the number of resources in such models, a classic result known as the competitive exclusion principle

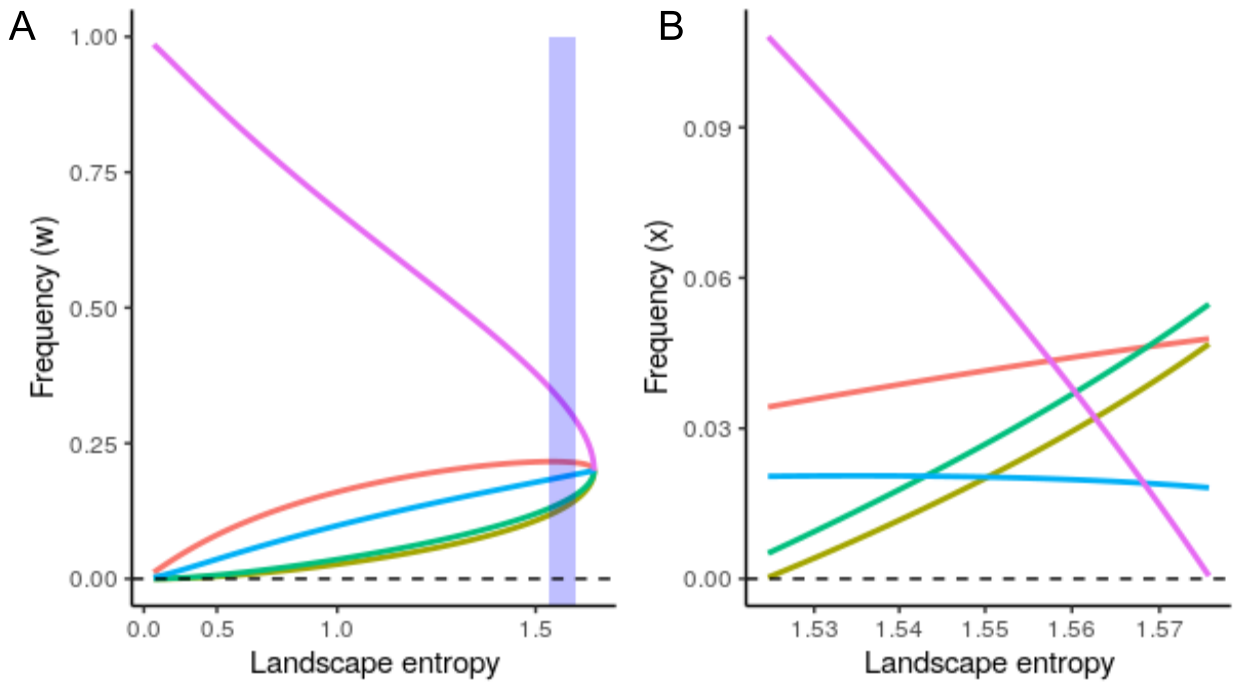

Figure 3.2: We illustrate the relationship between landscape parameters (A) and species' equilibrium frequencies (B) using a simulated community of habitat specialists. We sampled P such that each species had a strong advantage colonizing a distinct patch type, and $p_{ij} < m$ for non-preferred patches (parameters available at [166]). We then calculated species' frequencies ($\boldsymbol{x}^\star$) for landscapes ($\boldsymbol{w}$) ranging from a uniform environment dominated by one patch type, to equal frequency of all types. The full gradient of $\boldsymbol{w}$ parameters is shown in (A); the five species community is only feasible for a small subset (blue shading). In (B), we show species' frequencies, as a function of landscape diversity (measured in Shannon entropy), for the feasible range. Species' frequencies are not straightforwardly related to the availability of their preferred habitat types (indicated by matching colors), and species go extinct as $\boldsymbol{w}$ varies, even though all patch types are present. Surprisingly, even increasing the diversity (evenness) of the landscape drives some species extinct. To generate a gradient of $\boldsymbol{w}$, we selected parameters $\boldsymbol{v}$ compatible with feasibility and let $w_i = v_i^p / \sum_j v_j^p$ varying p from 0 to 10.

[141]. Our model equivalence provides a formal demonstration that this intuitive principle carries over to the context of environmental heterogeneity. Given this upper limit, we study coexistence assuming $\ell = n$, representing a fully "packed" consumer community. In this case, Eq. 3.2 has at most a single *coexistence equilibrium*, which is easily expressed in matrix form:

$$\begin{aligned} \boldsymbol{y}^\star &= m\, P^{-1}\mathbf{1} \\ \boldsymbol{x}^\star &= m\left(P^T\right)^{-1}\left(D(\boldsymbol{y}^\star)^{-1}\boldsymbol{w} - \mathbf{1}\right). \end{aligned} \tag{3.3}$$

Here we use the notation $\boldsymbol{y}^\star$ for the vector of equilibrium proportions (and similarly for $\boldsymbol{x}^\star$ and $\boldsymbol{w}$), and we collect the coefficients p_{ij} in the matrix P. We also use $D(\boldsymbol{y}^\star)$ for the diagonal matrix with non-zero elements given by $\boldsymbol{y}^\star$, and $\mathbf{1}$ for a vector of n ones.

Many important properties of this equilibrium are known. Coexistence of all n species requires that the equilibrium is biologically feasible, meaning that the components of $\boldsymbol{y}^\star$ and $\boldsymbol{x}^\star$ are all positive. In fact, it can be proven that this equilibrium is globally stable whenever it is feasible, and therefore coexistence is entirely controlled by feasibility in this model (see, e.g., [157]; for completeness, we provide a proof of this result in Supporting Information 3.6.1).

In accordance with the fact that $\boldsymbol{x}$ and $\boldsymbol{y}$ are proportions in our original framing of the model, we find that feasibility of $\boldsymbol{x}^\star$ requires $\sum_j y_j^\star < 1$. This means that there is an upper limit on m imposed by the matrix of establishment rates: $m < \mathbf{1}^T(P^{-1})\mathbf{1}$. Remarkably, the vacant patch equilibrium values, $\boldsymbol{y}^\star$, are completely unaffected by the underlying distribution of patch types in the environment, $\boldsymbol{w}$. As in consumer-resource models, this "shielded" behavior arises because the species in the system robustly drive the supply of vacant patches to a point determined only by their own demographic rates [241]. Feasibility of these values requires that every element of $P^{-1}\mathbf{1}$ is positive. Loosely, in ecological terms this expresses a

requirement that species are sufficiently similar in overall colonization ability (i.e., p_{ij} averaged across patch types), or sufficiently specialized on distinct habitat types (see Supporting Information 3.6.1 for detailed interpretation of this condition).

The equilibrium proportions for species themselves *are* sensitive to $\boldsymbol{w}$, but indirectly. Even if each species is specialized on a different patch type, the $\boldsymbol{x}^\star$ and $\boldsymbol{w}$ are not simply proportional, unless the species are all perfect specialists [241]. For example, in Fig. 3.2, we illustrate a scenario where each species is sufficiently specialized so that all non-preferred patches are net sinks (i.e., $p_{ij} < m$ for all $i \neq j$). Changing the distribution of patch types in the landscape can cause some species to go extinct, even though patches of all types remain available. Counterintuitively, this means that increasing the diversity (evenness) of habitat types will often, and sometimes drastically, decrease the species diversity of the system.

This kind of strong competitive interference can occur because the joint distribution of species and patch types reflects not just habitat preference, but also source-sink dynamics between patches. The potential for such dynamics in heterogeneous landscapes has long been noted [108, 106, 218]. In our model, we can examine this joint distribution more closely by returning to the "full" dynamics in Eq. 3.1. The hierarchical structure of Eqs. 3.1 and 3.2 immediately implies that each X_{ij} reaches a stable equilibrium value

$$X_{ij}^\star = \frac{1}{m}\, p_{ij}\, x_i^\star\, y_j^\star\,. \tag{3.4}$$

Here, and in Fig. 3.3, we see clearly that the net pattern of patch occupancy in an equilibrial landscape is shaped by the particular rates at which a focal species i can colonize and establish in patches of type j (p_{ij}), as well as the overall abundance of i and availability of j in the system ($x_i^\star y_j^\star$). These two factors can be identified with "species sorting" and "mass effects" processes, respectively, which are usually viewed as two ends of a continuum for metacommunity dynamics [139, 217]. While many studies of metacommunities focus on determining the importance of one or the other process in a particular community, our model

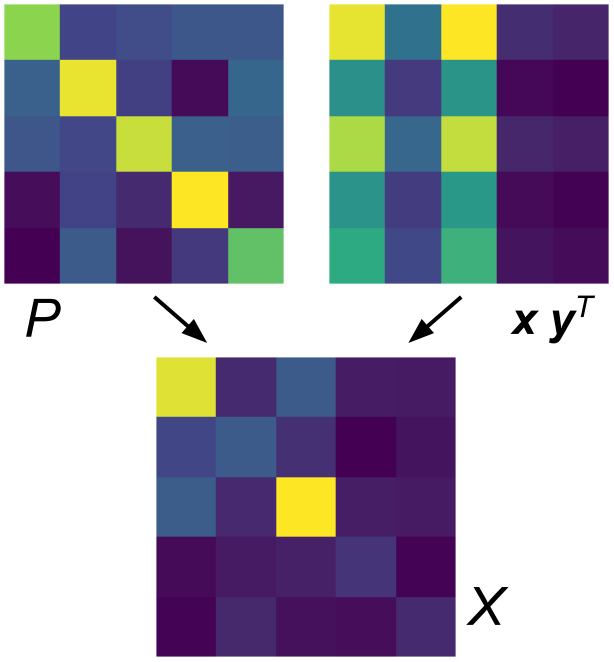

Figure 3.3: Pattern of habitat association reflects combination of species sorting and mass effects. The joint distribution of species and patch types at equilibrium, $X^{\star}_{ij}$ (Eq. 3.4), at bottom, is shaped by the matrix of colonization and establishment rates P (left) and the overall abundance of species and vacant patch types in the ecosystem $\boldsymbol{xy}^T$ (right). The left pattern sets an expectation based on species' habitat preferences (in this example, strong specialization on distinct patch types), while the right pattern shows the expected distribution if patches were homogeneous. The actual pattern of habitat association is the element-wise product of the two. Here each matrix is normalized so that the elements sum to one. Higher values are indicated by light colors (yellow), and low values by dark colors (blue).

quantitively predicts how the two should act together to shape observed patterns of habitat association.

3.3 Endogenous heterogeneity

Next, we consider how community dynamics change when patch heterogeneity is no longer a static feature of the environment, but an outcome of biotic feedbacks. For simplicity and for compatibility with the framework developed for exogeneous heterogeneity, we maintain the assumption that patches can be classified into distinct types, although now we speak of

patch *states*, since these attributes change through time. Each patch state is associated with a distinct species, reflecting the impacts of that species on local environmental conditions. For example, we might consider distinct soil microbial communities associated with particular host plants [27, 210, 191], immune statuses corresponding to recent infection history in vertebrate hosts [133], substrate morphologies shaped by benthic "ecosystem engineers" [145, 88], or chemical concentrations maintained by different bacterial strains [196, 9]. Thus, the number of species and patch states are both n, and we assume these are labelled so that state i corresponds to legacy effects of species i. As before, patch states affect the dynamics by governing the rate of colonization and establishment by each species in the community.

We approximate changes in local environmental conditions as discrete shifts between patch states. In a patch occupied for some time by species i, we assume that the local population of species i can drive a transition from the current patch state to state i at some rate d. In principle, this rate might depend on both the current patch type and the identity of the occupant species, but we focus on the case where d is constant. This scenario naturally describes systems where some external disturbance, occurring at a constant rate across the landscape, is needed to shift patches between alternative states, or where species all species modify their environment at roughly equal rates.

With biotic feedbacks operating, the distribution of patch states in the landscape, $\boldsymbol{w}$, is now a dynamic variable. But given a particular distribution of patch states $\boldsymbol{w}(t)$ at time t, we assume the instantaneous dynamics of colonization and extinction are exactly the same as in Eq. 3.1. This leads to the following model for a community with endogeneous heterogeneity:

$$\begin{aligned}
\frac{dx_i(t)}{dt} &= -mx_i(t) + x_i(t)\sum_{j=1}^{n} p_{ij}y_j(t) \\
\frac{dy_j(t)}{dt} &= m\big(w_j(t) - y_j(t)\big) - y_j(t)\sum_{i=1}^{n} p_{ij}x_i(t) \\
\frac{dw_k(t)}{dt} &= d\big(x_k(t) + y_k(t) - w_k(t)\big)
\end{aligned} \tag{3.5}$$

Intuitively, the total proportion of patches in state k increases when the number of patches occupied by species k, regardless of state, exceeds the total number of occupied patches in state k, regardless of occupant (given by $w_k(t) - y_k(t)$; see Supporting Information 3.6.2 for a detailed derivation of Eq. 3.5).

The dynamics of Eq. 3.5 can be much more complex than Eq. 3.2 – potentially including non-equilibrium coexistence or multistability – making it difficult to fully characterize the behavior of this model. To make progress, we first consider two limiting cases where patch dynamics and underlying landscape dynamics operate on very different timescales, permitting a natural simplification of the model via fast-slow decomposition [240, 179].

In the first case, all species modify their local environment extremely rapidly. Consequently, the state of a vacant patch will invariably reflect the identity of the most recent resident species. Formally, this scenario represents the limit where $d \to \infty$, and we can apply a fast-slow decomposition. Treating $\boldsymbol{x}(t)$ and $\boldsymbol{y}(t)$ as fixed, because these variables change slowly compared to the patch states, $\boldsymbol{w}(t)$, the $\frac{d\boldsymbol{w}(t)}{dt}$ become a set of n decoupled differential equations, each with a stable equilibrium where $w_k(x_k(t), y_k(t)) = x_k(t) + y_k(t)$. We take $\boldsymbol{w}$ to be at this equilibrium at all times and substitute in the dynamics for $\boldsymbol{y}(t)$ to produce the *slow system*:

$$\begin{aligned}\frac{dx_i(t)}{dt} &= -mx_i(t) + x_i(t)\sum_{j=1}^{n} p_{ij}y_j(t) \\ \frac{dy_j(t)}{dt} &= mx_j(t) - y_j(t)\sum_{i=1}^{n} p_{ij}x_i(t)\end{aligned} \tag{3.6}$$

In fact, this system is precisely the model we have studied previously [164].

At the opposite extreme, patches change state very slowly (that is, rarely). This limit corresponds to a system where patches resist modification – for example, where patch states are alternative stable states [189, 9] – but species occasionally drive patches from one state to another. Again, we consider a fast-slow decomposition, now with $d \to 0$. Taking $\boldsymbol{w}(t)$ as fixed over short timescales, we obtain a *fast system* that is identical to Eq. 3.2. Provided the equilibrium (Eq. 3.3) for this system is feasible, we have seen that it is globally stable, so we take $\boldsymbol{x}(t)$ and $\boldsymbol{y}(t)$ to be at this equilibrium (as a function of $\boldsymbol{w}(t)$) at all times. Then we find the slow system for the gradual evolution of patch states:

$$\frac{1}{d}\frac{d\boldsymbol{w}(t)}{dt} = \left(\left(D(P^{-1}\mathbf{1})P^T\right)^{-1} - I\right)\boldsymbol{w}(t) + m\left(P^{-1}\right)_A\mathbf{1} \tag{3.7}$$

Here I is the identity matrix of size n and S_A denotes the anti-symmetric part of a matrix, $S_A = S - S^T$. This system is a matrix differential equation, which is very amenable to analysis. In Supporting Information 3.6.2, we prove that Eq. 3.7 has a unique equilibrium solution, $\boldsymbol{w}^\star$, which is always feasible if $\boldsymbol{y}^\star = mP^{-1}\mathbf{1}$ is feasible, and which guarantees the feasibility of $\boldsymbol{x}^\star$. This equilibrium may be stable or unstable, depending on the structure of the colonization rate matrix P. We derive a simple graphical condition that characterizes the stability of Eq. 3.7 in terms of the eigenvalues of $PD(P^{-1}\mathbf{1})$, which is a weighted version of P reflecting the distribution of vacant patch states at equilibrium (see Fig. S1). This normalization by $P^{-1}\mathbf{1}$ removes any effect of the overall quality of different habitat types.

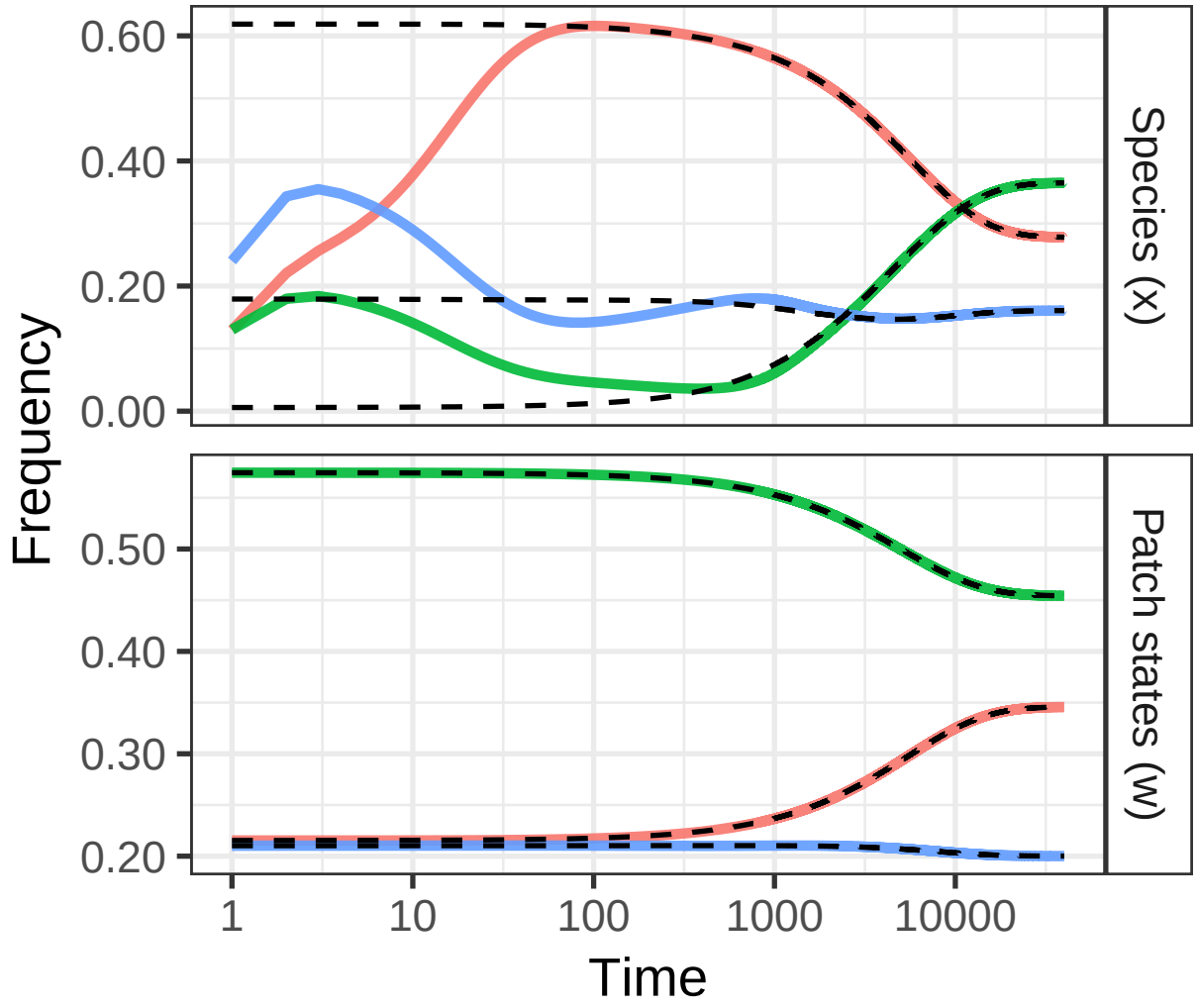

Figure 3.4: Stable feedback dynamics converge to fast-slow limit. Here we show the evolution of species frequencies (top) and the distribution of patch states (bottom) over time when feedbacks are slow. Colored lines indicate the solution obtained by numerically integrating Eq. 3.5 with $d = 10^{-5}$. Dashed lines show the predicted dynamics using the fast-slow decomposition. The predictions for patch states were obtained by solving the slow system (Eq. 3.7), and the predictions for species' frequencies were calculated from the predicted $\boldsymbol{w}(t)$ using Eq. 3.3 at each time point. The dynamics rapidly collapse to the slow manifold derived analytically. In these simulations, $m = 0.1$ and the elements of P were sampled symmetrically *iid* from the standard uniform distribution until a feasible and stable parameter set was found (parameters available at [166]). Note that time is shown on a log scale, to highlight dynamics on long and short timescales.

In the special case where P is symmetric (i.e., $p_{ij} = p_{ji}$), the analysis and interpretation of the model become even simpler. This kind of symmetry may arise naturally (at least approximately) in systems where the effect of one species' habitat modifications on another species' establishment rate depends on some measure of similarity between them. For example, the degree of "spillover" of Janzen-Connell effects between two tropical tree species is a function of their phylogenetic relatedness [75]. In this symmetric case, $\boldsymbol{x}^\star$, $\boldsymbol{y}^\star$, and $\boldsymbol{w}^\star$ all become proportional to $P^{-1}\mathbf{1}$. This equilibrium is stable if and only if P has exactly one positive eigenvalue. We prove this result in Supporting Information 3.6.2 and also show that this characterization of stability extends somewhat beyond the context of strict symmetry. For arbitrary P, if exactly one eigenvalue of $PD(P^{-1}\mathbf{1})$ lies in the right half of the complex plane, then the coexistence equilibrium is stable (although this condition is only *necessary* for stability if P is symmetric).

Precisely the same stability condition characterizes the dynamics of Eq. 3.6 when P is symmetric. Miller and Allesina [164] showed that P having exactly one positive eigenvalue can be interpreted as a quantitative generalization of the notion that each species must modify the environment in a way that disadvantages itself in order to generate negative frequency-dependent feedbacks that maintain diversity. The appearance of this stability criterion at both limiting extremes of Eq. 3.5 suggests that it applies more broadly to feedbacks on any timescale. Indeed, in Supporting Information 3.6.2, we prove that this condition characterizes local stability of the coexistence equilibrium when P is symmetric for any value of d. There are other qualitative similarities between the dynamics with very fast and very slow feedbacks. In particular, we have shown that feasibility in both cases depends only on $\boldsymbol{y}^\star$; there is always a distribution of patch states $\boldsymbol{w}^\star$ compatible with feasibility, and the system will evolve toward this configuration when a stability criterion is met. This behavior stands in contrast to the model with exogenous heterogeneity (Eq. 3.2), where any feasible equilibrium is stable, but feasiblity depends on $\boldsymbol{w}$.

The dynamics of fast and slow feedbacks are not entirely identical, however. The fast-feedback dynamics (Eq. 3.6) can exhibit stable limit cycles when P is not symmetric [164]. Because Eq. 3.7 is a linear system, this behavior is impossible when feedbacks occur on very long timescales. But as $d \to 0$, the model can still exhibit complex dynamics in the form of long transients [95]. In Fig. 3.5, we illustrate two interesting and ecologically relevant behaviors that can arise. First, if P meets the stability condition for the slow system (Eq. 3.7), then the dynamics will eventually reach a stable, feasible equilibrium. However, $\boldsymbol{w}(t)$ may transiently take on values that are incompatible with the feasibility of some species (i.e., some $x_i(w(t)) < 0$ for a range of t). In this case (Fig. 3.5A), the dynamics will "jump" between feasible subsystems where some species reach extremely low frequencies. In natural systems with finite size, this might lead to the extinction of these species before the coexistence equilibrium is reached. Alternatively, in very large systems or where there is a source of immigration that can rescue populations from rarity, the dynamics will be highly episodic as the system abruptly switches between feasible states, potentially over long times.

If instead P is not compatible with stability, some species will eventually be excluded from the system due to long-term feedbacks between the community and the landscape. On short timescales, however, the distribution of patch states is approximately constant, and the dynamics of Eq. 3.5 will closely resemble Eq. 3.2. In particular, species frequencies will be stable to perturbations. Thus, we can find surprising scenarios where a species rapidly recovers from reduction to low abundance in the short term, even though it is ultimately doomed to a gradual extinction (Fig. 3.5B).

These two scenarios illustrate that species' ability to invade when rare can change at different points in the dynamics, as the community modifies conditions across the landscape.

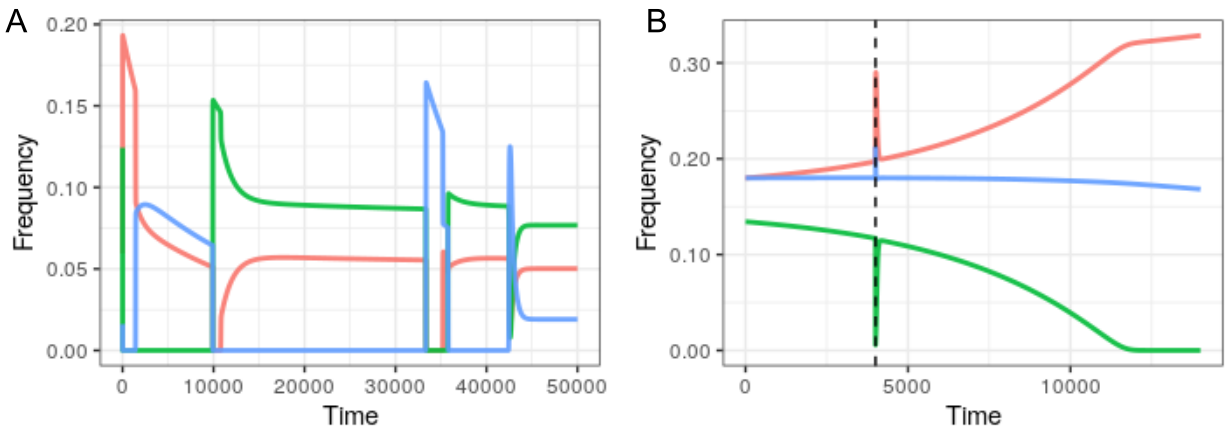

Figure 3.5: Complex transient dynamics when environmental feedbacks are much slower than community dynamics. Here we show species' frequencies ($\boldsymbol{x}(t)$) for the two scenarios described in the text. (A) When the slow system (Eq. 3.7) is stable, the ecosystem will eventually evolve toward a distribution of patch states such that species coexistence is feasible. However, if $\boldsymbol{w}$ is transiently incompatible with feasibility of the full community, the system will jump between (transiently) feasible sub-communities, leading to highly episodic dynamics. Each species reaches very low abundances during the transient dynamics, which would lead to extinctions in the absence of immigration or storage mechanisms (e.g., seed banks). (B) When the slow system is unstable, one or more species will eventually be excluded, but very gradually. During the transient period, the frequencies of all species are robust to perturbations. Here, the green species, which is driven to extinction by the long-term feedback dynamics, rapidly recovers from reduction to near extinction (dashed line) early in the dynamics. In these simulations, $m = 0.5$, $d = 10^{-5}$, and the elements of P were sampled *iid* from the standard uniform distribution until the desired properties were found (parameters available at [166]).

3.4 Discussion

Environmental heterogeneity is commonly understood to beget species diversity, but the converse can also be true. To better understand the relationships between the two, we introduced a simple, tractable modeling framework for species coexistence in an ecosystem where habitat heterogeneity is either a fixed feature of the landscape, or dynamically generated through biotic feedbacks. Our models, which are grounded in the metapopulation formalism, add to the rich literature on species coexistence in spatially-varying environments, and advance ecologists' growing understanding of feedbacks between multispecies communities and environmental variation. For fixed, or exogeneous, heterogeneity, our work extends classic models [108, 106, 218], recapitulates foundational theory in a new setting [48, 116, 47], and formalizes a connection between habitat partitioning and consumer-resource dynamics. In the context of endogenous heterogeneity, our model demonstrates how environmental modification by different species can lead to the stable maintenance of landscape and species diversity over long time scales, and clarifies the conditions under which these processes will occur. The minimal nature of our model makes it a promising tool to understand generic aspects of such feedbacks, which have been studied in many system-specific contexts [31, 133, 196].

Crucially, our approach also allows us to study exogenous and endogenous heterogeneity in a shared framework, revealing similarities and differences between coexistence mediated by both kinds of environmental variation. We showed that coexistence under endogenous heterogeneity is sensitive to the distribution of patch types in a landscape, but that the stability of a coexistence equilibrium is insensitive to the structure of species' colonization and establishment rates. When heterogeneity is endogenously generated, in contrast, the ecosystem has the capacity to "self-tune" the distribution of patch states to ensure feasibility. However, the landscape will only evolve toward this coexistence equilibrium if species' patch modifications generate negative frequency-dependent feedbacks. We derived quantitative criteria for such feedbacks to maintain coexistence, and showed that these same criteria

apply whether species modify the environment on very short or very long timescales. While the model dynamics are not identical at these two extremes, there are qualitative similarities that distinguish the endogenous cases from the exogenous one.

Although our models are quite abstract, they may nonetheless be useful for inference in natural systems. Eq. 3.4 expresses a relationship between the joint distribution of patch types and resident species at equilibrium ($X^{\star}_{ij}$), and the model parameters p_{ij}. An identical relationship holds for Eq. 3.5 once the distribution of patch states has equilibrated. We have discussed how this relationship expresses a net pattern of habitat association that emerges from the combined effects of species sorting and mass effects. By inverting this relationship, one can also obtain an estimator for each p_{ij} parameter (up to a constant factor, m) in terms of $X^{\star}_{ij}$ and the marginal frequencies $x^{\star}_{i}$ and $y^{\star}_{j}$. In principle, these frequencies could be computed in systems where well-resolved census and environmental data are available. Such data have been collected for plant communities [94, 192]. This method makes it possible to estimate dynamical model parameters from static, observational data, which is highly desirable for systems such as tropical forests where the slow pace of dynamics complicates experimental or time-series analysis. However, an important challenge to putting this approach into practice is defining operational patch types in context.

Our results suggest other practical considerations for inference and management in natural landscapes. For example, we found that manipulating the distribution of patch types in a landscape (with exogenous heterogeneity) can produce unexpected changes in the distribution of species frequencies. In particular, we illustrated a case where increasing habitat diversity quantitatively decreased species diversity qualitatively, even though all species were specialized on different habitat types [108, 218]. Without a very accurate knowledge of P, it is difficult to predict the effects of a perturbation to the landscape, and without considering the entire community context, it is impossible to determine important practical thresholds, such as the minimum abundance of a habitat type needed to sustain a species that relies on

it. As another example, we showed that biotic feedbacks can produce situations where all species are transiently resilient to perturbations, despite long-term dynamics that drive some of them to extinction. In such systems, efforts to characterize stability using experimental perturbations or analysis of population fluctuations over short timescales may be misleading about stability over longer timescales [95].

Of course, the abstract formulation of our model means that significant caveats may apply. We sought to explore the relationships between habitat heterogeneity, environmental feedbacks, and species coexistence in a minimal framework for these processes; therefore our model necessarily neglects other important processes present in real ecosystems. Following other patch models, our framework assumes no local co-occurrence of species, and therefore no direct species interactions. This allows us to isolate dynamics mediated by landscape heterogeneity, but direct interactions are certainly crucial in many systems, and within-patch dynamics might interact with regional dynamics in non-trivial ways. We also treat space implicitly in our model, but the spatial structure of ecological landscapes could shape how patch modification and dispersal interact. For example, a recent theoretical analysis incorporating both habitat partitioning and Janzen-Connell effects (endogenous heterogeneity) showed that these processes can combine to promote coexistence in a strongly synergistic manner when the spatial autocorrelation of patches is accounted for [223]. Even when only one source of heterogeneity is present, the spatial arrangement of patches could modulate our understanding of coexistence, for instance by reducing source-sink effects that limit the coexistence of imperfect habitat specialists [226].

Our approach also relies on a highly idealized implementation of environmental modification and legacy effects. We assume that patches can be classified into discrete types, and when heterogeneity is generated by the community, we assume that each species' effects on the environment can be summarized by a single patch state. This discreteness will only approximate the variation of environmental conditions in some natural systems, although in

others it may be apt. For instance, plant-associated microbial communities can differentiate into discrete types [27, 210, 191]. We also assume that when environmental conditions change, they do so by shifting abruptly between these discrete states. In reality, local conditions may change gradually, potentially reflecting the legacy effects of multiple past resident species at a single time, especially when change is slow (e.g., in the $d \to 0$ limit).

Intriguingly, one case where these simplifying assumptions might apply directly even in the $d \to 0$ limit comes from multi-strain pathogen systems [133]. It has long been known that a host's first infection by a pathogen can induce a lifelong imprinting effect, specific to the strain of first infection, that shapes future immune response [176]. This phenomenon, known as original antigenic sin, can have consequences at the level of population and strain dynamics. Recasting individual hosts as patches, and imprinting effects that modulate susceptibility as patch states, our model maps naturally onto these dynamics. Here, changes in the "landscape" occur not through shifts between states, but through demographic turnover that replaces imprinted hosts (lost to mortality) with naïve, newborn hosts on timescales much longer than infection dynamics. In Supporting Information 3.6.2, we show that an alternative model incorporating these processes behaves qualitatively identically to the model studied above. Our modeling approach could help explain how imprinting effects affect the maintenance of strain diversity. Interestingly, [164] showed that the stability criterion for symmetric feedbacks would imply a "burden of diversity" in such systems – greater strain diversity would raise the threshold for interventions aimed at eradicating the pathogen [97].

This example aside, our mathematical description of environmental modification is likely to be just a coarse approximation in many systems. Still, our approach provides a tractable way to link environmental conditions and community composition across varied timescales, offering a first step toward a more complete picture of these landscape feedbacks in a multispecies context. It has become increasingly clear that such feedbacks play a central and ubiquitous role in mediating interspecific interactions, whether maintaining species coex-

istence [31, 260], shaping patterns of abundandance and productivity [203, 155, 170], or driving species invasions [258, 250, 9]. Ecosystems are rarely a one-way street from landscape variation – set by abiotic features or "bottom-up" biotic process – to species diversity; understanding the dynamic interplay between environmental heterogeneity and "top-down" habitat modification is an important goal for ecology [57, 181, 170]. Simple models for these processes can illuminate essential features of each source of heterogeneity, and guide the way to unraveling how they interact and contribute to structuring natural communities.

3.5 Materials and methods

All computations were conducted in R (version 3.6.3). Where dynamics are shown, the model equations were integrated numerically using the deSolve package with the "ode45" Runge–Kutta method. Code to generate all figures and simulation results, including all parameters used in the text, is available on GitHub [166].

3.6 Supporting information

These supplementary materials are organized by the type of heterogeneity. We provide derivations, analysis, and commentary for the results stated in the Main Text.

3.6.1 Exogenous heterogeneity

In these sections, we derive and analyze the mathematical models for exogenous environmental heterogeneity (Eqs. 3.1-3.2) that appear in the Main Text.

Model reduction

We begin with the mathematical model

$$\begin{aligned}
\frac{dX_{ij}(t)}{dt} &= -m_{ij}X_{ij}(t) + p_{ij}y_j(t)\sum_{k=1}^{\ell} X_{ik}(t) \qquad \text{for } 1 \le i \le n \text{ and } 1 \le j \le \ell \\
\frac{dy_j(t)}{dt} &= \sum_{i=1}^{n} m_{ij}X_{ij}(t) - y_j(t)\sum_{i=1}^{n} p_{ij}\sum_{k=1}^{\ell} X_{ik}(t) \qquad \text{for } 1 \le j \le \ell
\end{aligned} \tag{3.8}$$

which is introduced and motivated in the Main Text. These dynamics can be viewed as a straightforward extension of classic metapopulation models to include ℓ patch types and n species, with colonization rates p_{ij} that depend on the combination of patch type and species identity.

The total number of patches of each type, whether vacant or occupied, is constant through the dynamics. Defining these quantities by $w_j = y_j(t) + \sum_i X_{ij}(t)$, we have that $\frac{dw_j}{dt} = 0$, which can be verified by summing the derivatives in Eq. 3.8. Naturally, then, we also have $\sum_j w_j$ constant, and we take this total to be 1, so that all model variables can be interpreted as proportions, or frequencies.

Assuming $m_{ij} = m$, as in the Main Text, we can simplify Eq. 3.8 by summing over patch types in the X_{ij}. We find that

$$\sum_j \frac{dX_{ij}(t)}{dt} = \frac{d\sum_j X_{ij}(t)}{dt} = -m\sum_j X_{ij}(t) + \sum_j p_{ij}y_j(t)\sum_{k=1}^{\ell} X_{ik}(t) \tag{3.9}$$

and, defining $x_i(t) = \sum_j X_{ij}(t)$, the total proportion of patches occupied by species i, we have the reduced model

$$\begin{aligned}
\frac{dx_i(t)}{dt} &= -mx_i(t) + x_i(t)\sum_{j=1}^{l} p_{ij}y_j(t) \\
\frac{dy_j(t)}{dt} &= m\sum_i X_{ij}(t) - y_j(t)\sum_{i=1}^{n} p_{ij}x_i(t) \ .
\end{aligned} \tag{3.10}$$

Eq. 3.10 still contains the quantities $\sum_i X_{ij}(t)$, which are the total proportions of occupied patches of type j. Because the total proportion of patches of each type is constant, we can express $\sum_i X_{ij}(t) = w_j - y_j(t)$ and re-write Eq. 3.10 only in terms of $x_i(t)$ and $y_j(t)$ variables:

$$\begin{aligned}\frac{dx_i(t)}{dt} &= -mx_i(t) + x_i(t)\sum_{j=1}^{\ell} p_{ij}y_j(t) \\ \frac{dy_j(t)}{dt} &= m\big(w_j - y_j(t)\big) - y_j(t)\sum_{i=1}^{n} p_{ij}x_i(t)\end{aligned} \tag{3.11}$$

This is Eq. 3.2 in the Main Text. Notice that Eq. 3.11 does not uniquely determine the dynamics of Eq. 3.8. However, we will see that a stable equilibrium for Eq. 3.11 implies a stable equilibrium solution for Eq. 3.8, so we concentrate on studying Eq. 3.11. As noted in the Main Text, Eq. 3.11 is typically a much smaller system than the full dynamics, because the size of this model grows with the sum of the number of patch types and species, rather than the product. Eq. 3.11 is also formally equivalent to widely-studied consumer-resource models with abiotic resources, making it possible to leverage known properties of such models.

Coexistence equilibrium and feasibility

In order to study the coexistence equilibrium (i.e. equilibrium where all species are present at positive abundances) of Eq. 3.11, it is convenient to express the model in matrix form. Using the notational conventions of the Main Text, we have

$$\begin{aligned}\frac{d\boldsymbol{x}(t)}{dt} &= -m\boldsymbol{x}(t) + D(\boldsymbol{x}(t))P\boldsymbol{y}(t) \\ \frac{d\boldsymbol{y}(t)}{dt} &= m\big(\boldsymbol{w} - \boldsymbol{y}(t)\big) - D(\boldsymbol{y}(t))P^T\boldsymbol{x}(t)\ .\end{aligned} \tag{3.12}$$

Here P is an $n \times \ell$ matrix. As discussed in the Main Text, coexistence of all species requires that $n \leq \ell$. We focus on the case where $n = \ell$, and so P is a square matrix. However, we note that there is a growing literature on typical properties of this model (in the consumer-resource context) when $n < \ell$, which could be applied to understand coexistence in heterogeneous landscapes using the equivalence established here [241, 60]. We will also assume that P is invertible, which requires that there are differences among species in their ability to colonize different patch types.

Under these assumptions, the coexistence equilibrium frequencies can be obtained by setting the derivatives in Eq. 3.12 to zero, and then solving for $\boldsymbol{x}^\star$ and $\boldsymbol{y}^\star$. We find

$$\begin{aligned}\boldsymbol{y}^\star &= m\,P^{-1}\mathbf{1} \\ \boldsymbol{x}^\star &= m\left(P^T\right)^{-1}\Big(D(\boldsymbol{y}^\star)^{-1}\boldsymbol{w} - \mathbf{1}\Big)\ .\end{aligned} \tag{3.13}$$

Feasibility of this equilibrium requires that all $P^{-1}\mathbf{1} > 0$, and that $\sum_j y_j^\star = m\mathbf{1}^T P\mathbf{1} < 1$. The latter condition effectively sets an upper bound on the local extinction rate, m; the condition can always be met if this rate is sufficiently small. Feasibility of the $\boldsymbol{x}^\star$ is also sensitive to the distribution of patch types, $\boldsymbol{w}$, as explored in the Main Text. Our analysis of the model with endogeneous heterogeneity, below, will imply that, if $\boldsymbol{y}^\star$ is feasible, there is always at least one admissible (i.e. positive and summing to one) $\boldsymbol{w}$ such that $\boldsymbol{x}^\star$ is feasible. Thus, the condition $P^{-1}\mathbf{1} > 0$ plays a fundamental role in determining whether species coexist.

We briefly consider the interpretation of this condition in ecological terms. Fully char-

acterizing the relationship between P and feasibility is a difficult problem with no simple account despite significant study of the same underlying mathematical relationship in other contexts [205, 213, 204, 190]. This condition expresses the fact that $P\boldsymbol{y} = \mathbf{1}$ must have a positive solution, or in other words, there must be some possible distribution of available patch types such that all species attain equal effective colonization rates (i.e. colonization rate averaged over the distribution of available patch types: $\sum_j p_{ij} y_j$). More loosely, we can interpret this condition as requiring that all species are sufficiently similar in overall colonization ability, or sufficiently specialized on distinct habitat types, or some combination of the two.

To justify this statement, we first re-write P in a more interpretable form. One can think of $\bar{p}_i = \frac{1}{\ell} \sum_j p_{ij}$ as summarizing the overall colonization ability of species i – this is the average colonization rate for species i across all patch types. We can express P as

$$P = \ell D(\bar{\boldsymbol{p}}) Q \tag{3.14}$$

where Q is a row stochastic matrix. The elements of Q represent the *relative establishment ability* of each species in different patch types. Intuitively, Q captures the degree of specialization of each species – if the elements of Q are of similar magnitude within a row, the corresponding species is not strongly specialized on a particular habitat.

Now we can show that if all species are exactly equal in overall colonization ability, or perfectly specialized on distinct habitat types, then coexistence is always feasible. In the first case, $\bar{p}_i = \bar{p}$ for all species, so $P^{-1}\mathbf{1} = \frac{1}{\bar{p}\ell} Q^{-1}\mathbf{1}$. Because Q is row stochastic, Q^{-1} is also, and so $\boldsymbol{y}^\star = \frac{m}{\bar{p}\ell}\mathbf{1}$, which is all positive. In the second case, Q is the identity matrix, so P is a positive diagonal matrix, and $y_i^\star = \frac{m}{\bar{p}_i \ell} > 0$. These two extreme cases show that when all species have equal overall colonization ability, coexistence is feasible regardless of specialization, and similarly when all species are perfectly specialized, coexistence is feasible regardless of overall colonization abilities.

Next we develop a quantitative version of the statement that some combination of equality and specialization is necessary for feasibility. Assume that all species are able to colonize and establish in all habitat types at some non-zero rate. Let q' be the minimum element of Q (i.e. the smallest relative establishment ability of any species in any patch type). q' provides one measure of specialization in the community. Larger q' implies less overall specialization, while small q' means that there is at least one species that relies on certain habitat types much less than others. We prove that there is now a limit on how much any two species can differ in their overall colonization ability before feasible coexistence is precluded. Assume that two species, i and j, have $\bar{p}_i = \epsilon \bar{p}_j$. For feasible coexistence, there must be some positive $\boldsymbol{y}$ such that

$$\sum_k q_{ik} y_k = \frac{1}{\epsilon} \quad \text{and} \quad \sum_k q_{jk} y_k = 1 \tag{3.15}$$

From the former equality we have $\sum_k y_k \geq \frac{1}{\epsilon}$, because the elements of Q are between zero and one. Then we know that the latter sum is at least equal to $\frac{q'}{\epsilon}$. If $\epsilon < q'$, then this sum is greater than one, which contradicts the equilibrium conditions. Thus, any two species in the community must be have overall colonization abilities within a factor of $\frac{1}{q'}$, and we have a quantitative statement of the notion that a certain degree of specialization requires a sufficient amount of similarity among species for coexistence. We make no attempt to sharpen this bound; we simply emphasize that these two ecologically meaningful attributes are constrained by one another.

Stability analysis

It is known, in the context of consumer-resource theory, that the coexistence equilibrium of Eq. 3.11 is always globally stable if it is feasible (see e.g. [157]). Global stability means that trajectories of the system will approach the equilibrium from any initial condition where

all species are present. For completeness, we outline a proof of this fact by constructing a Lyapunov function for the dynamics.

A Lyapunov function for an autonomous dynamical system $\frac{d\boldsymbol{z}}{dt} = g(\boldsymbol{z})$, with $\boldsymbol{z} \in \mathbb{R}^n$, is a continuous scalar function $V : \mathbb{R}^n \to \mathbb{R}$ that has continuous first derivatives and satisfies the following:

1. $V(\boldsymbol{z}) > 0$ except for an equilibrium point $\boldsymbol{z}^\star$, where $V(\boldsymbol{z}^\star) = 0$
2. $\frac{dV}{dt} < 0$ except when $\boldsymbol{z} = \boldsymbol{z}^\star$, where $\frac{dV}{dt} = 0$

In words, V is a positive function that is strictly decreasing through the dynamics, until reaching a minimum at $\boldsymbol{z}^\star$. The existence of such a function implies that the point $\boldsymbol{z}^\star$ is globally Lyapunov stable. For a thorough discussion of Lyapunov functions and global stability, see [35, 89].

Unfortunately, there is no general method to construct Lyapunov functions. However, we illustrate how one can sometimes be found using a technique called *Generalized Lotka-Volterra (GLV) embedding*, which exploits the facts that (i) a large class of differential equations can be recast as GLV systems, and [234] (ii) well-studied candidate Lyapunov functions for GLV systems are known [78]. Thus, GLV embedding removes some of the need for "divine inspiration" that is usually require to find Lyapunov functions. For more detailed exposition of this method, see [199, 234, 164].

Eq. 3.11 is not a GLV system, but we can define the new variables $r_j(t) = \frac{1}{y_j(t)}$ and "recast" the model as the larger system

$$\begin{aligned}
\frac{dx_i(t)}{dt} &= x_i(t)\left(-m + \sum_{j=1}^{\ell} p_{ij} y_j(t)\right) \\
\frac{dy_j(t)}{dt} &= y_j(t)\left(-m + w_j r_j(t) - \sum_{i=1}^{n} p_{ij} x_i(t)\right) \\
\frac{dr_j(t)}{dt} &= r_j(t)\left(m - w_j r_j(t) + \sum_{i=1}^{n} p_{ij} x_i(t)\right)
\end{aligned} \tag{3.16}$$

subject to the constraints $r_j(0) = \frac{1}{y_j(0)}$ on the initial conditions. This system *is* a GLV model. If we define the vector of abundances $\boldsymbol{z}(t) = (\boldsymbol{x}(t), \boldsymbol{y}(t), \boldsymbol{r}(t))$, Eq. 3.16 can be written as $\frac{d\boldsymbol{z}(t)}{dt} = D(\boldsymbol{z}(t))\,(M\boldsymbol{z}(t) + \lambda)$ with

$$M = \begin{pmatrix} 0 & P & 0 \\ -P^T & 0 & D(\boldsymbol{w}) \\ P^T & 0 & -D(\boldsymbol{w}) \end{pmatrix} \quad \text{and} \quad \lambda = \begin{pmatrix} -m\mathbf{1} \\ -m\mathbf{1} \\ m\mathbf{1} \end{pmatrix}. \tag{3.17}$$

Now we that we have a GLV system, we can try to apply the well-known candidate Lyapunov function [78]

$$V(\boldsymbol{z}(t)) = \sum_i \gamma_i \left(z_i(t) - z_i^\star - z_i^\star \log\left(\frac{z_i(t)}{z_i^\star}\right)\right) \tag{3.18}$$

where $\boldsymbol{\gamma}$ is a vector of non-negative constants, and $z_i^\star$ is the equilibrium value of the corresponding component of $\boldsymbol{z}$. Defined this way, V is positive everywhere except at the coexistence equilibrium [78]. The time derivative of V is given by

$$\dot{V}(\boldsymbol{z}(t)) = (\boldsymbol{z}(t) - \boldsymbol{z}^\star)^T \left(D(\boldsymbol{\gamma})M + M^T D(\boldsymbol{\gamma})\right)(\boldsymbol{z}(t) - \boldsymbol{z}^\star) \tag{3.19}$$

and thus we seek a choice of $\boldsymbol{\gamma}$ such that $\dot{V}(\boldsymbol{z}(t)) \leq 0$ for all times. Consider $\gamma = (\mathbf{1}, \mathbf{1}, \mathbf{0})^T$. Then we find

$$\dot{V}(\boldsymbol{z}(t)) = 2(\boldsymbol{y}(t) - \boldsymbol{y}^\star)^T D(\boldsymbol{w})(\boldsymbol{r}(t) - \boldsymbol{r}^\star)\,. \tag{3.20}$$

But we know that $r_j(t) - r_j(t)^\star = \frac{1}{y_j(t)} - \frac{1}{y_j^\star} = -\frac{y_j(t)-y_j^\star}{y_j(t)y_j^\star}$ and so

$$\dot{V}(\boldsymbol{z}(t)) = -2\sum_j \frac{w_j\left(y_j(t) - y_j^\star\right)^2}{y_j(t)y_j^\star} \leq 0\,. \tag{3.21}$$

This expression is actually zero whenever $\boldsymbol{y}(t) = \boldsymbol{y}^\star$, regardless of whether $\boldsymbol{x}(t)$ is also at equilibrium. But we note that if $\boldsymbol{y}(t) = \boldsymbol{y}^\star$ and $\boldsymbol{x}(t) \neq \boldsymbol{x}^\star$, then $\frac{d\boldsymbol{y}(t)}{dt} \neq 0$ and the trajectory leaves the set where $\dot{V}(\boldsymbol{z}(t)) = 0$. Thus, LaSalle's invariance principle guarantees that the coexistence equilibrium is globally stable.

The stability of this equilibrium for Eq. 3.11 immediately implies that the full model in Eq. 3.8 also reaches a stable coexistence equilibrium. Taking $\boldsymbol{x}$ and $\boldsymbol{y}$ at equilibrium, the dynamics for the joint distribution of species and patch types become:

$$\frac{dX_{ij}(t)}{dt} = -mX_{ij}(t) + p_{ij}y_j^\star x_i^\star\ . \tag{3.22}$$

These equations are now uncoupled from one another, and each has a stable (noting that $-m$ is always negative) equilibrium given by Eq. 3.4 in the Main Text.

3.6.2 Endogenous heterogeneity

In these sections, we derive and analyze the mathematical models for endogenous environmental heterogeneity (Eqs. 3.5-3.7) that appear in the Main Text. We also introduce an alternative model where environmental modification is tied to demographic turnover in a host population, or strong disturbances that revert patches to a "naïve" state. We show that our major conclusions are robust to this difference in model particulars.

Model reduction

As described in the Main Text, we now consider a scenario where the type of each patch is not fixed, but instead patches can be in one of n states, corresponding to the n species in the community. When a patch in state j is occupied by species i, at some rate it may shift to state i. This provides a phenomenological way to model habitat modification by each species, which can change the state of the environment over some characteristic timescale. Combining these new processes with the assumptions outlined for dynamics with exogenous heterogeneity, we have a model analogous to Eq. 3.8, which in the most general case is given by

$$\begin{aligned} \frac{dX_{ij}(t)}{dt} &= -m_{ij}X_{ij}(t) + p_{ij}y_j(t)\sum_{k=1}^{\ell} X_{ik}(t) - d_{ij}X_{ij}(t) + \delta_{ij}\sum_{k} d_{ik}X_{ik}(t) \\ \frac{dy_j(t)}{dt} &= \sum_{i=1}^{n} m_{ij}X_{ij}(t) - y_j(t)\sum_{i=1}^{n} p_{ij}\sum_{k=1}^{\ell} X_{ik}(t) \end{aligned} \tag{3.23}$$

Here δ_{ij} is the Kronecker delta, which equals one when $i = j$ and zero otherwise. In this model, we automatically have $1 \leq i, j \leq n$ by assumption. In general, the rate at which species i modifies patches in state j might depend on both i and j, as shown here. Following the exogeneous case, however, we assume $m_{ij} = m$ and $d_{ij} = d$ and track the dynamics for $x_i(t) = \sum_j X_{ij}(t)$. In this case, we must also track the dynamics of patch states, since these are not fixed. We define $w_k(t) = y_k(t) + \sum_i X_{ik}(t)$. Using these definitions to compute sums of the derivatives in Eq. 3.23, we write the reduced model

$$\begin{aligned}
\frac{dx_i(t)}{dt} &= -mx_i(t) + x_i(t)\sum_{j=1}^{n} p_{ij}y_j(t) \\
\frac{dy_j(t)}{dt} &= m\big(w_j(t) - y_j(t)\big) - y_j(t)\sum_{i=1}^{n} p_{ij}x_i(t) \\
\frac{dw_k(t)}{dt} &= d\big(x_k(t) + y_k(t) - w_k(t)\big)
\end{aligned} \tag{3.24}$$

which is Eq. 3.5 in the Main Text.

As described in the Main Text, we can study this model in two limits ($d \to \infty$ and $d \to 0$, corresponding to very fast and very slow feedbacks) where the equations become simplified. These fast-slow decompositions rely on Tikhonov's theorem [240], and are valid whenever the coexistence equilibrium for the relevant fast system is feasible and stable. We know that stability will hold in all cases, and in the limit $d \to \infty$, feasibility is also guaranteed. In this fast limit, Eq. 3.24 becomes identical to the model studied by [164]. We refer the reader to this study for detailed analysis of the model dynamics. However, we note that Miller and Allesina showed that when $P = P^T$, the coexistence equilibrium is stable if and only if P has exactly one positive eigenvalue. This condition reappears in the analysis below. Miller and Allesina additionally discuss the ecological interpretation of this eigenvalue condition.

Stability for slow feedbacks

In the slow limit ($d \to 0$), we take

$$\begin{aligned}
\boldsymbol{y}(t) &= m\, P^{-1}\mathbf{1} \\
\boldsymbol{x}(t) &= m\left(P^T\right)^{-1}\Big(D(\boldsymbol{y}(t))^{-1}\boldsymbol{w}(t) - \mathbf{1}\Big)
\end{aligned} \tag{3.25}$$

assuming that these fast variables rapidly approach their equilibrium given $\boldsymbol{w}(t)$, and then substitute into the equations for $\frac{d\boldsymbol{w}(t)}{dt}$ to obtain the slow system

$$\begin{aligned}\frac{1}{d}\frac{d\boldsymbol{w}(t)}{dt} &= m\left(P^T\right)^{-1}\left(D(m\,P^{-1}\mathbf{1})^{-1}\boldsymbol{w}(t)-\mathbf{1}\right)+m\,P^{-1}\mathbf{1}-\boldsymbol{w}(t)\\ &= \left(\left(D(P^{-1}\mathbf{1})P^T\right)^{-1}-I\right)\boldsymbol{w}(t)-m\left(\left(P^{-1}\right)^T-P^{-1}\right)\mathbf{1}\end{aligned} \tag{3.26}$$

which is Eq. 3.7 in the Main Text. This decomposition holds when $\boldsymbol{y}(t)$ and $\boldsymbol{x}(t)$ are feasible, which may not be true for all initial conditions $\boldsymbol{w}$ (see discussion in Main Text).

Eq. 3.26 is a linear matrix equation with several special properties. The constraint $\sum_k w_k(t) = 1$ implies that the dynamics should be confined to the simplex. These dynamics can be expressed in terms of the eigenvectors and eigenvalues of $A = \left(D(P^{-1}\mathbf{1})P^T\right)^{-1} - I$. We note that $D(P^{-1}\mathbf{1})P^T$ is column stochastic, so this matrix has a right eigenvector, which we denote $\boldsymbol{v}$, with an associated eigenvalue of 1. Because the matrix is non-negative, $\boldsymbol{v}$ is in fact the Perron eigenvector of $D(P^{-1}\mathbf{1})P^T$, and it is also non-negative [109]. It is easy to see that $A\boldsymbol{v} = 0$, which means that the dynamics have no component in this direction. The remaining eigenvectors of A have components that sum to zero, as we verify by considering

$$\mathbf{1}^T\boldsymbol{u} = \frac{1}{\lambda}\mathbf{1}^T A\boldsymbol{u} = 0 \tag{3.27}$$

for any eigenvector u with associated eigenvalue $\lambda \neq 0$. Here we used the fact that $\mathbf{1}$ is a left eigenvector of A with an associated eigenvalue of zero. Because the dynamics can be written as a linear combination of zero-sum eigenvalues, the dynamics for $\boldsymbol{w}$ are zero-sum, and remain in the simplex, as expected.

Taking this constraint into account, Eq. 3.7 has a unique equilibrium given by

$$\boldsymbol{w}^\star = mP^{-1}\mathbf{1} + k\boldsymbol{v} \tag{3.28}$$

where $\boldsymbol{v}$ is the eigenvector defined above, normalized such that $\mathbf{1}^T\boldsymbol{v} = 1$, and k is the quantity $1 - m\mathbf{1}^T P^{-1}\mathbf{1}$. We can verify that

$$\begin{aligned}
\frac{1}{d}\frac{d\boldsymbol{w}^\star}{dt} &= \left(\left(D(P^{-1}\mathbf{1})P^T\right)^{-1} - I\right)\boldsymbol{w}^\star - m\left(\left(P^{-1}\right)^T - P^{-1}\right)\mathbf{1} \\
&= \left(\left(D(P^{-1}\mathbf{1})P^T\right)^{-1} - I\right)\left(mP^{-1}\mathbf{1} + k\boldsymbol{v}\right) - m\left(\left(P^{-1}\right)^T - P^{-1}\right)\mathbf{1} \\
&= m\left(D(P^{-1}\mathbf{1})P^T\right)^{-1} P^{-1}\mathbf{1} - mP^{-1}\mathbf{1} + 0 - m\left(\left(P^{-1}\right)^T - P^{-1}\right)\mathbf{1} \\
&= m\left(P^{-1}\right)^T\mathbf{1} - mP^{-1}\mathbf{1} - m\left(\left(P^{-1}\right)^T - P^{-1}\right)\mathbf{1} \\
&= 0\ .
\end{aligned} \tag{3.29}$$

Provided that $P^{-1}\mathbf{1} > 0$ and $m\mathbf{1}^T P^{-1}\mathbf{1} < 1$ (the feasibility conditions for $\boldsymbol{y}$ in the fast system), this equilibrium is feasible. It also implies a feasible equilibrium for the species frequencies, given by

$$\begin{aligned}
\boldsymbol{x}^\star &= m\left(P^T\right)^{-1}\left(D(\boldsymbol{y}^\star)^{-1}\boldsymbol{w}^\star - \mathbf{1}\right) \\
&= m\left(P^T\right)^{-1}\left(D(mP^{-1}\mathbf{1})^{-1}\left(mP^{-1}\mathbf{1} + k\boldsymbol{v}\right) - \mathbf{1}\right) \\
&= m\left(P^T\right)^{-1}\left(\mathbf{1} + kD(mP^{-1}\mathbf{1})^{-1}\boldsymbol{v} - \mathbf{1}\right) \\
&= k\left(D(P^{-1}\mathbf{1})P^T\right)^{-1}\boldsymbol{v} \\
&= k\boldsymbol{v}
\end{aligned} \tag{3.30}$$

Here we used the definition of $\boldsymbol{v}$, and the fact that $\boldsymbol{v}$ is a Perron eigenvector implies that all components are positive.

It is worth noting that because the existence of this equilibrium is independent of the timescales of the dynamics, these equilibrium calculations apply for Eq. 3.24, for any choice of d.

Finally, we consider the stability of this equilibrium (assuming again that $d \to 0$). Trajectories of Eq. 3.26 will approach $\boldsymbol{w}^\star$ from any initial condition if and only if the matrix A has eigenvalues with all negative real parts (excepting the zero eigenvalue, which corresponds to directions forbidden by the zero-sum constraint). Equivalently, $\left(D(P^{-1}\mathbf{1})P^T\right)^{-1}$ must have eigenvalues with real part less than 1. To relate this condition to the eigenvalues of $D(P^{-1}\mathbf{1})P^T$ (or, equivalently, $PD(P^{-1}\mathbf{1})$, which shares the same eigenvalues), suppose that this matrix has an eigenvalue $a + bi$. The eigenvalues of an inverse matrix are the inverses of the eigenvalues, so $\left(D(P^{-1}\mathbf{1})P^T\right)^{-1}$ has a corresponding eigenvalue with real part $\frac{a}{a^2+b^2}$. Thus, we require that $\frac{a}{a^2+b^2} < 1$ or equivalently $(a - \frac{1}{2})^2 + b^2 > \left(\frac{1}{2}\right)^2$. Overall, the Perron-Frobenius theorem implies that $a^2 + b^2 < 1$ (because $D(P^{-1}\mathbf{1})P^T$ has an eigenvalue 1), and stability requires that $(a - \frac{1}{2})^2 + b^2 > \left(\frac{1}{2}\right)^2$. In graphical terms, the eigenvalues of $D(P^{-1}\mathbf{1})P^T$ must lie within a crescent-shaped region in the complex plane, within a circle of radius 1 centered at the origin, and outside of a circle of radius $\frac{1}{2}$ centered at $a = \frac{1}{2}$ (see Fig. 3.6). From this geometric picture, we immediately see that if all but one eigenvalue (the Perron eigenvalue) of $D(P^{-1}\mathbf{1})P^T$ have negative real part, this is sufficient to ensure stability.

The matrix $PD(P^{-1}\mathbf{1})$ defines a natural normalization of P in this context – multiplying by the diagonal matrix $D(P^{-1}\mathbf{1})$ maps every eigenvalue into the unit disk. In more ecological terms, this normalization also removes any effect of differences in overall quality between patches. To see this, decompose P as $QD(P^T\mathbf{1})$, where Q is a column stochastic matrix and $P^T\mathbf{1}$ are the column sums of P. Any differences in the overall quality of patches are captured by $P^T\mathbf{1}$. Now we see that $PD(P^{-1}\mathbf{1})$ is completely insensitive to $P^T\mathbf{1}$: we have $P^{-1}\mathbf{1} = D(P^T\mathbf{1})^{-1}Q^{-1}\mathbf{1}$, and so

$$PD(P^{-1}\mathbf{1}) = QD(P^T\mathbf{1})D(P^T\mathbf{1})^{-1}D(Q^{-1}\mathbf{1}) = QD(Q^{-1}\mathbf{1})\,. \tag{3.31}$$

In general, it is not possible to relate this stability condition more directly to P. However,

in the special case where P is symmetric (i.e. $P = P^T$), this stability condition reduces to the statement that the coexistence equilibrium is stable if and only if P has exactly one positive eigenvalue. This because $PD(P^{-1}\mathbf{1})$ is similar to the matrix $S = D(P^{-1}\mathbf{1})^{1/2}PD(P^{-1}\mathbf{1})^{1/2}$ (and therefore shares the same eigenvalues), and S is congruent to P (and therefore shares the same number of positive, negative, and zero eigenvalues) [109]. This conclusion follows from Sylvester's law of inertia and relies on the symmetry of P. This symmetry also ensures that P (and consequently S and $PD(P^{-1}\mathbf{1})$) has strictly real eigenvalues. From Fig. 3.6, it is apparent that along the real line, the region of stability reduces to the interval $(-1, 0)$. In other words, the eigenvalues of P (excepting the Perron eigenvalue, as usual) must be negative.

Stability for symmetric feedbacks on arbitrary timescales

The appearance of the necessary and sufficient stability condition *P has exactly one positive eigenvalue* for symmetric feedbacks at two opposite limits of the dynamics suggests that this condition should apply more broadly for Eq. 3.24 with feedbacks on any timescale (i.e any choice of d). Here, we prove that this is indeed the case. In particular, we show that this condition characterizes the local stability of the coexistence equilibrium of Eq. 3.24 whenever P is symmetric.

If $P = P^T$, the equilibrium frequencies found in the previous section simplify dramatically. We find $\boldsymbol{y}^\star = mP^{-1}$, $\boldsymbol{x}^\star = k'\boldsymbol{y}^\star$ and $\boldsymbol{w} = (1 + k')\boldsymbol{y}^\star$, where $k' = \frac{1}{m\mathbf{1}^T P^{-1}\mathbf{1}} - 1$. That is, all three equilibrium vectors become proportional to $P^{-1}\mathbf{1}$. This is easily verified by noting that $P^{-1}\mathbf{1}$ is a right eigenvector of $D(P^{-1}\mathbf{1})P^T = D(P^{-1}\mathbf{1})P$ with an associated eigenvalue of 1.

This simple form for the coexistence equilibrium of Eq. 3.24 makes it possible to analyze the Jacobian matrix for these dynamics at equilibrium. We find the Jacobian

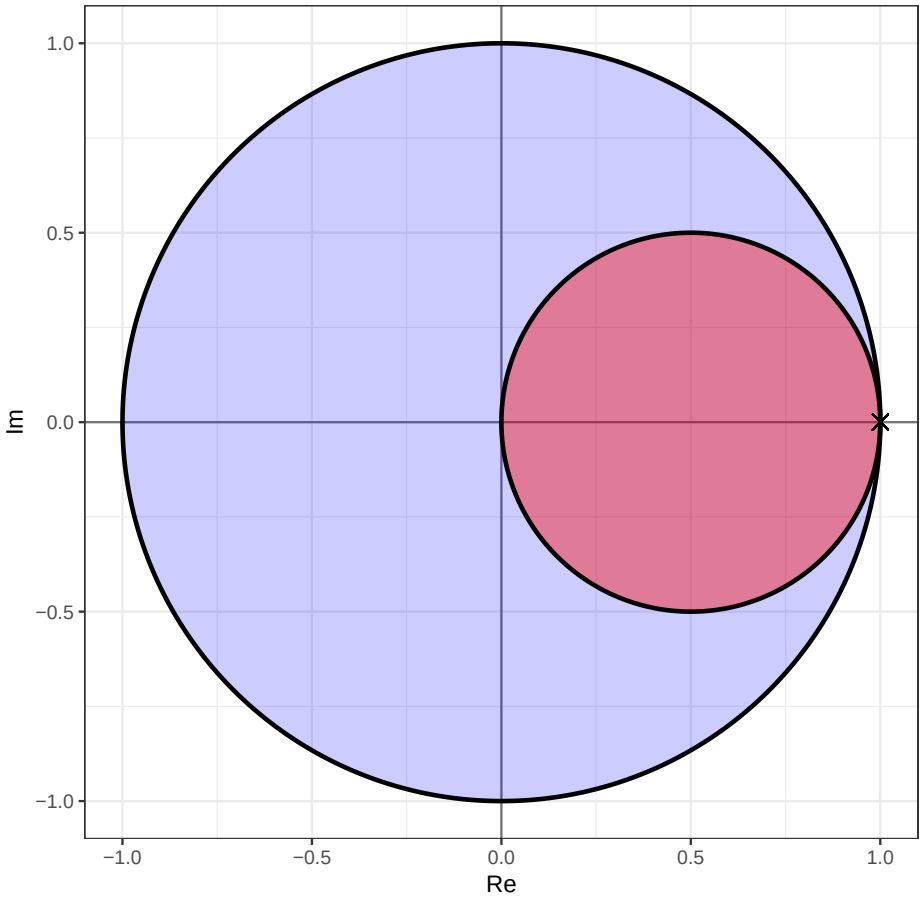

Figure 3.6: Graphical stability condition for Eq. 3.26. Stability of the coexistence equilibrium is determined by the eigenvalues of $D(P^{-1}\mathbf{1})P^T$ (or, equivalently, $PD(P^{-1}\mathbf{1})$). This matrix has a Perron (dominant) eigenvalue $\lambda = 1$, indicated here by a black X. The remaining $n-1$ eigenvalues fall within the unit disk in the complex plane (light blue shaded region). The coexistence equilibrium is stable if these remaining eigenvalues all lie outside of a disk of radius $\frac{1}{2}$ centered at $\frac{1}{2}$ on the real line (red shaded region). Thus, there is a crescent-shaped stability region which must contain the non-Perron eigenvalues in order for the dynamics to be stable. Notice that if all non-Perron eigenvalues have negative real part, then they necessarily lie in the stability region, so this condition is sufficient to ensure stability. When P is a symmetric matrix, all eigenvalues of $PD(P^{-1}\mathbf{1})$ lie on the real line, so negativity of the non-Perron eigenvalues becomes necessary, as well as sufficient, for stability.

$$J = \begin{pmatrix} 0 & k'D(\boldsymbol{y}^\star)P & 0 \\ -D(\boldsymbol{y}^\star)P^T & -m(k'+1)I & mI \\ dI & di & -dI \end{pmatrix} \tag{3.32}$$

It is actually more convenient to work with another matrix, J', that is similar to J, and thus shares the same eigenvalues [109]. We first define the change of basis matrix

$$U = \begin{pmatrix} D(\boldsymbol{y}^\star)^{1/2} & 0 & 0 \\ 0 & D(\boldsymbol{y}^\star)^{1/2} & 0 \\ 0 & 0 & D(\boldsymbol{y}^\star)^{1/2} \end{pmatrix} \tag{3.33}$$

and then define $J' = U^{-1}JU$. More explicitly, we have

$$J' = \begin{pmatrix} 0 & mk'S & 0 \\ -mS & -m(k'+1)I & mI \\ dI & di & -dI \end{pmatrix} \tag{3.34}$$

where $S = D(P^{-1}\mathbf{1})^{1/2}PD(P^{-1}\mathbf{1})^{1/2}$. Following [164], we use the ansatz that the eigenvectors of J' all take the form $(\boldsymbol{u}_i, c_1\boldsymbol{u}_i, c_2\boldsymbol{u}_i)^T$, where $\boldsymbol{u}_i$ is the ith eigenvector of S, and c_1 and c_2 are undetermined constants. We will show that each eigenpair of S generates three associated eigenpairs of J', and the eigenvalues of S control the signs of the eigenvalues of J'.

With our ansatz, each eigenvalue of J' satisfies

$$J' \begin{pmatrix} \boldsymbol{u}_i \\ c_1\boldsymbol{u}_i \\ c_2\boldsymbol{u}_i \end{pmatrix} = \lambda \begin{pmatrix} \boldsymbol{u}_i \\ c_1\boldsymbol{u}_i \\ c_2\boldsymbol{u}_i \end{pmatrix} \tag{3.35}$$

and taking the matrix multiplication by blocks yields the following system of equations:

$$
\begin{aligned}
mk'\lambda(S)_i \boldsymbol{u}_i &= \lambda \boldsymbol{u}_i \\
-m\lambda(S)_i \boldsymbol{u}_i - m(k'+1)\boldsymbol{u}_i + m\boldsymbol{u}_i &= c_1 \lambda \boldsymbol{u}_i \\
d(\boldsymbol{u}_i + c_1 \boldsymbol{u}_i - c_2 \boldsymbol{u}_i) &= \lambda c_2 \boldsymbol{u}_i
\end{aligned}
\tag{3.36}
$$

where $\lambda(S)_i$ is the ith eigenvalue of S (which appears when we consider the definition of $\boldsymbol{u}_i$). Provided suitable constants exist, this system of equations confirms our ansatz for the form of the eigenvectors of J'. These equations imply the scalar system

$$
\begin{aligned}
mk'\lambda(S)_i &= \lambda \\
-m\lambda(S)_i - m(k'+1) + m &= c_1 \lambda \\
d(1 + c_1 - c_2) &= \lambda c_2
\end{aligned}
\tag{3.37}
$$

and using substitution for c_1 and c_2, we can reduce this system further to the cubic equation

$$
\lambda^3 + (m(k'+1) + d)\lambda^2 + (k'm^2\lambda(S)_i^2 + dk'm)\lambda + dk'm^2\lambda(S)_i(\lambda(S)_i - 1) = 0\,. \tag{3.38}
$$

We note that the coefficients of the first three terms are positive for any choice of the model parameters. The constant term is negative if $\lambda(S)_i > 0$, and positive if $\lambda(S)_i < 0$ (noting that the eigenvalues of S must be less than 1 in magnitude – see discussion in the previous section). Descartes's rule of signs implies that number of positive and negative roots is controlled by the sign of the constant terms, and therefore by the sign of $\lambda(S)_i$. If $\lambda(S)_i < 0$, there are zero positive roots; if $\lambda(S)_i < 0$, there is exactly one positive root. There is one special case to consider: we know that S has an eigenvalue of 1, and when $\lambda(S)_i = 1$, the constant term in the equation above vanishes, leading to a root $\lambda = 0$. This is consistent

with our expectation that there is one direction pointing "out" of the simplex, along which the dynamics cannot change.

Overall, this analysis shows that each eigenvalue of S generates three eigenvalues of J', and the number of positive eigenvalues of J' is exactly one less than the number of positive eigenvalues of S. In particular, J' has all non-positive eigenvalues if and only if S has exactly one positive eigenvalue. Because S and P are symmetric and congruent, Sylvester's law of inertia dictates that the number of positive eigenvalues of P and S are the same, and we recover the conjectured stability condition [109].

An alternative model

In some cases, it is natural to assume that changes in patch state are mediated by significant disturbance events that remove any species present and reset the patch to a "naïve" state. In the context of immune imprinting, discussed in the Main Text, this might actually represent the replacement of an old patch (host) by a new one, due to births and deaths in the host population. In other contexts, we might simply imagine severe perturbations, such as fire, that clear the patch. Then the new state is determined by the next species to occupy this naïve patch.

In this section, we introduce a modification of Eq. 3.24 that incorporates this kind of process. We show that this modified model behaves qualitatively like Eq. 3.24 when disturbance events are very rare and naïve patches are re-colonized sufficiently quickly.

We consider the model

$$\begin{aligned}
\frac{dx_i(t)}{dt} &= -mx_i(t) + x_i(t)\sum_{j=1}^{n} p_{ij}y_j(t) + cx_i(t)\Big(1 - \sum_{j=1}^{n} w_j(t)\Big) - dx_i(t) \\
\frac{dy_j(t)}{dt} &= m\big(w_j(t) - y_j(t)\big) - y_j(t)\sum_{i=1}^{n} p_{ij}x_i(t) - dy_j(t) \\
\frac{dw_k(t)}{dt} &= cx_k(t)\Big(1 - \sum_{j=1}^{n} w_j(t)\Big) - dw_k(t)
\end{aligned} \tag{3.39}$$

where all variables have the same interpretation as before. Now d is interpreted as the rate of disturbance in the system, and the new parameter c is the rate at which all species colonize naïve patches. The frequency of naïve patches is represented implicitly as $1 - \sum_{j=1}^{n} w_j(t)$, which we henceforth denote by $z(t)$ for concision. In this model, all patches are subject to disturbance, which leads to losses from the $\boldsymbol{x}$ and $\boldsymbol{y}$ variables, and changes in the distribution of patch states ($\boldsymbol{w}$) occur as naïve patches are colonized by different species, which set the state of the patch.

In the limit where $d \to 0$ and assuming $z(t)$ is of the same order as d, we can apply a fast-slow decomposition and show that the dynamics of Eq. 3.39 are essentially identical to the slow limit of Eq. 3.24. By taking $z(t)$ to be small, we are assuming that naïve patches are recolonized sufficiently quickly (relative to d) so that the frequency of naïve patches in the landscape is small. We will show that this assumption is consistent with the equilibrium behavior for $z(t)$.

In this limit, we take $\frac{d\boldsymbol{x}(t)}{dt} = 0$ and $\frac{d\boldsymbol{y}(t)}{dt} = 0$, assuming that these variables change and equilibrate much more rapidly than the $\boldsymbol{w}(t)$ (more formally, we notice that all terms in $\frac{d\boldsymbol{w}(t)}{dt}$ are of order d, taking $d \to 0$). Then we obtain

$$\begin{aligned}\boldsymbol{y}(t) &= (m + d - cz(t))\, P^{-1}\mathbf{1} \\ \boldsymbol{x}(t) &= \left(P^T\right)^{-1}\left(mD(\boldsymbol{y}(t))^{-1}\boldsymbol{w}(t) - (m+d)\mathbf{1}\right)\end{aligned} \tag{3.40}$$

which is nearly identical to equation Eq. 3.25. Now we consider the dynamics of $z(t)$, given by

$$\frac{dz(t)}{dt} = -\frac{d\sum_j w_j(t)}{dt} = d(1 - z(t)) - cz(t)\sum_{j=1}^{n} x_j(t) \tag{3.41}$$

Using Eq. 3.40, we have

$$\begin{aligned}\frac{dz(t)}{dt} = \frac{1}{m + d - cz(t)}\times \\ \left(c(d+m)(1+cq)z(t)^2 - (cm(1+qm) + d(c+m+d+2cqm+cqd))\, z(t) + (m+d)d\right)\end{aligned} \tag{3.42}$$

where $q = \mathbf{1}^T P^{-1}\mathbf{1}$. Under our assumptions that d and $z(t)$ are small, the prefactor is approximately equal to $\frac{1}{m}$, and in particular, it will be positive. This means the dynamics of $z(t)$ are controlled by the quadratic factor. This factor can be well-approximated by

$$f(z(t)) = cm(1+cq)z(t)^2 - cm(1+mq)z(t) + md\,. \tag{3.43}$$

One root of $f(z(t))$ is small – using a binomial approximation, this root is approximately $\frac{d}{c(1+mq)}$. This root is associated with a stable equilibrium point for $\frac{dz(t)}{dt}$, which we can verify by noting that $f(z(t))$ is negative above this root and positive below. Thus, our initial assumption that $z(t)$ is of order d is supported. For $z(0)$ small enough (precisely how small will depend on the other root), $z(t)$ will approach an equilibrium $z^\star \approx \frac{d}{c(1+mq)}$. In other

words, provided the proportion of patches in the naïve state is initially small, it will remain small through the dynamics.

Finally, we can consider the slow system

$$\frac{d\boldsymbol{w}(t)}{dt} = \left(\frac{cmz(t)}{m+d-cz(t)}\left(D(P^{-1}\mathbf{1})P^T\right)^{-1} - dI\right)\boldsymbol{w}(t) - c(m+d)z(t)\left(P^{-1}\right)^T\mathbf{1} \quad (3.44)$$

After sufficiently long times, we can take $z(t) \approx z^\star$ in these dynamics. In this case, Eq. 3.44 becomes a linear matrix equation, very similar to Eq. 3.26. The matrix that multiplies $\boldsymbol{w}(t)$ shares the same eigenvectors as the matrix A in Eq. 3.26; however the eigenvalues of the two differ. As we have seen previously, $\left(D(P^{-1}\mathbf{1})P^T\right)^{-1}$ has an eigenvalue of 1, and so the matrix coefficient in this case has an eigenvalue

$$\lambda = \frac{cmz^\star}{m+d-cz^\star} - d \; = -\frac{cq(m+d)z^\star}{1-z^\star} \quad (3.45)$$

where the last equality follows from the equilibrium condition for $z(t)$ (i.e. setting $\frac{dz(t)}{dt} = 0$). This eigenvalue is always negative, consistent with our conclusion that the proportion of naïve patches, and so the sum of $\boldsymbol{w}(t)$, converges to equilibrium. The remaining eigenvectors of $\left(D(P^{-1}\mathbf{1})P^T\right)^{-1}$ sum to 0, as shown previously. So, as in the original model, the remaining dynamics occur in a manifold where $\sum_j w_j$ is constant. What are the eigenvalues for these directions? Denoting the eigenvalues of $\left(D(P^{-1}\mathbf{1})P^T\right)^{-1}$ by λ', we have

$$\lambda = \frac{cmz^\star}{m+d-cz^\star}\lambda' - d \approx \frac{d}{1+mq}\lambda' - d \quad (3.46)$$

using our approximation $z^\star = \frac{d}{c(1+mq)}$. This implies that if $\mathrm{Re}(\lambda') < 1+mq$, then $\lambda < 0$. In particular, if $\mathrm{Re}(\lambda') < 1$, the real part of the corresponding λ will always be negative. This is exactly the stability condition we found for the original model, and we see that the conclusions for our original model apply here qualitatively.

CHAPTER 4

METAPOPULATIONS WITH HABITAT MODIFICATION

4.1 Introduction

Many interactions between species are realized indirectly, through effects on a shared environment. For example, consumers compete indirectly by altering resource availability [244, 46]. However, the ways that species affect and are affected by their environment extend far beyond the consumption of resources. Across the tree of life, and over a tremendous range of spatial scales, organisms make complex and sometimes substantial changes to the physical and chemical properties of their local environment [120, 250, 196, 148]. Many species also impact local biotic factors; for example, plant-soil feedbacks are often driven by changes in soil microbiome composition [250, 31, 188, 155].

Numerous studies have recognized and discussed the ways such changes can mediate interactions between species, as well as the obstacles to modeling these complex, indirect interactions [96, 31, 196, 119, 169]. In some instances, the effects of environmental modification by one species on another can be accounted for implicitly in models of direct interactions [253, 46, 3], or within the well-established framework of resource competition [169, 194]. But in many other cases, new modeling approaches are necessary.

Because the range of ecosystems where interactions are driven by environmental modification is wide and varied, many parallel strands of theory have developed for them. Examples include "traditional" ecosystem engineers [86, 259, 111, 131, 197], plant-soil feedbacks [31, 198, 250], and chemically-mediated interactions between microbes [169, 196]. Similar dynamics underlie Janzen-Connell effects, where individuals (e.g., tropical trees) modify

Miller, Zachary R., and Stefano Allesina. "Metapopulations with habitat modification." *Proceedings of the National Academy of Sciences* 118, no. 49 (2021).

their local environment by supporting high densities of natural enemies [118, 54, 15, 188], and immune-mediated pathogen competition, where pathogen strains modify their hosts by inducing specific immunity [85, 11, 76, 50]. These last two examples highlight that environmental modification might be "passive", in the sense that it is generated by the environment itself.

While each of these systems has attracted careful study, it is difficult to elucidate general principles for the dynamics of environmentally-mediated interactions without a simple, shared theoretical framework. Are there generic conditions for the coexistence of many species in these systems? What are typical relationships between diversity and ecosystem productivity or robustness? We especially lack theoretical expectations for high-diversity communities, as most existing models focus on the dynamics of one or two species [31, 86, 259, 250].

To begin answering these questions, we introduce and analyze a flexible model for species interactions mediated by environmental modification. Two essential features of these interactions – which underlie the difficulty integrating them into standard ecological theory – are that environmental modifications are localized in space and persistent in time [96]. To capture these aspects, we adopt the metapopulation framework, introduced by Levins [144], which provides a minimal model for population dynamics with distinct local and global scales. Metapopulation models underpin a productive and diverse body of theory in ecology [92, 91], including various extensions to study multi-species communities [139, 82]. Here, we adopt the simplest such extension, by assuming zero-sum dynamics and an essentially horizontal community [245, 81]. Our modeling framework accommodates lasting environmental modification by introducing a versatile notion of "patch memory", in which the state of local sites depends on past occupants.

In line with evidence from a range of systems, we find that patch memory can support the robust coexistence of any number of species, even in an initially homogeneous landscape. We

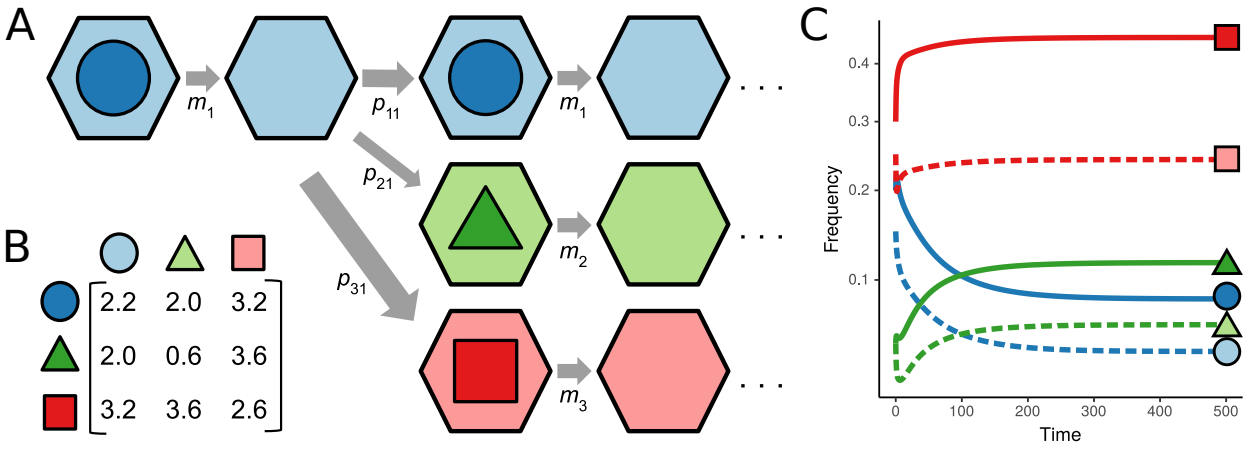

Figure 4.1: Metapopulation model with patch memory effects. (A) Schematic view of the model. Patches (hexagons) may be occupied by any of n (here, 3) species (distinguished by color and shape). Upon local extinction of the resident species, which happens at rate m_i, a patch becomes vacant, but retains a "memory" of the last resident (light color). The memory state of a vacant patch determines the rate at which it is (successfully) re-colonized by each species in the community (arrow thickness proportional to rate p_{ij}). Note that colonization events occur at a rate proportional to the frequency of the colonizing species ($p_{ij}x_i$), while local extinction rates are constant per patch. Dynamics for the 3-species community with colonization rates (P matrix) given in (B) are shown in (C). The frequency of patches occupied by each species (x_i) is shown with solid lines of the corresponding color, while vacant patches in each memory state (y_i) are shown with dashed lines. In this example, the colonization rate matrix is symmetric and has exactly one positive eigenvalue, so the community exhibits stable coexistence (see section Symmetric memory effects). In (C), $m = 1$ for all species.

derive quantitative conditions for species' coexistence and show how they connect to existing conceptual models. Importantly, these conditions apply even as several model assumptions are relaxed. We also investigate an emergent relationship between species diversity and robustness, demonstrating that our modeling framework can provide new insight for a variety of systems characterized by localized environmental feedbacks.

4.2 Results

4.2.1 Model

We consider a community of n species inhabiting a landscape composed of many local patches, all linked by dispersal. At any time, each patch may be occupied by a single species or vacant. A patch becomes occupied by colonization from another patch, and is made vacant by local extinction. In contrast to traditional metapopulation models, vacant patches are not homogeneous. Instead, each vacant patch may be in one of n states, corresponding to its last resident, and modeling the effects of modification by that resident. We refer to these modifications collectively as patch memory effects. The ability of species to successfully establish in a patch is sensitive to environmental state, and consequently the state of a vacant patch determines the rate at which it is recolonized by any species in the community.

A simple model for community dynamics incorporating these processes (Fig. 4.1) is:

$$\begin{aligned} \frac{dx_i(t)}{dt} &= -m_i\, x_i(t) + x_i(t) \sum_{j=1}^{n} p_{ij}\, y_j(t) \\ \frac{dy_i(t)}{dt} &= m_i\, x_i(t) - y_i(t) \sum_{j=1}^{n} p_{ji}\, x_j(t) \end{aligned} \tag{4.1}$$

where $x_i(t)$ is the proportion of patches occupied by species i at time t and $y_i(t)$ is the proportion of vacant patches in state i (i.e., last occupied by species i). The parameters $p_{ij} \geq 0$ specify the rate at which species i can colonize patches in state j. The local extinction rate for species i is given by $m_i > 0$.

This system has close connections to existing ecological models. Eq. (4.5) reduces to the Levins' metapopulation model when $n = 1$. Neglecting memory effects, the underlying n-species model is conceptually similar to a lottery system [206, 261]. And the full system

is closely related to models of infectious disease with multiple strains and partial immunity. As indicated above, when hosts are viewed as patches, with memory effects provided by immunological memory, strain competition is characterized by precisely the kind of dynamics that motivate this study. In fact, our model can be seen as a simplification of the model by Andreasen *et al.* [11], describing a system with short-term immunity in which only the most recent infection is tracked. As widely discussed in the literature on metapopulation dynamics [92] and compartmental models in epidemiology [63], the form of Eq. (4.5) reflects several standard assumptions: most notably, that the number of patches is large and fixed, and that colonizers or propagules disperse randomly across the landscape. Depending on the context, patches may represent local populations with fast within-patch dynamics, or sites holding a single individual, such as trees in a forest [245].

Patch memory effects in this model are entirely captured by the matrix of species-by-state colonization rates, $P = (p_{ij})$. Rather than track the (potentially many) internal properties of each patch that affect and are affected by resident species, we incorporate them implicitly through these rates. A change in patch state may increase or decrease the rate of colonization by each species, as a net result of factors that facilitate or impede successful establishment. This simplification permits us to model scenarios where the factors mediating patch memory are unknown or complex, and to apply a common modeling framework across systems where these mechanisms differ. Our approach builds on a rich literature modeling metapopulation dynamics in heterogeneous landscapes [142, 106, 8]; however, in our model environmental heterogeneity is generated by the community itself.

We also suppose that the state of a vacant patch depends only the last resident species, and only affects species' colonization rates, not local extinction rates. Both of these features reflect an underlying assumption that species modify their local environment on a shorter timescale compared to that of extinction. The modifications of each species "overwrite" previous alterations, such that the earlier occupancy history of a patch has negligible effect

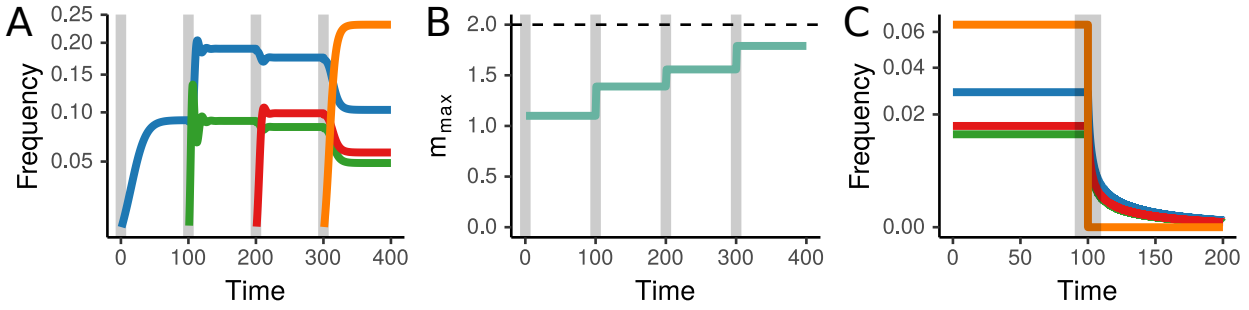

Figure 4.2: Diversity and coexistence with species-specific memory effects. We consider a pool of 4 species with negative memory effects $\boldsymbol{\alpha}$ = (-0.9, -1.9, -1.6, -0.4) and $\beta = 2$. These species coexist stably from any non-zero initial condition, provided that the common extinction rate, m, is not too large. The maximum sustainable extinction rate, denoted $m_{\max}$, is a function of the species present. As successive species join the community (A), $m_{\max}$ increases (B). Species introductions are marked with vertical gray lines. While $m_{\max}$ always increases with diversity, eventually saturating at $m_{\max} = \beta$ (dashed line in (B)), the frequency of individual species may increase or decrease. For example, in (A) the equilibrium frequency of species 1 (blue) increases when species 2 (green) joins the community, but decreases with each subsequent species introduction. (C) The positive relationship between $m_{\max}$ and species richness means that whole-community collapse is possible when diversity is reduced. Here, all species can coexist with $m = 1.57$, but when species 4 (orange) is removed at time $t = 100$ (vertical gray bar), $m_{\max}$ drops below m, and all species go extinct. In (A), on the other hand, $m = 1$, which permits coexistence at any level of richness. For clarity, unoccupied patch frequencies are not shown.

on current colonization rates. This kind of behavior arises naturally when all species modify a small number of shared environmental features, such as pH or physical structure, and new changes necessarily efface old ones [196, 148]. It is also likely to be a good approximation for many communities where modifications wane without maintenance (see below), resulting in patch memory that is effectively characterized by the most recent occupant [58].

When there is no patch memory (i.e., $p_{ij} = p_{ik}$ for all i, j, and k), the model does not generally admit a biologically feasible equilibrium (an equilibrium with all positive frequencies). The only robust outcome in this case is the eventual extinction of all but one species. However, with patch memory, any number of species may potentially coexist at equilibrium. For a community of n species, this full coexistence equilibrium is unique if it exists. Assuming P is invertible, the steady-state frequencies for vacant patches are simply $\boldsymbol{y}^\star = P^{-1}\boldsymbol{m}$, where $\boldsymbol{m} = (m_1, m_2 \ldots m_n)$. In general, $\boldsymbol{x}^\star$, the vector of steady-state frequencies for the n species, is obtained by solving an eigenvector problem with no closed form solution (although $\boldsymbol{x}^\star$ can be written explicitly under special conditions). However, the signs of $\boldsymbol{x}^\star$, and thus the feasibility of the equilibrium state, can always be determined from $\boldsymbol{y}^\star$ alone. In Supporting Information 4.5.1, we show that the conditions $y_i^\star > 0$ for all i and $\sum_i y_i^\star < 1$ are necessary and sufficient for feasibility.

In this study, we are interested in understanding the long-term dynamics of the model. We first consider cases in which P is highly structured, allowing a complete characterization of the long-term dynamics. Then, we go on to examine conditions for coexistence in more general parameterizations of the model.

4.2.2 Species-specific memory effects

When patch memory effects are species-specific, the colonization rate matrix, P, has a very simple structure:

$$p_{ij} = \begin{cases} \beta + \alpha_i \,, & i = j \\ \beta \,, & i \neq j \end{cases} \quad . \tag{4.2}$$

Here, $\beta \geq 0$ is the "background" rate of colonization, and α_i expresses the patch memory effects of species i on conspecifics. We allow each α_i to be positive or negative, subject to $\alpha_i > -\beta$ (ensuring colonization rates are non-negative). This form of P models a community where every species modifies and responds to unique properties of the local environment. A number of important and well-studied ecological processes are characterized by this kind of memory effect; for example, local enhancement of specialized natural enemies [118, 54] or specific mycorrhizal symbionts [236] in plant communities, and multi-strain disease dynamics with weak cross immunity [50]. Previous theoretical and empirical studies suggest that memory effects leading to positive intraspecific feedback ($\alpha_i > 0$) should be destabilizing, while negative feedback ($\alpha_i < 0$) provides a source of self-regulation, thereby promoting species diversity [118, 54, 31, 250, 196].

If all species have identical local extinction rates, m—as, for example, among demographically equivalent species or when extinction is driven by external disturbance—the steady-state abundance of a species i is:

$$x_i^\star = \frac{1}{\alpha_i} \left(\frac{R(\boldsymbol{\alpha})^{-1} + \beta - m}{1 + \beta\, R(\boldsymbol{\alpha})} \right). \tag{4.3}$$

The quantity $R(\boldsymbol{\alpha}) = \sum_i \frac{1}{\alpha_i}$ summarizes the net memory effects in the community. Because the factor in parenthesis in Eq. 4.3 does not depend on i, feasibility of the equilibrium (with corresponding $\boldsymbol{y}^\star$) requires that all α_i have the same sign. In Supporting Information 4.5.2, we show that if all $\alpha_i > 0$, the coexistence equilibrium is unstable whenever $n > 1$. When all $\alpha_i < 0$, the equilibrium is instead globally stable, so that coexistence is robust to any

perturbation of species frequencies short of extinction. These results align precisely with previous studies that identify stable coexistence with negative environmental feedback.

This highly idealized scenario provides insight into the relationship between diversity and coexistence that extends to systems with more general memory effects. Assuming now that $\alpha_i < 0$ for all i, $\boldsymbol{x}^\star$ will be feasible (and therefore stable) if and only if the common local extinction rate is not too large:

$$m < R(\boldsymbol{\alpha})^{-1} + \beta \quad . \tag{4.4}$$

The stability criteria imply that this bound on m is strictly increasing as new species are added to the community (Fig. 4.2A-B). In other words, the model exhibits a positive relationship between diversity and community robustness, defined here as the capacity to tolerate increased disturbance or more marginal environmental conditions (i.e., larger m). This effect arises as each new species in the system effectively dilutes the (negative) specific patch memory effects experienced by others. At the same time, however, all species compete for a fixed number of patches. These contrasting effects of diversity are manifest in the relationship between the equilibrium abundance of a focal species, i, and $R(\boldsymbol{\alpha})$ (i.e., a measure of effective species diversity). When diversity is low, $R(\boldsymbol{\alpha})^{-1}$ is very large and negative. Here, $x_i^\star$ may be increased by the arrival of new species. As more species join the community, however, the beneficial dilution effect of diversity quickly saturates, and $x_i^\star$ begins to decrease due to the competitive effect of each new species (see, for example, the dynamics of species 1 in Fig. 4.2A). This transition occurs at the critical value $R(\boldsymbol{\alpha}) = \frac{1}{m-\beta}(1 + \sqrt{\frac{m}{\beta}})$.

The results of this section are largely unchanged by variation in local extinction rates among species. When the rates m_i differ, the coexistence equilibrium can become unfeasible; however, the (global) stability of any internal equilibrium point depends only on the signs of α_i. Additionally, there remains a well-defined positive diversity-robustness relationship (see Supporting Information 4.5.2).

4.2.3 Symmetric memory effects

Next, we consider the more general class of symmetric memory effects, i.e., $p_{ij} = p_{ji}$ for all i and j. This kind of rate structure may arise whenever patch memory effects depend on some measure of similarity between species. For example, if the local abundances of different predators (pathogens, mutualists, etc.) determine establishment rates, and resident species drive recruitment of their respective predators, then the rates $p_{ij} = p_{ji}$ will depend on the number of shared predators of species i and j. Similarly, for bacterial species with different preferences for environmental pH, and which modify the pH according to their preference, the induced memory effects would be symmetric. This kind of symmetry is considered typical in immune cross-reactivity, as well [224].

For two species, any symmetric matrix can be written in the same form as Eq. 4.2, so the results of the previous section apply. Assuming feasibility, the two-species equilibrium is globally stable if and only if $p_{12} = p_{21} > \max(p_{11}, p_{22})$, regardless of m_1 and m_2. As noted above, this requirement captures the notion that negative feedbacks must predominate in the system for coexistence to be stable. When this condition is met, each species has an advantage colonizing patches last occupied by the other, which generates negative frequency dependence. But how does this intuition generalize to larger communities where patch memory effects cannot be neatly partitioned into intra- and inter-specific components?

In more diverse communities, a different approach is needed to assess stability. Under the assumption of identical local extinction rates (as discussed above) we can study the local stability of the coexistence equilibrium for any n. The weaker notion of local stability characterizes the system's response to small perturbations from equilibrium. For symmetric P, we show (Supporting Information 4.5.3) that the coexistence equilibrium will be locally stable whenever P has exactly one positive eigenvalue (Fig. 4.3). Because P is non-negative, it is guaranteed to have a positive eigenvalue, called the Perron eigenvalue. Thus, our stability condition requires that this is the *only* positive eigenvalue of P.

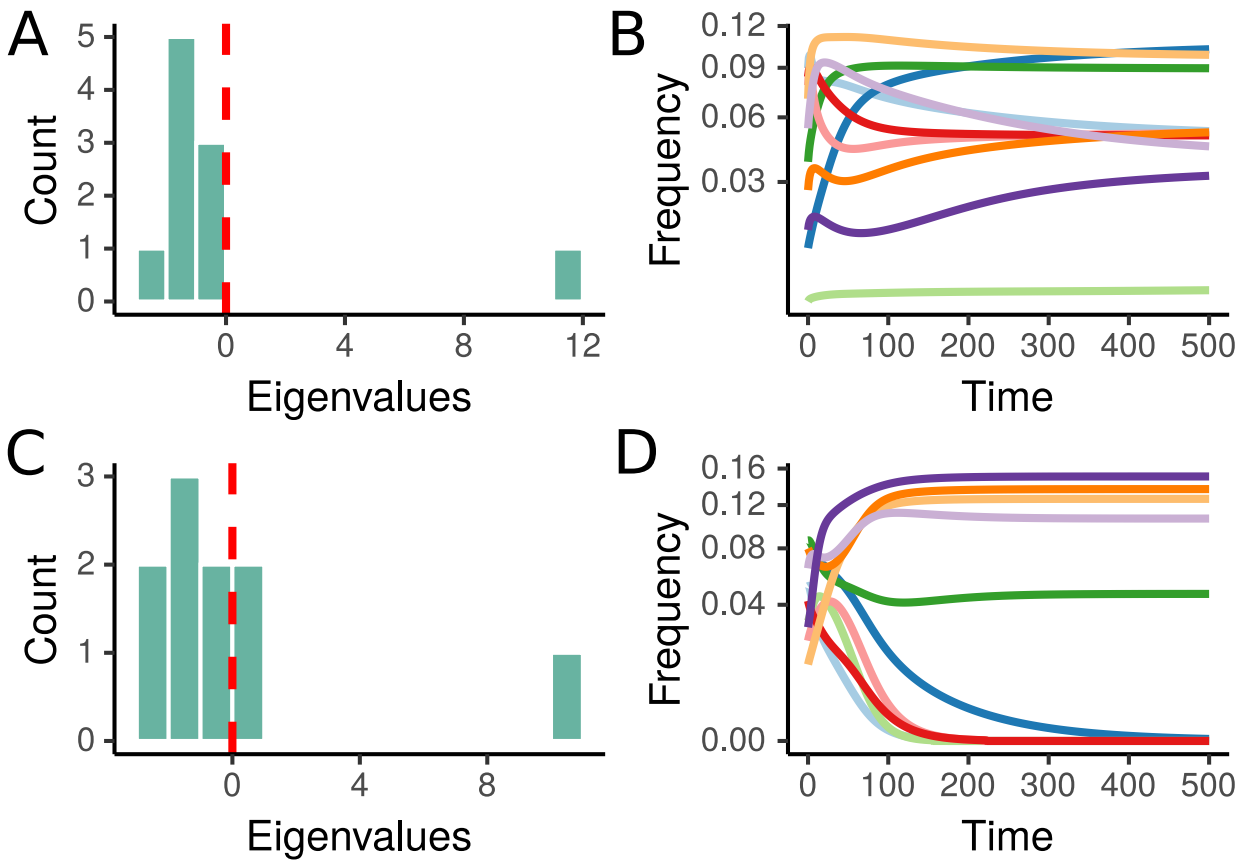

Figure 4.3: Stability criterion for symmetric memory effects. (A) When the colonization rate matrix P has exactly one positive eigenvalue, any feasible equilibrium is locally stable. (B) Coexistence emerges through the dynamics for the 10-species community corresponding to (A). (C) When P has any additional positive eigenvalues, the coexistence equilibrium is unstable. (D) For the 10-species community corresponding to (C), 5 species go extinct, despite the existence of a feasible equilibrium. The dynamics prune the community to a subset that meets the coexistence criteria. In (B) and (D), $m = 1$ for all species. For clarity, vacant patch frequencies are not shown. All parameter values can found in the online code [165].

In general, there is no simple characterization of this stability condition in terms of inequalities between elements of P, as was possible for $n = 2$. However, we can find separate necessary and sufficient conditions for a positive symmetric matrix to have exactly one positive eigenvalue [183]. These partial characterizations provide biological intuition for the stability condition. First, a necessary condition: $p_{ij} \geq \min(p_{ii}, p_{jj})$ for all i and j, to have the possibility of coexistence. On the other hand, if $p_{ij} > \frac{1}{n}\sum_{k=1}^{n} p_{ik}$ for all $i \neq j$, then a feasible coexistence equilibrium is guaranteed to be stable. Naturally, the second condition is stronger than the first, and in fact implies $p_{ij} > \max(p_{ii}, p_{jj})$. Fig. 4.1B-C shows an example of a stable system that meets the first (necessary) condition, but not the second. Both conditions place limits on the strength of same-species memory effects (i.e., the magnitudes of p_{ii}) relative to inter-specific effects. In this way, the requirement that P has exactly one positive eigenvalue is a natural generalization of the intuitive notion that all species must be at a disadvantage when colonizing patches last occupied by conspecifics.

While this characterization of stable coexistence relies on local stability and identical local extinction rates, extensive numerical evidence suggests that stability is in fact global and unaffected by different m_i (Supporting Information 4.5.3), as can be proved in the more tractable species-specific case. Expressing equilibrium frequencies (and therefore characterizing feasibility) is also less straightforward for arbitrary n. However, the symmetry of P means that $\boldsymbol{x}^\star$ will be proportional to $\boldsymbol{y}^\star$ (see Supporting Information 4.5.1). Because $\boldsymbol{y}^\star$ solves a linear system of equations, a number of techniques may be applied to characterize feasibility and the distribution of species abundances in special cases, such as communities structured by phylogeny or functional groups [214], or when colonization rates are randomly distributed [213]. Additionally, we can ask how diversity affects the "community-wide" feasibility condition, $\sum_i y_i^\star < 1$. In the previous section, this condition gave rise to a positive relationship between diversity and robustness (i.e., the range of m values compatible with coexistence). In Supporting Information 4.5.3, we prove that the same is true here: For any

symmetric system with equal rates m, the stability criterion induces a positive diversity-robustness relationship. Specifically, whenever a species is added to a coexisting community and the augmented equilibrium is stable, $m_{\max}$ must increase. In other words, a coexisting community is always more robust than any of its subsets. While this result alone gives no indication of the strength of the relationship, we show that the robustness benefit of increasing species diversity can be substantial in simulated communities with randomly-distributed memory effects.

4.2.4 Nonsymmetric memory effects

When patch memory effects are not symmetric, a wide variety of dynamics are possible, including non-equilibrium coexistence. To illustrate the range of outcomes, we consider two particular structures for P. We will see that these examples also shed light on typical behaviors for nonsymmetric systems.

Our first example extends the symmetric case to allow variation in dispersal ability. We have so far implicitly assumed that species have equal dispersal rates in defining p_{ij}, which, in practice, represents a composite of two factors: dispersal (ability to reach a new patch) and establishment (ability to successfully establish residence). If each species now has a characteristic dispersal rate, c_i, and the establishment rates $P' = (p'_{ij})$ have a symmetric structure, then $p_{ij} = c_i\, p'_{ij}$ and P is *symmetrizable*. While the colonization rate matrix is nonsymmetric, we find that stability is governed solely by the eigenvalues of the establishment rate matrix, P', according to the stability condition for symmetric matrices (Supporting Information 4.5.4).

In our second example, P is proportional to a cyclic permutation matrix. Here, patches last occupied by species i may only be colonized by species j, patches vacated by j may only be colonized by k, and so on, forming a loop. This intransitive structure is well-known to ecologists, as in the three-species "rock-paper-scissors" dynamics [6]. In our model, this kind

of P matrix can be seen as a caricature of successional dynamics or facilitation cascades [239], where each species modifies the environment in a way that leads to colonization by the next in the cycle. Strictly interpreted, this structure assumes that the successional process forms a closed loop [249, 198], but these dynamics might also approximate transitive succession in the presence of disturbance [8].

Assuming identical local extinction rates, m, and colonization rates, c, all species have equal equilibrium frequencies. In contrast to our previous cases, the stability of this equilibrium now depends on the magnitude of m (see Supporting Information 4.5.4). For sufficiently small m, the coexistence equilibrium is locally stable and approached by damped oscillations. However, when $n > 2$ there is a threshold value, m_c, above which the equilibrium point loses stability and the dynamics approach a stable limit cycle. The amplitude of these cycles increases sharply as m increases, making coexistence above m_c tenuous in any real system where environmental and demographic fluctuations would be present. When m is sufficiently large, feasibility is lost altogether. For example, the three species community shown in Fig. 4.4A begins to cycle at $m_c = 2/9$ and loses feasibility at $m_{\max} = 1/3$. Unlike the symmetric cases, this feasibility threshold decreases as n increases, so that diverse communities are actually less robust to elevated local extinction rates.

These qualitative behaviors are shared by many nonsymmetric systems. For randomly-distributed P, a progression from stable coexistence, to limit cycles, to species extinctions is often observed as m increases and abundances decrease (e.g., Fig. 4.4B; see Supporting Information 4.5.4 for additional simulations). The frequent appearance of a bifurcation point at high m indicates that coexistence mediated by nonsymmetric memory effects is "fragile" in marginal environments. As disturbance increases or environmental quality deteriorates, these systems can collapse sooner than expected on the basis of abundance declines alone (i.e., before feasibility is lost).

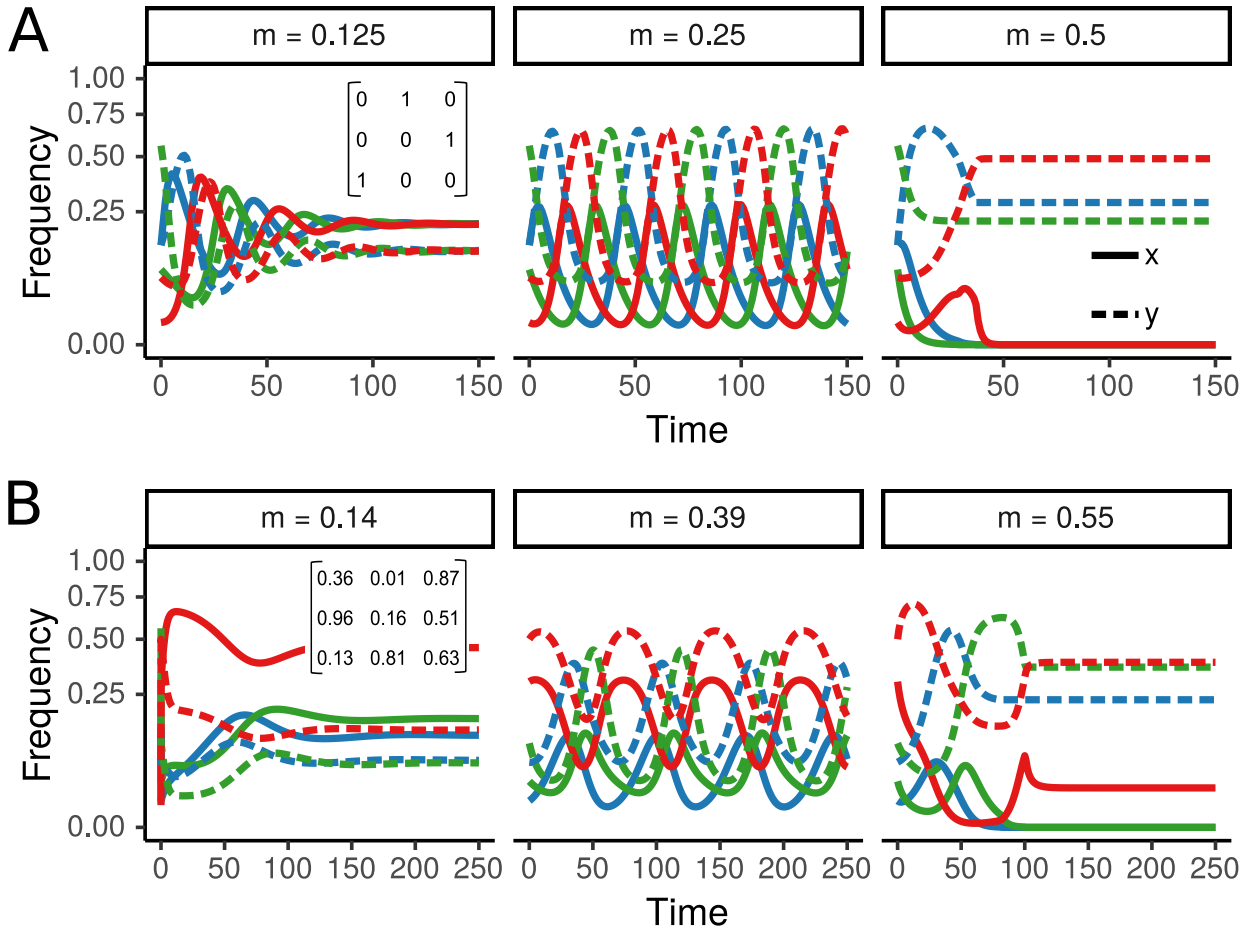

Figure 4.4: Loss of stability with nonsymmetric memory effects. When P is nonsymmetric, the long-term dynamics can depend on the magnitude of local extinction (m), even when all species experience equal extinction rates. (A) For the 3-species community with cyclic memory effects, a stable equilibrium exists at low m, but gives way to limit cycles at $m = 2/9$. Beyond $m = 1/3$, all species go extinct. (B) This qualitative progression is often observed for nonsymmetric matrices sampled at random, for example the 3-species community shown here. The frequencies of patches occupied by each species (x_i) are shown with solid lines, while unoccupied patches in each memory state (y_i) are shown with dashed lines.

4.2.5 Waning memory

Our model assumes that patch memory persists indefinitely, until a patch is re-colonized. This may be reasonable when the mechanisms mediating patch memory are durable, or when the typical time to re-colonization is short. However, in many systems, we expect patch memory effects to decay in time. For example, nutrient concentrations might re-equilibrate, and physical modifications may erode. This assumption is particularly problematic for modeling pathogen strain competition, where our model is best viewed as an approximation to systems with short-term immunological memory (i.e., immunity well-characterized by the last infection). Clearly this is at odds with the indefinite persistence of memory effects in the absence of new colonization.

To relax the persistent memory assumption, we extended our model to include an additional "naïve" state (see Supporting Information 4.5.5). Our extended model mirrors Eq. (4.5), except that vacant patches of each type i decay into a naïve state at a constant rate, d_i, simulating waning patch memory. Each species colonizes naïve patches at a constant rate, c_i, regardless of the identity of the previous resident.

How do these changes affect the long-term dynamics? For simplicity, we analyze the case where P is symmetric, and all species have equal demographic rates m, c, and d. Under these assumptions, the conditions for coexistence of n species are very closely related to those found without waning memory. In particular, the requirement that P must have exactly one positive eigenvalue for stability still holds. Now, however, this condition only indicates local, not global, stability of the coexistence equilibrium. This distinction is important because the model can exhibit bistability (discussed below). As before, feasibility of the coexistence equilibrium depends on the signs of $\boldsymbol{y}^\star \propto P^{-1}\mathbf{1}$, in addition to a community-wide condition on the demographic parameters.

The space of outcomes, including global stability of the coexistence equilibrium, bistability, or no feasible equilibrium, is presented graphically in Fig. 4.5A, and derived in Supporting

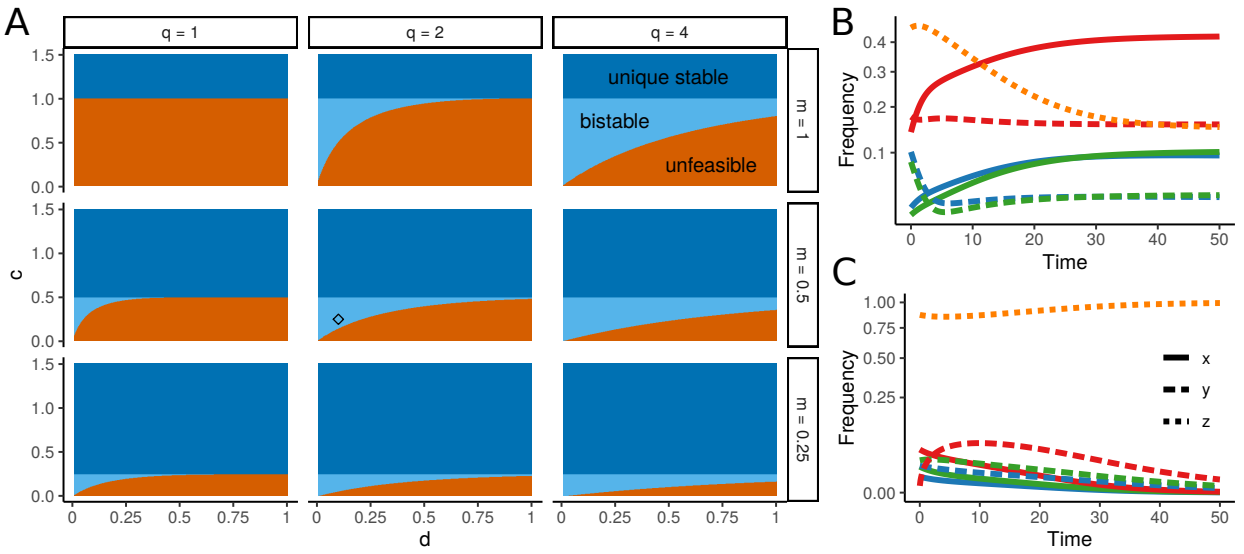

Figure 4.5: Coexistence conditions for waning (symmetric) memory effects. (A) Assuming P has exactly one positive eigenvalue and $P^{-1}\mathbf{1} > 0$ elementwise, the long-term dynamics depend on the relationship between demographic parameters m (local extinction rate), d (memory decay rate), c (colonization rate for naïve patches), and q (a statistic quantifying the effective community-wide colonization rate; see main text and Supporting Information 4.5.5). When $c > m$, there is a unique, stable coexistence equilibrium for all d and q (dark blue). When $c < m$, there may be no feasible equilibrium (orange). However, coexistence is possible when d is sufficiently small, and c and q are sufficiently large. In that case (light blue), there is a strong Allee effect. Coexistence is locally stable, but requires that species are not too rare initially. (B) and (C) show two possible outcomes for the parameter combination indicated by the black diamond in (A). (B) When initial frequencies of community members are high enough, all 3 species coexist stably. (C) When naïve patches are initially abundant, the community collapses and all species go extinct. In (B) and (C), the frequencies of patches occupied by each species (x_i) are shown with solid lines, unoccupied patches in each memory state (y_i) are shown with dashed lines, and naïve patches (z) are shown with dotted orange line. The matrix P used for this example is from Fig. 1.1B.

Information 4.5.5. The primary determinant of coexistence is the ratio between c and m: When $c > m$, the coexistence equilibrium is always feasible, and the only stable fixed point. When $c < m$, coexistence may be impossible (no feasible equilibrium) or contingent on initial conditions (bistability). In this second regime, the coexistence equilibrium is locally stable, but a community-wide Allee effect operates at low species abundances. If the initial fraction of naïve patches is not too large, all species coexist, while if naïve patches are very abundant, all species go extinct.

This strong Allee effect is present when $c < m$, d is small, and the net colonization rate of patches with memory (measured by a summary statistic of P, $q = (\mathbf{1}^T P^{-1} \mathbf{1})^{-1}$) is sufficiently large. These conditions correspond to an ecosystem where no species is able to colonize naïve patches fast enough to outpace local extinction ($c < m$), but patch memory effects facilitate colonization overall, and memory effects are sufficiently durable to influence the dynamics. Negative feedbacks for each species maintain diversity, while a positive community-wide feedback maintains the growth rates of all species once their frequencies exceed a certain threshold. This picture can become much more complicated if species vary significantly in their rates of memory decay and naïve patch colonization. In this general setting, it is possible for Allee effects to emerge on multiple timescales, leading to more complex multistability.

4.3 Discussion

Species interactions mediated by local environmental feedbacks are ubiquitous in natural systems and arise from many different proximal mechanisms. We presented a highly simplified but flexible model for the dynamics of such communities, with the goal of elucidating general principles that govern coexistence across these disparate settings. Our model recapitulates behaviors observed empirically and in system-specific theory, namely coexistence of many species maintained by negative feedbacks [31, 188, 155, 15, 76]. By virtue of the simplicity of

the model, we were able to derive precise conditions for this coexistence, in addition to novel predictions regarding diversity and community robustness, and the emergence of bistability when memory effects are impermanent.

Our central finding, that patch memory effects allow the potential coexistence of any number of species, shares close conceptual similarities with models of facilitation-driven coexistence [162], particularly microbial crossfeeding [40, 156]. In these phenomena and our model, high species diversity can be maintained because community members generate elevated environmental heterogeneity relative to the abiotic background. But in contrast to crossfeeding models, where the number of coexisting species is eventually bounded by the number of distinct resources produced and consumed, our model of patch memory automatically produces the possibility of coexistence no matter how many species are added to the community.

Of course, the possibility of coexistence is no guarantee that it will be realized. We have shown that there are nontrivial – but interpretable – conditions for the feasibility and stability of equilibria in our model. These conditions are unlikely to be met when parameters are drawn at random. However, a number of ecological and evolutionary mechanisms are known that may structure memory effects in way that would promote coexistence [76, 31, 118, 54]. Our model can provide theoretical guidance to help understand these mechanisms and their associated colonization rate structures. For example, there has been significant debate over the degree of enemy specialization needed to produce coexistence through Janzen-Connell effects, which can be modeled (in a simplistic way) through our framework [69, 211, 207]. And for symmetric memory effects, the stability condition we derived offers a natural and precise generalization of the rule that environmental modification must produce negative feedbacks for every species.

Aside from clarifying and generalizing the conditions for coexistence, our model makes several distinct predictions about the relationship between diversity and robustness. When

memory effects are symmetric, more diverse communities can tolerate higher local extinction rates. This phenomenon is due to "dilution effects" closely related to those studied in disease ecology [53]. If memory effects decay in time, the benefits of diversity may be even greater. In the bistable regime, high diversity in terms of species richness *and* relative abundance is needed to maintain coexistence. However, a negative relationship between diversity and robustness is observed when communities form a successional cycle, indicating that varied behaviors are possible even in this simple model, and that qualitatively distinct rate structures can support coexistence.

In the cases where diversity promotes robustness, coexistence may be sensitive to species loss as a result. Fig. 4.2C shows an example where the removal of a single species causes the extinction of the entire community. In the waning memory model, even perturbing some species to low abundance may cause such a collapse. These outcomes are most likely in marginal environments (high m). The dependence of long-term outcomes on the magnitude of m – observed in the nonsymmetric case, as well, through the loss of stability as m increases – is a surprising behavior that has no analog in simple models of community dynamics that do not incorporate local environmental feedbacks (e.g., generalized Lotka-Volterra models).

Our model is not meant to capture the detailed behavior of any particular community, but instead to highlight and investigate the essential dynamics common to a range of systems. This approach strikes a balance between models that explicitly incorporate the mechanisms of environmental modification [74, 196, 172] and those that fold environmental modification into direct interactions between species [46, 253, 3]. We view our approach as complementary to both. Despite its simplicity, our model exhibits rich and informative dynamics. It may also be possible to parameterize and test our model in empirical systems where investigators have measured parameters akin to our colonization rate matrices [31, 188, 250].

Inevitably, this approach requires us to make several strong assumptions about the underlying metapopulation dynamics of the community. For instance, we ignore the possibility

of age or stage structures; complex spatial structures; co-occupancy of patches; and direct interactions between species. Many or all of these factors will be present in natural landscapes, and each has been shown to affect the dynamics of model communities [261, 91, 82]. However, by omitting these and other factors known to shape community dynamics, we are able to isolate the behavior of environmentally-mediated interactions, especially in relation to species coexistence. Integrating additional processes will likely raise interesting questions. To take one example, strong spatial structure, which is a central feature of many of the systems discussed here, might stabilize oscillatory dynamics, like those shown in Fig. 4.4, by coupling out of sync patches [198] or distributing oscillations over space [127]. Alternatively, though, localized dispersal could lead to spatial segregation of species, decoupling the successional cycles or negative feedbacks that sustain community diversity.

We have shown that our main findings are robust to relaxing one central assumption of the model – the permanence of memory effects – although qualitatively new behaviors arise in this case, as well. Many natural systems likely violate our model assumptions in the opposite direction, by exhibiting memory effects that endure beyond each new colonization event. Adaptive immunity, where memory effects may be lifelong, is an obvious example [85, 76, 50], but many others are possible. It is straightforward to extend our model to include longer-term memory effects, but not to analyze such extensions, which require a precipitous expansion of the state space and model complexity [11, 76]. It may be possible to consider other approximations, such as memory influencing extinction rates, or patch memory of the last two or three occupants – although even characterizing the behavior of our simple model under the most general (nonsymmetric) parameterizations remains an open problem. Expanding ecological theory to account for environmental feedbacks – beyond resource competition – on multiple spatial and temporal scales remains a key challenge and opportunity for further investigation.

4.4 Materials and methods

All computations (simulations and calculation of eigenvalues) were conducted in R (version 3.6.3). Where dynamics are shown, the model equations (Eq. 4.5) were solved numerically using the deSolve package with the "ode45" Runge-Kutta method. Coexistence conditions shown in Fig. 4.5A were obtained using Mathematica (see Supporting Information 4.5.5 for details). Code to generate all figures and simulation results is available on GitHub [165].

4.5 Supporting information

4.5.1 Model equations and coexistence equilibrium

Model equations

It is convenient to express our model (Eq. 4.1 in the main text) in matrix form:

$$\begin{aligned} \frac{d\boldsymbol{x}(t)}{dt} &= D(\boldsymbol{x}(t))\left(-\boldsymbol{m} + P\boldsymbol{y}(t)\right) \\ \frac{d\boldsymbol{y}(t)}{dt} &= \left(D(\boldsymbol{m}) - D(\boldsymbol{y}(t))P^T\right)\boldsymbol{x}(t) \end{aligned} \tag{4.5}$$

Here, $D(\boldsymbol{z})$ denotes a diagonal matrix with vector $\boldsymbol{z}$ on the diagonal. Vectors $\boldsymbol{x}(t) \in \mathbb{R}^n$ and $\boldsymbol{y}(t) \in \mathbb{R}^n$ express the frequency (at time t) of patches occupied by species i and vacant patches last occupied by species i ("in state i"), respectively. $\boldsymbol{m} \in \mathbb{R}^n$ is a vector of local extinction rates, $m_1, \ldots, m_n > 0$, and $P \in \mathbb{R}^{n\times n}$ is a matrix of non-negative colonization rates.

As discussed in the main text, this system of equations generalizes Levins's classical metapopulation model in two ways: (i) there are n species in the landscape, which interact by competing for patches, and (ii) vacant patches retain a "memory" of their last resident species, which determines the rate of re-colonization by every species in the community. The

fact that each patch may be occupied by only a single species at any time (and therefore species compete for free patches) means that every patch is counted exactly once in the state variables $\boldsymbol{x}(t)$ and $\boldsymbol{y}(t)$. This implies zero-sum dynamics, as verified by summing:

$$\sum_i \frac{dx_i(t)}{dt} + \frac{dy_i(t)}{dt} = \sum_i \left(-m_i\, x_i(t) + x_i(t) \sum_{j=1}^{n} p_{ij}\, y_j(t) + m_i\, x_i(t) - y_i(t) \sum_{j=1}^{n} p_{ji}\, x_j(t) \right) = 0\,.$$

Patches, therefore, are never created or destroyed through the dynamics. Since the invariant quantity $T = \sum_{i=1}^{n} x_i + \sum_{i=1}^{n} y_i$ is arbitrarily determined by the initial conditions, we assume throughout that $T = 1$; in other words, $\boldsymbol{x}(t)$ and $\boldsymbol{y}(t)$ are frequencies.

In the following sections, we analyze the model (Eq. 4.5) in detail for arbitrary n and considering a range of assumptions.

Coexistence equilibrium

The system defined by Eq. 4.5 admits 2^n equilibria, corresponding to distinct combinations of species presence/absence (and counting the degenerate equilibrium with $\boldsymbol{x}(t) = 0$). In this study, we are primarily interested in the existence and stability of the unique equilibrium where all species (and patch states) are present at non-zero frequency – we refer to this as the *coexistence equilibrium*. To solve for the coexistence equilibrium (frequencies $\boldsymbol{x}^\star$ and $\boldsymbol{y}^\star$, dropping the time dependence), we first set $\frac{d\boldsymbol{x}}{dt} = 0$, which yields the linear system

$$P\boldsymbol{y}^\star = \boldsymbol{m} \tag{4.6}$$

for $\boldsymbol{y}^\star$. When P has full rank, the equilibrium frequencies are found by matrix inversion: $\boldsymbol{y}^\star = P^{-1}\boldsymbol{m}$. Invertibility of P requires (at a minimum) that patch memory effects operate in the system. If not, then $p_{ij} = p_{ik} = p_i$ for all i, j, and k (i.e., P has constant rows), which means P is a rank-one matrix, and therefore non-invertible for any $n > 1$. In this

case, Eq. 4.6 admits a solution only if $\boldsymbol{m}$ is exactly proportional to the columns of P. If not, there is no equilibrium at all. However, even if this proportionality holds, there is no robust equilibrium. This situation, corresponding to a perfect trade-off in species' colonization and extinction rates, is degenerate, and unbiological for two reasons: (i) it requires fine-tuning of the parameters, and (ii) there are infinitely many equilibria, which means that all but one species will eventually drift to zero frequency (extinction) in a system of finite size. For the rest of the analysis, we assume that memory effects do operate, and that the colonization rate structure is non-degenerate, so P is invertible.

Solving for the equilibrium species frequencies $\boldsymbol{x}^\star$ is less straightforward. Substituting $\boldsymbol{y}^\star = P^{-1}\boldsymbol{m}$ into $\frac{d\boldsymbol{y}}{dt}$ gives us the system

$$\left(D(\boldsymbol{m}) - D(P^{-1}\boldsymbol{m})P^T\right)\boldsymbol{x}^\star = 0. \tag{4.7}$$

Let us define $Q = D(\boldsymbol{m}) - D(P^{-1}\boldsymbol{m})P^T$. The equilibrium frequencies $\boldsymbol{x}^\star$ correspond to the one-dimensional null space of Q, or equivalently, an eigenvector of Q with eigenvector 0. In general, then, there is no closed form expression for $\boldsymbol{x}^\star$ (although these frequencies are easily computed numerically). However, for the important purpose of determining whether the coexistence equilibrium is biologically feasible (having all positive components), it is not necessary to compute $\boldsymbol{x}^\star$ – only $\boldsymbol{y}^\star$ is needed. This is because the matrix $-Q^T$ has the special structure of a transition rate matrix, which means that it satisfies:

1. $-q_{ii} > 0$ for all i
2. $-q_{ij} < 0$ for all $i \neq j$
3. $\sum_i q_{ij} = 0$ for all j .

All three conditions are easily verified by observing that $Q = D(P\boldsymbol{y}^\star) - D(\boldsymbol{y}^\star)P^T$ (using the equilibrium relationship $\boldsymbol{m} = P\boldsymbol{y}^\star$). Every transition rate matrix possesses a zero

eigenvalue corresponding to an eigenvector of constant sign (the stationary distribution of the corresponding continuous-time Markov chain). This establishes that either all $x_i > 0$ or all $x_i < 0$. Eq. 4.7 determines $\boldsymbol{x}^\star$ only up to a multiplicative constant; in order to determine the constant (and thus the sign), we invoke the fact that $1 = \sum_{i=1}^{n} x_i + \sum_{i=1}^{n} y_i$. Let C be the sum of $\boldsymbol{x}^\star$ at equilibrium. Then we have

$$\begin{aligned} 1 &= \mathbf{1}^T(\boldsymbol{x} + \boldsymbol{y}) \\ &= C + \mathbf{1}^T P^{-1}\boldsymbol{m} \end{aligned} \tag{4.8}$$

and so

$$C = 1 - \mathbf{1}^T P^{-1}\boldsymbol{m} \tag{4.9}$$

where $\mathbf{1}^T$ is a vector of n ones. Combining these facts, all components of $\boldsymbol{x}^\star$ are positive only if $\mathbf{1}^T P^{-1}\boldsymbol{m} < 1$; in other words, only if the vacant patch frequencies sum to less than 1.

The coexistence equilibrium is therefore feasible if and only if both $P^{-1}\boldsymbol{m} > 0$, elementwise, and $\mathbf{1}^T P^{-1}\boldsymbol{m} < 1$. Clearly these two criteria may be checked without reference to $\boldsymbol{x}^\star$.

Equilibrium species frequencies in special cases

Under various conditions, it becomes possible to express the equilibrium species frequencies in a straightforward way. Most notably, when P is symmetric (i.e., $P = P^T$), the species frequencies $\boldsymbol{x}^\star$ are proportional to the vacant patch frequencies $\boldsymbol{y}^\star$. This is verified by setting $\boldsymbol{x}^\star = k\boldsymbol{y}^\star$, where k is a constant of proportionality, and then substituting into Eq. 4.7:

$$
\begin{aligned}
(D(\boldsymbol{m}) - D(P^{-1}\boldsymbol{m})P^T)\,\boldsymbol{x} &= k(D(\boldsymbol{m}) - D(P^{-1}\boldsymbol{m})P)P^{-1}\boldsymbol{m} \\
&= k(D(\boldsymbol{m})P^{-1}\boldsymbol{m} - D(P^{-1}\boldsymbol{m})\boldsymbol{m}) \\
&= 0.
\end{aligned} \tag{4.10}
$$

As when assessing feasibility, the constant k must be determined using the zero-sum constraint. We find

$$
k = \frac{1}{\sum \boldsymbol{y}^\star} - 1 = \frac{1}{\mathbf{1}^T P^{-1}\boldsymbol{m}} - 1. \tag{4.11}
$$

It is also possible to write $\boldsymbol{x}^\star$ directly when P is symmetrizable, meaning P is of the form DS, where D is a diagonal matrix and S is symmetric. Then, we find $\boldsymbol{y}^\star = S^{-1}D^{-1}\boldsymbol{m}$ and, following a calculation similar to Eq. 4.10, $\boldsymbol{x}^\star = kD^{-1}\boldsymbol{y}^\star = k(DSD)^{-1}\boldsymbol{m}$, with k once again a constant to be determined.

An explicit expression for $\boldsymbol{x}^\star$ is possible in other circumstances, as well, but these two cases will be needed in the following sections.

4.5.2 Species-specific memory effects

Simplest case

We begin by studying the simplest non-trivial parameterization of the model. Let $P = D(\boldsymbol{\alpha}) + \beta J$, where $\boldsymbol{\alpha} = (\alpha_1, \ldots, \alpha_n)^T$ is a vector of species-specific memory effects (of any sign) and $\beta > 0$ expresses the background colonization rate for all species. We must have $\alpha_i \geq -\beta$ to ensure all rates are non-negative. Here, J denotes the $n \times n$ matrix of ones, $J = \mathbf{1}\mathbf{1}^T$. Initially, we will assume that all species experience identical local extinction rates, m.

Under these assumptions, P is a rank-one perturbation of a diagonal matrix, and it

is possible to compute P^{-1} using the Sherman-Morrison formula [109]. We find that the equilibrium frequencies are

$$y_i^\star = \frac{1}{\alpha_i}\left(\frac{m}{1+\beta\, R(\boldsymbol{\alpha})}\right) \tag{4.12}$$

where $R(\boldsymbol{\alpha})$ is the sum of reciprocals of the α_i, $R(\boldsymbol{\alpha}) = \sum_i \frac{1}{\alpha_i}$. Using Eqs. 4.10 and 4.11, we also have

$$x_i^\star = \frac{1}{\alpha_i}\left(\frac{R(\boldsymbol{\alpha})^{-1}+\beta-m}{1+\beta\, R(\boldsymbol{\alpha})}\right). \tag{4.13}$$

In Eq. 4.13, the factor in parentheses has no dependence on i. This shows that the equilibrium frequency of each species is inversely proportional to the strength of its memory effects. This also makes clear that the equilibrium can only be feasible if all α_i share the same sign. We will assume this is case; otherwise, coexistence of all species at equilibrium is not possible, and some species will go extinct.

Global stability

For this equilibrium to be an attractor of the system, it must be stable as well as feasible. We would ideally like to know whether the equilibrium is *globally stable*, meaning the dynamics approach the equilibrium from any initial condition (assuming all species are initially present at some non-zero frequency). Global stability can be established by constructing a Lyapunov function for the dynamics. A Lyapunov function for an autonomous dynamical system $\frac{d\boldsymbol{z}}{dt} = g(\boldsymbol{z})$, with $\boldsymbol{z} \in \mathbb{R}^n$, is a continuous scalar function $V : \mathbb{R}^n \to \mathbb{R}$ that has continuous first derivatives and satisfies the following:

1. $V(\boldsymbol{z}) > 0$ except for an equilibrium point $\boldsymbol{z}^\star$, where $V(\boldsymbol{z}^\star) = 0$
2. $\frac{dV}{dt} < 0$ except when $\boldsymbol{z} = \boldsymbol{z}^\star$, where $\frac{dV}{dt} = 0$

In words, V is a positive function that is strictly decreasing through the dynamics, until reaching a minimum at $\boldsymbol{z}^\star$. The existence of such a function implies that the point $\boldsymbol{z}^\star$ is globally Lyapunov stable. For a thorough discussion of Lyapunov functions and global stability, see [35, 89].

Unfortunately, there is no general method to construct Lyapunov functions. For some well-studied models in ecology, including MacArthur's consumer-resource model [149] and the generalized Lotka-Volterra (GLV) model [78], candidate Lyapunov functions are known, and can be used to show global stability under appropriate parameterizations. While our model is not among these, we take advantage of an embedding technique from dynamical systems theory to make use of the known results for GLV.

Brenig [36] has shown that GLV is a canonical model, in the sense that any quasi-polynomial (QP) system of ordinary differential equations can be recast into GLV form through a change of variables. QP systems take the form

$$\frac{du_i}{dt} = u_i \left(\lambda_i + \sum_{j=1}^{m} A_{ij} \prod_{k=1}^{l} u_k^{B_{jk}} \right), \quad i = 1, ..., l \tag{4.14}$$

where A is an $l \times m$ matrix and B is an $m \times l$ matrix, with $m \geq l$. Many ecological models are in QP form, including ours. By casting our model from QP into GLV form, it becomes possible to use a class of candidate Lyapunov functions for GLV to prove global stability. Typically, this process requires an enlargement of the state space, and therefore the embedded dynamics are subject to constrained initial conditions. As we will show, these constraints are crucial for our stability analysis.

More concretely, our model is a QP system with $\boldsymbol{u}(t) = (\boldsymbol{x}(t), \boldsymbol{y}(t))^T$, $\boldsymbol{\lambda} = (-\boldsymbol{m}, 0)^T$, and A and B are block-structured matrices

$$A = \begin{pmatrix} 0 & P & 0 \\ -P^T & 0 & mI \end{pmatrix} \quad B = \begin{pmatrix} I & 0 \\ 0 & I \\ I & -I \end{pmatrix} \tag{4.15}$$

where each block is $n \times n$ (so $l = 2n$ and $m = 3n$). Such a system can be recast into GLV form with state variables

$$z_i = \prod_{j=1}^{m} u_j^{B_{ij}}, \quad i = 1, ..., m \tag{4.16}$$

and dynamics given by

$$\frac{d\boldsymbol{z}}{dt} = D(\boldsymbol{z})(B\boldsymbol{\lambda} + BA\boldsymbol{z}). \tag{4.17}$$

For more details, see [36, 100, 234]. In our particular case, this procedure amounts to defining the new variables $r_i = \frac{x_i}{y_i}$, with the resulting $3n$-"species" GLV system defined by variables $\boldsymbol{z}(t) = (\boldsymbol{x}(t), \boldsymbol{y}(t), \boldsymbol{r}(t))^T$, growth rates $B\boldsymbol{\lambda} = (-\boldsymbol{m}, 0, -\boldsymbol{m})^T$, and interaction matrix

$$BA = \begin{pmatrix} 0 & P & 0 \\ -P^T & 0 & mI \\ P^T & P & -mI \end{pmatrix}. \tag{4.18}$$

The interaction matrix for this larger system is singular, and the models defined by Eq. 4.5 and Eqs. 4.17-4.18 are equivalent only on the manifold where $r_i = \frac{x_i}{y_i}$ for all i.

All of these manipulations finally put us in a position to try applying a well-known family of candidate Lyapunov functions for GLV. The function

$$V(\boldsymbol{z}) = \sum_i \sigma_i \left(z_i - z_i^\star - z_i^\star \log\left(\frac{z_i}{z_i^\star}\right)\right), \tag{4.19}$$

with non-negative constants σ_i, is smooth and always positive except at $V(\boldsymbol{z}^\star) = 0$. Thus,

V is a Lyapunov function for the GLV system with equilibrium $\boldsymbol{z}^\star$ if there is a choice of $\boldsymbol{\sigma}$ such that $\frac{dV}{dt} < 0$ for all $\boldsymbol{z} \neq \boldsymbol{z}^\star$ [78]. The quantity $\frac{dV}{dt}$ conveniently reduces to

$$(\boldsymbol{z} - \boldsymbol{z}^\star)^T \left(\frac{D(\boldsymbol{\sigma})M + M^T D(\boldsymbol{\sigma})}{2} \right) (\boldsymbol{z} - \boldsymbol{z}^\star) \tag{4.20}$$

where M is the interaction matrix (in our case, $M = BA$).

We can now show that the equilibrium found in Eqs. 4.12-4.13 is globally stable for our simplest model. Let $\boldsymbol{\sigma} = (\mathbf{1}, \mathbf{1}, \frac{-1}{k+1} D(\boldsymbol{\alpha})^{-1}\mathbf{1})^T$, where k is the constant of proportionality $\frac{R(\boldsymbol{\alpha})+\beta-m}{m}$. We use the short-hand $\Delta\boldsymbol{x} = \boldsymbol{x} - \boldsymbol{x}^\star$, and similarly for $\boldsymbol{y}$ and $\boldsymbol{r}$. Evaluating Eq. 4.20, and noting the symmetry of P, yields

$$\frac{dV}{dt} = m\Delta\boldsymbol{y}^T\Delta\boldsymbol{r} - \frac{m}{k+1}(\Delta\boldsymbol{x} + \Delta\boldsymbol{y})^T P D(\boldsymbol{\alpha})^{-1}\Delta\boldsymbol{r} + \frac{m^2}{k+1}\Delta\boldsymbol{r}^T D(\boldsymbol{\alpha})^{-1}\Delta\boldsymbol{r} \tag{4.21}$$

$$= m\Delta\boldsymbol{y}^T\Delta\boldsymbol{r} - \frac{m}{k+1}(\Delta\boldsymbol{x} + \Delta\boldsymbol{y})^T (D(\boldsymbol{\alpha}) + \beta J) D(\boldsymbol{\alpha})^{-1}\Delta\boldsymbol{r} + \frac{m^2}{k+1}\Delta\boldsymbol{r}^T D(\boldsymbol{\alpha})^{-1}\Delta\boldsymbol{r} \tag{4.22}$$

which simplifies to

$$= m\Delta\boldsymbol{y}^T\Delta\boldsymbol{r} - \frac{m}{k+1}(\Delta\boldsymbol{x} + \Delta\boldsymbol{y})^T \Delta\boldsymbol{r} + \frac{m^2}{k+1}\Delta\boldsymbol{r}^T D(\boldsymbol{\alpha})^{-1}\Delta\boldsymbol{r} \tag{4.23}$$

$$= \frac{-m}{k+1}(\Delta\boldsymbol{x} - k\Delta\boldsymbol{y})^T \Delta\boldsymbol{r} + \frac{m^2}{k+1}\Delta\boldsymbol{r}^T D(\boldsymbol{\alpha})^{-1}\Delta\boldsymbol{r} \tag{4.24}$$

using the zero-sum constraint, $(\Delta\boldsymbol{x} + \Delta\boldsymbol{y})^T J = 0$. Next we recall that $r_i = \frac{x_i}{y_i}$, which, along with the proportionality of $\boldsymbol{y}^\star$ and $\boldsymbol{x}^\star$, implies that $\Delta\boldsymbol{r} = D(\boldsymbol{y})^{-1}(\Delta\boldsymbol{x} - k\Delta\boldsymbol{y})$, and so

$$\frac{dV}{dt} = \frac{1}{k+1}(-m\Delta\boldsymbol{r}^T D(\boldsymbol{y})\Delta\boldsymbol{r} + m^2\Delta\boldsymbol{r}^T D(\boldsymbol{\alpha})^{-1}\Delta\boldsymbol{r}). \tag{4.25}$$

Because the frequencies $\boldsymbol{y}$ are always non-negative, and $\Delta \boldsymbol{r}^T D(\boldsymbol{y}) \Delta \boldsymbol{r}$ is a quadratic form, the first term is always negative. The second term is always negative if $D(\boldsymbol{\alpha})^{-1}$ is a negative definite matrix. This requires $\alpha_i < 0$ for all i. These calculations show that when all species have negative memory effects, the coexistence equilibrium is globally stable. It is straightforward to show using similar arguments that if all $\alpha_i > 0$, the coexistence equilibrium is never stable, except when $n = 1$. In other words, when species exhibit positive memory effects, the only long-term outcome is monodominance.

While our Lyapunov function can be written entirely in terms of the original model variables and parameters as

$$\begin{aligned} V &= \sum_i x_i - x_i^\star - x_i^\star \log\left(\frac{x_i}{x_i^\star}\right) + y_i - y_i^\star - y_i^\star \log\left(\frac{y_i}{y_i^\star}\right) - \frac{1}{(k+1)\alpha_i}\left(\frac{x_i}{y_i} - k - k\log\left(\frac{x_i}{k y_i}\right)\right) \\ &= \sum_i -x_i^\star \log\left(\frac{x_i}{x_i^\star}\right) - y_i^\star \log\left(\frac{y_i}{y_i^\star}\right) - \frac{1}{(k+1)\alpha_i}\left(\frac{x_i}{y_i} - k - k\log\left(\frac{x_i}{k y_i}\right)\right) \end{aligned} \tag{4.26}$$

and verified without reference to the GLV embedding, we trace the process of recasting in GLV form to demonstrate the utility of this approach. The difficulty of generating suitable Lyapunov functions – which is usually seen a matter of inspired guesswork or laborious trial-and-error – is a major obstacle to their wider application. The canonical status of GLV, and the potential to exploit this fact for constructing Lyapunov functions, has been known for decades, but very rarely utilized in ecology (but see [199]). Our derivation illustrates how GLV embedding can systematize the search for a Lyapunov function, by reducing the problem to a choice of appropriate constants (here, σ_i). In many cases, this is likely to be a more fruitful effort than divining an appropriate function directly.

Feasibility and diversity

We now return to consideration of feasibility. We have seen that feasibility requires that all α_i share a common sign, and stability requires that all $\alpha_i < 0$. When these conditions are satisfied, what else is needed to guarantee feasibility? The remaining criterion is a community-wide condition:

$$m < R(\boldsymbol{\alpha})^{-1} + \beta. \tag{4.27}$$

When this inequality holds, and assuming all $\alpha_i < 0$, both $\boldsymbol{x}^\star$ and $\boldsymbol{y}^\star$ are strictly positive. Eq. 4.27 gives an upper bound on the local extinction rate that the coexisting community can tolerate. Because $\alpha_i < 0$, the quantity $R(\boldsymbol{\alpha})^{-1}$ is always negative, but it increases toward zero as any new species is added to the community. As a consequence, the maximum m compatible with feasibility, $m_{\max}$, increases with diversity, as well. This implies a positive diversity-robustness relationship: Assuming some environmental component to m (habitat quality, external disturbance rate, etc.), more speciose communities can tolerate environments that would drive a subset of the species to extinction. In this scheme, species with weaker memory effects (i.e. α_i closer to 0) contribute more strongly to raising $m_{\max}$. Intuitively, these species are more abundant at equilibrium, and more effectively dilute the negative memory effects of other species. As species join the community, $m_{\max}$ increases to an asymptotic upper bound at $m_{\max} = \beta$. In this limit, the memory effects in the system are so diluted that the effective colonization rate for all species is just β, the background rate.

It is indicative of the contrasting effects of diversity in this model that species with weak negative memory effects provide a strong community benefit (higher $m_{\max}$) but also occupy a large fraction of patches. Coexisting communities blur the distinction between mutualism and competition, as species benefit one another through a dilution effect, but compete for available patches. One consequence is a non-monotonic relationship between

diversity and equilibrium frequency. Consider the equilibrium value, $x_i^\star$, for a focal species as the community composition varies with m constant. Adding or removing species affects $x_i^\star$ through the quantity $R(\boldsymbol{\alpha})$, which we take for a moment as a continuous variable, R, that ranges from $\frac{1}{m-\beta}$ (species i alone with strong negative memory effects) to $-\infty$ (very many species, or species with very weak negative memory effects). The derivative of $x_i^\star$ with respect to R is

$$\frac{dx_i^\star}{dR} = \frac{-1}{\alpha_i}\left(\frac{1}{R^2} - \frac{m\beta}{(1+\beta R)^2}\right) \tag{4.28}$$

which changes sign as R tends toward $-\infty$. For $R \approx \frac{1}{m-\beta}$, recalling that $\alpha_i < 0$, we have $\frac{dx_i^\star}{dR} > 0$, indicating that $x_i^\star$ increases with increasing diversity (decreasing R). However, as R becomes very negative, $\frac{dx_i^\star}{dR}$ approaches 0 from above. The sign of $\frac{dx_i^\star}{dR}$ changes once at

$$R = \frac{1}{m-\beta}\left(1 + \sqrt{\frac{m}{\beta}}\right) \tag{4.29}$$

which can be found by setting Eq. 4.28 equal to 0 (the other root always falls above $\frac{1}{m-\beta}$). Once R drops below the critical value in Eq. 4.29, any increase in diversity decreases R further, decreasing $x_i^\star$, as well.

Variation in local extinction rates

How does this picture change when species differ in their local extinction rates? Now, we allow each species to have a distinct local extinction rate, $m_i > 0$. It turns out that stability is unaffected by this variation, although feasibility may be. And while the relationship between diversity and robustness becomes more complex in this case, we will see that there is still a well-defined positive relationship between the two.

Using the Sherman-Morrison formula, as before, we find

$$y_i^\star = \frac{1}{\alpha_i}\left(m_i - \frac{\beta(\sum_j \frac{m_j}{\alpha_j})}{1+\beta R(\boldsymbol{\alpha})}\right). \tag{4.30}$$

Using Eq. 4.11, we also have

$$x_i^\star = \frac{1}{\alpha_i}\left(m_i - \frac{\beta(\sum_j \frac{m_j}{\alpha_j})}{1+\beta R(\boldsymbol{\alpha})}\right)\left(\frac{1+\beta R(\boldsymbol{\alpha})}{\sum_j \frac{m_j}{\alpha_j}} - 1\right). \tag{4.31}$$

As before, all α_i must share the same sign for feasibility. For stability, this common sign must be negative. This can be verified using a Lyapunov function of the same form as Eq. 4.19, but with $\boldsymbol{\sigma} = \{\mathbf{1}, \mathbf{1}, \frac{-1}{k+1} D(\boldsymbol{m}) D(\boldsymbol{\alpha})^{-1}\mathbf{1}\}$.

The requirement that $\alpha_i < 0$ induces a positive diversity-robustness relationship in this case, as well. The picture is complicated by the fact that each species may react differently to a set of environments – a favorable environment for one species (decreased m_i) may be unfavorable for another (increased m_j). However, any community-environment pair can be characterized by a weighted average of of the local extinction rates: $w(\boldsymbol{m}) = \sum_j \left(\frac{R(\boldsymbol{\alpha})}{\alpha_j}\right) m_j$. Then a community-wide feasibility condition, directly analogous to Eq. 4.27, is

$$w(\boldsymbol{m}) < R(\boldsymbol{\alpha})^{-1} + \beta\,. \tag{4.32}$$

The interpretation of Eq. 4.32 is nearly identical to Eq. 4.27: $R(\boldsymbol{\alpha})^{-1}$ is negative and increasing with species richness, so diverse communities are able to tolerate higher $w(\boldsymbol{m})$.

Unlike the constant m case, Eq. 4.32 is not sufficient for feasibility. We also find a requirement that no particular m_i is too much larger than the rest. From Eq. 4.31, one can show that the inequality

$$\frac{m_i}{w(\boldsymbol{m})} < \frac{\beta R(\boldsymbol{\alpha})}{1+\beta R(\boldsymbol{\alpha})} \tag{4.33}$$

must hold for all i. This feasibility condition sets an upper bound on the ratio of each species'

local extinction rate to the weighted average of the whole community. When diversity is low, this condition is not very restrictive, but as diversity increases and $R(\boldsymbol{\alpha})$ decreases toward $-\infty$, the allowable variation in m_i becomes very small.

4.5.3 Symmetric memory effects

In this section we consider arbitrary symmetric memory effects (i.e., $P = P^T$). For two species, every symmetric matrix has constant off-diagonals, so the results of the previous section apply. For $n > 2$, we derive a stability condition that naturally, but precisely, generalizes the intuitive notion that all species must have a disadvantage colonizing "their own" vacant patches (patches of type i, for species i), compared to vacant patches in other states.

As n grows, it quickly becomes impractical to write the equilibrium frequencies explicitly. The general feasibility conditions in Supporting Information 4.5.1 must be checked in each case. For the remainder of this section we assume the coexistence equilibrium is feasible and focus on its stability properties. In subsection Feasibility and Diversity, we return to consider the diversity-robustness relationship, as suggested by Eqs. 4.27 and 4.32.

Local stability

Allowing P to be an arbitrary (non-negative) symmetric matrix makes the problem of constructing a Lyapunov function much more difficult. Instead, we consider the *local* stability of the coexistence equilibrium. Once again, we begin by assuming m is identical for all species. However, in subsection Relaxing Assumptions we present numerical evidence that any locally stable equilibrium is in fact globally stable, and that variation in local extinction rates never affects stability.

Local stability of the coexistence equilibrium depends on the real parts of the eigenvalues of the Jacobian matrix, $J^\star$, evaluated at $(\boldsymbol{x}^\star, \boldsymbol{y}^\star)^T$. Due to the zero-sum constraint, the

model dynamics are confined to the simplex, and there is necessarily one zero eigenvalue, which corresponds to an eigenvalue pointing "out" of the simplex. This eigenvalue has no bearing on stability. The coexistence equilibrium is then locally asymptotically stable if and only if the remaining $2n-1$ eigenvalues of $J^\star$ all have negative real part. In general, we have the Jacobian

$$J^\star = \begin{pmatrix} 0 & D(\boldsymbol{x}^\star)P \\ D(\boldsymbol{m}) - D(\boldsymbol{y}^\star)P^T & -D(P^T\boldsymbol{x}^\star) \end{pmatrix} \tag{4.34}$$

or, using the equilibrium relationship $D(\boldsymbol{m})\boldsymbol{x}^\star = D(\boldsymbol{y}^\star)P^T\boldsymbol{x}^\star$,

$$J^\star = \begin{pmatrix} 0 & D(\boldsymbol{x}^\star)P \\ D(\boldsymbol{m}) - D(\boldsymbol{y}^\star)P^T & -D(\boldsymbol{y}^\star)^{-1}D(\boldsymbol{m})D(\boldsymbol{x}^\star) \end{pmatrix} \tag{4.35}$$

which simplifies considerably to

$$J^\star = \begin{pmatrix} 0 & kD(\boldsymbol{y}^\star)P \\ mI - D(\boldsymbol{y}^\star)P & -kmI \end{pmatrix} \tag{4.36}$$

under the assumptions $P = P^T$ and $m_i = m$.

It is actually more convenient to work with another matrix, J', which is *similar* to $J^\star$. As such, $J^\star$ and J' share the same eigenvalues. Let us define the change of basis matrix

$$U = \begin{pmatrix} D(\boldsymbol{y}^\star)^{1/2} & 0 \\ 0 & D(\boldsymbol{y}^\star)^{1/2} \end{pmatrix} \tag{4.37}$$

Then J' is given by

$$\begin{aligned} J' &= U^{-1} J^\star U \\ &= \begin{pmatrix} 0 & kD(\boldsymbol{y}^\star)^{1/2} PD(\boldsymbol{y}^\star)^{1/2} \\ mI - D(\boldsymbol{y}^\star)^{1/2} PD(\boldsymbol{y}^\star)^{1/2} & -kmI \end{pmatrix} \end{aligned} \tag{4.38}$$

For simplicity we introduce the shorthand $S = D(\boldsymbol{y}^\star)^{1/2} PD(\boldsymbol{y}^\star)^{1/2}$. Now we will see that the eigenvalues of J' can be written in terms of the eigenvalues of S. The ith eigenvalue of J', denoted λ_i, satisfies

$$J' \begin{pmatrix} \boldsymbol{u}_i \\ \boldsymbol{v}_i \end{pmatrix} = \lambda_i \begin{pmatrix} \boldsymbol{u}_i \\ \boldsymbol{v}_i \end{pmatrix} \tag{4.39}$$

for the corresponding eigenvector $(\boldsymbol{u}_i, \boldsymbol{v}_i)^T$, with components $\boldsymbol{u}_i$ and $\boldsymbol{v}_i$ each of length n. This gives us the system of equations

$$\begin{aligned} kS\boldsymbol{v}_i &= \lambda_i \boldsymbol{u}_i \\ m\boldsymbol{u}_i - S\boldsymbol{u}_i - mk\boldsymbol{v}_i &= \lambda_i \boldsymbol{v}_i. \end{aligned} \tag{4.40}$$

We notice that Eq. 4.40 can satisfied by $\boldsymbol{u}_i = c\boldsymbol{v}_i$, for an undetermined constant c, whenever $\boldsymbol{v}_i$ is an eigenvector of S. Denote the corresponding eigenvalue of S as $\lambda(S)_i$, which must equal $\frac{c}{k}\lambda_i$, according to the first equation. Assuming $\lambda_i \neq 0$, we can then re-write the second equation entirely in terms of $\boldsymbol{v}_i$:

$$mk\frac{\lambda(S)_i}{\lambda_i}\boldsymbol{v}_i - k\frac{\lambda(S)_i}{\lambda_i} S\boldsymbol{v}_i - mk\boldsymbol{v}_i = mk\frac{\lambda(S)_i}{\lambda_i}\boldsymbol{v}_i - k\frac{\lambda(S)_i^2}{\lambda_i}\boldsymbol{v}_i - mk\boldsymbol{v}_i = \lambda_i \boldsymbol{v}_i \tag{4.41}$$

which yields the scalar equation

$$\begin{aligned} 0 &= mk\frac{\lambda(S)_i}{\lambda_i} - k\frac{\lambda(S)_i^2}{\lambda_i} - mk - \lambda_i \\ &= \lambda_i^2 + km\lambda_i + k\lambda(S)_i(\lambda(S)_i - m). \end{aligned} \tag{4.42}$$

Eq. 4.42 has the solutions

$$\lambda_i = \frac{-km \pm \sqrt{(km)^2 - 4k\lambda(S)_i(\lambda(S)_i - m)}}{2}. \tag{4.43}$$

We can see that each eigenvalue of S determines a pair of eigenvalues J', which we write as λ_i^+ and λ_i^-. If the coexistence equilibrium is feasible, $-km$ will always be negative, and so λ_i^- will have negative real part. The real part of λ_i^+ will be negative if $\lambda(S)_i < 0$ or $\lambda(S)_i > m$, and exactly zero when $\lambda(S)_i = 0$ or m. In fact, one eigenvalue of S is equal to m, with corresponding eigenvector $D(\boldsymbol{y}^\star)^{1/2}\mathbf{1}$. This is easy to verify:

$$\begin{aligned} SD(\boldsymbol{y}^\star)^{1/2}\mathbf{1} &= D(\boldsymbol{y}^\star)^{1/2}PD(\boldsymbol{y}^\star)^{1/2}D(\boldsymbol{y}^\star)^{1/2}\mathbf{1} \\ &= D(\boldsymbol{y}^\star)^{1/2}PD(\boldsymbol{y}^\star)\mathbf{1} \\ &= mD(\boldsymbol{y}^\star)^{1/2}PP^{-1}\mathbf{1} \\ &= mD(\boldsymbol{y}^\star)^{1/2}\mathbf{1}. \end{aligned} \tag{4.44}$$

This eigenpair generates the expected zero eigenvalue of J'.

The matrix S and its eigenvector $D(\boldsymbol{y}^\star)^{1/2}\mathbf{1}$ are both non-negative, so m is the Perron eigenvalue of S [109]. This implies that all other eigenvalues of S are smaller than m in magnitude. In particular, there is no $\lambda(S)_i > m$. This means that the coexistence equilibrium is stable if an only if m is the sole positive eigenvalue of S. Because S and P are symmetric and *congruent*, Sylvester's law of inertia guarantees that they share the same number of positive, negative, and zero eigenvalues [109]. Thus, we can equivalently state

that the coexistence equilibrium is stable if and only if P has a single positive eigenvalue.

This kind of matrix (nonnegative, symmetric, with exactly one positive eigenvalue) has previously been associated with the stable maintenance of polymorphisms in models in population genetics (e.g. [128, 110, 123]). These and other studies [18, 184, 183] have produced several characterizations of this class of matrix, which allow us to develop some biological intuition for the stability condition (see main text).

Relaxing assumptions

While the analysis above relies on the assumption $m_i = m$ and shows only local stability, numerical simulations suggest that the same stability condition holds regardless of $\boldsymbol{m}$ (assuming feasibility), and that this stability is global in character.

To examine the consequences of variation in $\boldsymbol{m}$, we drew random symmetric P matrices with $n = 4$ and $p_{ij} = p_{ji} \sim U[0, 1]$, and numerically checked local stability for different choices of $\boldsymbol{m}$. To assess whether the stability criterion derived with constant m remained necessary and sufficient for stability in this generalized setting, we collected 1000 randomly distributed P matrices with exactly one positive eigenvalue (putatively stable) and 1000 matrices with additional positive eigenvalues (putatively unstable). For each matrix, we considered 1000 random $\boldsymbol{m}$ vectors. To avoid sampling many choices of $\boldsymbol{m}$ incompatible with feasibility, which would be computationally costly, we first sampled a vector $\boldsymbol{l}$ uniformly from the n-simplex, which we took to be proportional to $\boldsymbol{y}^\star$ (and consequently $\boldsymbol{x}^\star$). Then we computed $\boldsymbol{m}$ as $cP\boldsymbol{l}$ where c is a scalar uniformly distributed between 0 and 1. Finally, the equilibrium frequencies were computed accordingly. This sampling strategy is commonly used to draw random parameters compatible with feasibility (see, for example, [45, 200, 72]). Across all 10^6 combinations of P and $\boldsymbol{m}$ for each stability category (stable or unstable), we found that the stability of the system with variation in m_i was always correctly predicted by the stability of the associated system with no variation. This suggests that the condition P

has exactly one positive eigenvalue is necessary and sufficient for stability of any community with symmetric memory effects, regardless of the values of each species' local extinction rates.

To check whether local stability implies global stability in this model, we again drew random symmetric P matrices with $n = 4$ and $p_{ij} = p_{ji} \sim U[0, 1]$. For these simulations, we only retained P matrices with exactly one positive eigenvalue, and sampled until we collected 1000 such matrices. For each realization of P, we calculated $m_{\max}$ and set $m = \frac{1}{2}m_{\max}$ for all species. Then we numerically integrated the model dynamics from 100 random initial conditions, sampled uniformly from the $2n$-simplex. In each case, we integrated the dynamics for 5000 time steps, and then checked if the trajectory had converged to the coexistence equilibrium. If not, we integrated for another 5000 time steps, and repeated this procedure up to 10 times. For all 10^5 combinations of P and initial conditions, we observed convergence to the equilibrium. This consistency strongly suggests that any locally stable equilibrium is also globally stable in our (symmetric) model. It is unnecessary to check the converse, in this case, because local instability implies that trajectories will always eventually move away from the equilibrium, regardless of initial conditions.

R scripts implementing these simulations are available on GitHub [165].

Feasibility and diversity

Motivated by our analysis of the model with species-specific memory effects, it is natural to ask whether this stability condition for symmetric memory effects also induces a positive diversity-robustness relationship. To make this question precise we maintain the assumption of identical m for all species, and consider the notion of an *assembly sequence* [215]. An assembly sequence is a sequence of sets of species beginning with a single species, and where each set contains the preceding set along with one additional species. For instance, $\{i\}$, $\{i, j\}$, $\{i, j, k\}$, where i, j and k are species labels, is an assembly sequence of length 3. For

any set of species there is an upper bound, $m_{\max}$, on m for feasibility of the coexistence equilibrium. We ask whether, for any coexisting set of species S, $m_{\max}$ increases along any assembly sequence that ends at S.

For this question to be meaningful, each set of species along the assembly sequence should coexist (for suitable m). Even if the equilibrium frequencies for S all share the same sign, there is no guarantee that this property will hold for a subset. Thus, we need to assume this property holds for each set along the assembly sequence. On the other hand, given (potential) feasibility, it *is* the case that, if the equilibrium for S is stable, then every subset will also be stable [18]. This is a straightforward consequence of the *eigenvalue interlacing theorem for bordered matrices* [109], which we will rely on again to prove that $m_{\max}$ is increasing along any assembly sequence. For our purposes, the theorem states that, if P^k is a $k \times k$ symmetric matrix and P^{k-1} is the matrix obtained by deleting the last row and column of P^k, then their respective eigenvalues, λ_i^k and λ_i^{k-1}, can be ordered as:

$$\lambda_1^k \geq \lambda_1^{k-1} \geq \lambda_2^k \geq \lambda_2^{k-1} \cdots \geq \lambda_{k-1}^{k-1} \geq \lambda_k^k. \tag{4.45}$$

Using Eq. 4.45, along with the Perron-Frobenius theorem [109], we see that if P^k is a positive symmetric matrix with exactly one positive eigenvalue, then P^{k-1} must be as well. For any set of species, S, we can always order the corresponding colonization rate matrix, P, so that a subset of interest is obtained by sequentially removing the last row and column of P; the stability of any subset follows inductively.

We will also use the identity [121]

$$q_{ii}^{k-1} = q_{ii}^k - \frac{q_{in}^k}{q_{ni}^k} q_{nn}^k \quad \forall i = 1, \ldots, k-1 \tag{4.46}$$

which relates the elements of inverse matrices $(P^{k-1})^{-1} = (q_{ij}^{k-1})$ and $(P^k)^{-1} = (q_{ij}^k)$.

We are now in a position to prove the statement that $m_{\max}$ increases along any assembly

sequence terminating in a coexisting set of species, S. $m_{\max}$ can be computed from Eq. 4.11, which gives

$$m_{\max} = \frac{1}{\mathbf{1}^T P^{-1} \mathbf{1}}. \tag{4.47}$$

We see that $m_{\max}$ is a decreasing function of the quantity $\mathbf{1}^T P^{-1} \mathbf{1}$. Thus, for S with k species and the preceding subset with $k-1$ species, we have $m^k_{\max} \geq m^{k-1}_{\max}$ if and only if $\mathbf{1}^T (P^k)^{-1} \mathbf{1} \leq \mathbf{1}^T (P^{k-1})^{-1} \mathbf{1}$. To manipulate this second inequality, we introduce the matrix $(\tilde{P}^{k-1})^{-1}$, which is just $(P^{k-1})^{-1}$ with a row and column of zeros appended. Now both $(P^k)^{-1}$ and $(\tilde{P}^{k-1})^{-1}$ are $k \times k$, so we can subtract:

$$\mathbf{1}^T (P^k)^{-1} \mathbf{1} - \mathbf{1}^T (P^{k-1})^{-1} \mathbf{1} = \mathbf{1}^T \left((P^k)^{-1} - (\tilde{P}^{k-1})^{-1} \right) \mathbf{1} = \mathbf{1}^T R \, \mathbf{1} \leq 0. \tag{4.48}$$

Using Eq. 4.46, the elements of R are simply $(r_{ij}) = \frac{(q^k_{in})^2}{q^k_{nn}}$. Clearly the sign of the quadratic form in Eq. 4.48 is determined by the sign of q^k_{nn}. If this sign is always negative (or zero), then the inequality holds. As we have noted that the rows and columns of P can be re-ordered to make any species the nth, we now show that $q^k_{nn} \leq 0$ by proving that every diagonal element of $(P^k)^{-1}$, the inverse of a positive symmetric matrix with exactly one positive eigenvalue, is non-positive.

This can be done by induction. In Eq. 4.48, we have at least $k = 2$. Taking this as our base case and computing the inverse explicitly we find

$$(P^{k=2})^{-1} = \frac{1}{\det(P^{k=2})} \begin{pmatrix} p_{22} & -p_{12} \\ -p_{21} & p_{11} \end{pmatrix} \tag{4.49}$$

which must have non-positive diagonal elements because $P^{k=2}$ is non-negative and the determinant is strictly negative. Now, in the induction step, we prove that if $q^{k-1}_{ii} \leq 0$ for

all $i = 1, \dots k-1$, then $q_{ii}^k \leq 0$ for all $i = 1, \dots k$, as well. Here we use a proof by contradiction. First assume that $q_{kk}^k > 0$. Then, using Eq. 4.46, we must have $q_{ii}^k \geq q_{ii}^{k-1}$ for all $i = 1, \dots k-1$. This implies that $\mathrm{Tr}((P^k)^{-1}) > \mathrm{Tr}((P^{k-1})^{-1})$. But the eigenvalues of $(P^k)^{-1}$ and $(P^{k-1})^{-1}$, which are $\frac{1}{\lambda_i^k}$ and $\frac{1}{\lambda_i^{k-1}}$, respectively, obey

$$\frac{1}{\lambda_1^{k-1}} \geq \frac{1}{\lambda_1^k} \geq 0 \geq \frac{1}{\lambda_k^k} \geq \frac{1}{\lambda_{k-1}^{k-1}} \cdots \geq \frac{1}{\lambda_2^{k-1}} \geq \frac{1}{\lambda_2^k}. \tag{4.50}$$

using Eq. 4.45 and the fact that both matrices have exactly one positive eigenvalue. These inequalities imply that $\mathrm{Tr}((P^k)^{-1}) < \mathrm{Tr}((P^{k-1})^{-1})$, a contradiction. Thus, we conclude that $q_{kk}^k < 0$. In this case, Eq. 4.46 shows that $q_{ii}^k \leq q_{ii}^{k-1}$ for all $i = 1, \dots k-1$. These inequalities establish that if $q_{ii}^{k-1} \leq 0$ for all $i = 1, \dots k-1$, then $q_{ii}^k \leq 0$ for all $i = 1, \dots k$, so altogether we have shown that $q_{ii}^k \leq 0$ for any $k \geq 2$ and i.

Combined with the results above, this ultimately establishes that $m_{\max}^k \geq m_{\max}^{k-1}$ at every step along a (coexisting) assembly sequence. In this setting, a species-rich community can always tolerate a higher local extinction rate than any subset of its species. Notice that, if m is constant, these results also imply that the total fraction of occupied patches at equilibrium increases along any assembly sequence. This kind of positive diversity-productivity relationship is commonly observed in empirical studies [107, 99, 246]. In our model, the relationships between diversity-robustness and diversity-productivity are closely connected, because the robustness benefit of diversity arises from a positive "dilution effect" of a more productive community, as discussed in the main text.

While we have shown here that the conditions for coexistence generically induce a positive diversity-robustness relationship, we are not able to quantify the magnitude of this effect, as in Eqs. 4.27 and 4.32. To get a sense of the possibilities, we simulated 500 assembly sequences, each terminating in a distinct coexisting community of 5 species. The matrix P for each community was drawn at random with $p_{ij} = p_{ji} \sim U[0, 1]$ i.i.d. for simplicity. We discarded matrices that did not permit coexistence, and sampled until we obtained 500 that

did. For every community, we calculated $m_{\max}$ first for species 1 alone, then species 1 and 2 together, and so on, up to the full 5 species. If any subset along the assembly sequence lacked a feasible equilibrium, the entire sequence was discarded. As a comparison, we also simulated 500 assembly sequences terminating in communities having equilibria that were potentially feasible (i.e., $P^{-1}\mathbf{1} > 0$, elementwise), but unstable. Our procedure for these communities was identical, except that matrices were checked for instability, rather than stability. The results of these numerical experiments are shown in Fig. 4.6. For stable communities, $m_{\max}$ always increases with richness, as expected, and grows more than twofold on average from 1-species to 5-species communities. For unstable communities, we never observed $m_{\max}$ increase consistently along an assembly sequence, and Fig. 4.6 shows no trend in the average change of $m_{\max}$ with richness. This comparison makes it clear that the positive diversity-robustness relationship seen in coexisting communities is a consequence of the stability condition, rather than the feasibility conditions.

4.5.4 Nonsymmetric memory effects

When P is no longer symmetric, we are unable to find a general characterization of $\boldsymbol{m}$ and P yielding coexistence. Many behaviors are possible, including non-point attractors. While a complete picture of the model dynamics awaits further study, we consider two special (but nonsymmetric) structures that are potentially biologically relevant and amenable to closer study. In subsection Simulating Dynamics for Random Nonsymmetric Memory Effects, we also present the outcomes of numerical simulations with many nonsymmetric colonization rate matrices sampled at random. These results illustrate general patterns in the dynamics across parameter space.

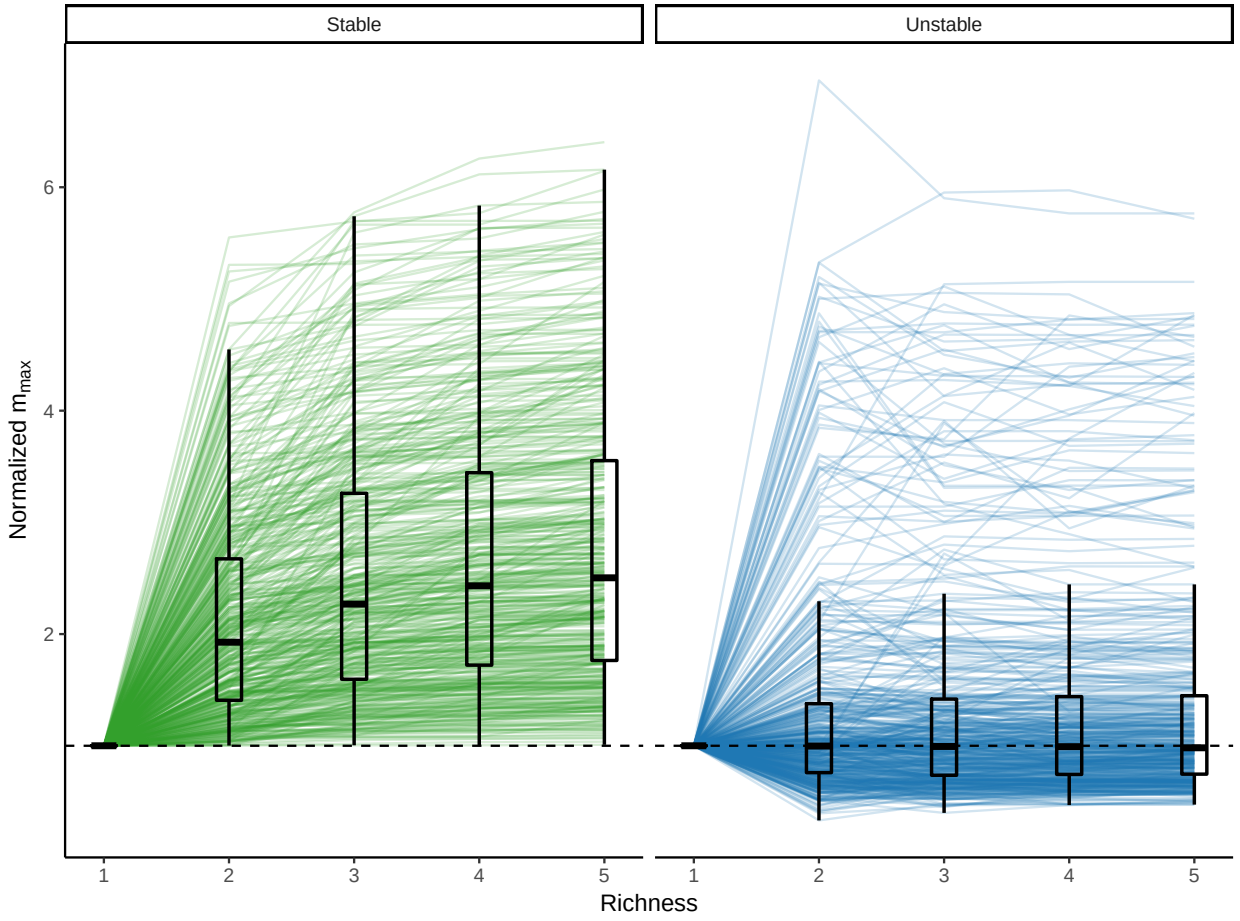

Figure 4.6: Coexistence criteria induce a positive relationship between diversity and robustness. Along 500 random assembly sequences leading to coexisting communities of 5 species, $m_{\max}$ always increases (left). When the final community does not coexist, $m_{\max}$ is never strictly increasing. Here we show a normalized measure of $m_{\max}$ for each assembly sequence, obtained by dividing $m_{\max}$ at each level of richness by its value for the first species alone. See Supporting Information 4.5.3 for simulation details.

Symmetrizable matrices

In Supporting Information 4.5.3, we implicitly assumed equal dispersal rates in defining the rates p_{ij}, which in fact represent a composite of two factors: dispersal (ability to reach a new patch) and establishment (ability to successfully establish residence). If each species has a characteristic dispersal rate, c_i, and now we assume the establishment rates p'_{ij} are symmetric, then $p_{ij} = c_i\, p'_{ij}$, and P is called *symmetrizable*. This kind of matrix is nonsymmetric, but can be made symmetric by pre-multiplication with a diagonal matrix. Extensive simulations suggest that stability in this case is controlled entirely by P', the matrix of establishment rates. In particular, to examine the consequences of variation in $\boldsymbol{c}$, we drew random symmetric P matrices with $n = 4$ and $p'_{ij} = p'_{ji} \sim U[0, 1]$ and numerically checked local stability of the coexistence equilibrium for different choices of $\boldsymbol{c}$. This procedure followed closely the analysis of variation in $\boldsymbol{m}$, discussed in Supporting Information 4.5.3. To assess whether the stability criterion derived with equal dispersal rates remained necessary and sufficient for stability in this generalized setting, we used 1000 randomly distributed P' matrices with exactly one positive eigenvalue (putatively stable) and 1000 matrices with additional positive eigenvalues (putatively unstable). For each matrix, we considered 1000 random $\boldsymbol{c}$ vectors. To avoid sampling many choices of $\boldsymbol{c}$ incompatible with feasibility, which would be computationally costly, we first sampled a vector $\boldsymbol{l}$ uniformly from the simplex, which we took to be proportional to $\boldsymbol{y}^\star$. Then we computed $D(\boldsymbol{c})^{-1}$ as $P'\boldsymbol{l}$ and chose m (equal for all species) uniformly distributed between 0 and 1. Finally, the equilibrium frequencies were computed accordingly. This sampling strategy is commonly used to draw random parameters compatible with feasibility (see, for example, [45, 200, 72]). Across all 10^6 combinations of P' and $\boldsymbol{c}$ for each stability category (stable or unstable), we found that the stability of the system with variation in c_i was always correctly predicted by the stability of the associated system with no variation. This suggests that the condition P' *has exactly one positive eigenvalue* is necessary and sufficient for stability of any community with

symmetric memory effects, regardless of the values of each species' colonization ability.

R scripts implementing these simulations are available on GitHub [165].

Successional cycles

One tractable special case is when P takes the form of a cyclic permutation matrix. As discussed in the main text, this choice of P can be viewed as a simple model for successional dynamics. And we will see that this case illustrates some general features for nonsymmetric P, as well.

A cyclic permutation matrix can be written as

$$Q = \begin{pmatrix} 0 & 0 & \dots & 0 & 1 \\ 1 & 0 & \dots & 0 & 0 \\ 0 & \ddots & \ddots & \vdots & \vdots \\ \vdots & \ddots & \ddots & 0 & 0 \\ 0 & \dots & 0 & 1 & 0 \end{pmatrix} \tag{4.51}$$

assuming species are labeled in the appropriate order. When $n = 3$, this yields the well-known "rock-paper-scissors" dynamics. The key property of this kind of matrix, for our purposes, is that $Q^{-1} = Q^T$. We will use this fact to write the equilibrium frequencies and study the local stability of the coexistence equilibrium.

We assume that all species have identical local extinction rates m and colonization rates c (i.e., $P = cQ$) for simplicity. The equilibrium frequencies for a community of n species are then

$$\begin{aligned} y_i^\star &= \frac{m}{c} \\ x_i^\star &= \frac{1}{n} - \frac{m}{c}, \quad \text{for all } i. \end{aligned} \tag{4.52}$$

The only condition for feasibility in this case is that $m < \frac{c}{n}$. Although P is nonsymmetric, the equivalence of species in this highly idealized case means that $\boldsymbol{y}^\star$ and $\boldsymbol{x}^\star$ are both constant, and therefore proportional. Abusing notation slightly, we let $k = \frac{c}{mn} - 1$ be the constant of proportionality.

The Jacobian evaluated at the coexistence equilibrium is given by

$$J^\star = \begin{pmatrix} 0 & k\frac{m}{c}P \\ mI - \frac{m}{c}P^T & -kmI \end{pmatrix} \tag{4.53}$$

which yields the system of equations

$$\begin{aligned} k\frac{m}{c}P\boldsymbol{v}_i &= \lambda_i \boldsymbol{u}_i \\ m\boldsymbol{u}_i - \frac{m}{c}P^T\boldsymbol{u}_i - km\boldsymbol{v}_i &= \lambda_i \boldsymbol{v}_i \end{aligned} \tag{4.54}$$

for the ith eigenvalue and eigenvector of $J^\star$. Using the fact that $P^T = c^2 P^{-1}$, and assuming $\lambda_i \neq 0$, we can re-arrange Eq. 4.54 to obtain

$$P\boldsymbol{v}_i = (c + \frac{c}{m}\lambda_i + \frac{c}{km^2}\lambda_i^2)\boldsymbol{v}_i \tag{4.55}$$

which implies that the eigenvalues of $J^\star$ and Q are related by

$$\lambda(Q)_i = 1 + \frac{1}{m}\lambda_i + \frac{1}{km^2}\lambda_i^2. \tag{4.56}$$

Solving for λ_i, we find

$$\lambda_i = \frac{-km\left(1 \pm \sqrt{1 - \frac{4}{k}(1 - \lambda(Q)_i)}\right)}{2}. \tag{4.57}$$

The quantity km is always positive when the coexistence equilibrium is feasible, so the real

parts of the λ_i will be all negative if and only if $1 > \text{Re}\left(\sqrt{1-\frac{4}{k}(1-\lambda(Q)_i)}\right)$ for every $\lambda(Q)_i$. In general, $\lambda(Q)_i$ may be complex, so we write these eigenvalues more explicitly as $\lambda(Q)_i = a + bi$. The real part of a complex square root then gives us

$$\begin{aligned} 1 &> \text{Re}\left(\sqrt{1-\frac{4}{k}(1-\lambda(Q)_i)}\right) \\ &= \sqrt{\frac{1-\frac{4}{k}+\frac{4}{k}a+\sqrt{(1-\frac{4}{k}+\frac{4}{k}a)^2+(\frac{4}{k}b)^2}}{2}} \\ &= \sqrt{\frac{1-\frac{4}{k}+\frac{4}{k}a+\sqrt{1-\frac{8}{k}(1-\frac{4}{k})(1-a)}}{2}} \end{aligned} \tag{4.58}$$

using the fact that $a^2 + b^2 = 1$ for any permutation matrix to obtain the last line. This expression can be simplified substantially to produce the equivalent inequality

$$k > a + 1 \tag{4.59}$$

or

$$m < \frac{c}{n(a+2)}. \tag{4.60}$$

Finally, we consider the eigenvalues of Q, which are the nth roots of unity, with real parts $a_k = \cos\left(\frac{2\pi k}{n}\right)$ for $k = 0, ..., n-1$. For $k = 0$, the associated λ_i is the (structural) zero eigenvalue of J. The relevant bound for m is found by considering the largest (non-trivial) value of a_k, which is $\cos\left(\frac{2\pi}{n}\right)$, for $k = 1$. This gives us the stability threshold

$$m_c = \frac{c}{n\left(\cos\left(\frac{2\pi}{n}\right)+2\right)}. \tag{4.61}$$

When $m < m_c$, the coexistence equilibrium is stable. For $n > 2$, this threshold is always less than the threshold for feasibility, $m_{\max} = \frac{c}{n}$. For the range of m values in between, $m_c < m < m_{\max}$, we observe limit cycles (Fig. 4.7). Numerical evidence shows that the

amplitude of these cycles grows rapidly as m increases, so that for $n \geq 3$, all species go extinct even before $m_{\max}$ is reached (Fig. 4.8). The parameter space where stable coexistence is possible shrinks rapidly as n increases; for large n, we have $m_c \approx \frac{c}{3n}$. As one might expect, higher colonization rates increase the stability threshold, as well as the feasibility threshold. Both are proportional to c, so that the stable fraction of feasible parameter space has no dependence on c.

Simulating dynamics for random nonsymmetric memory effects

The previous sections suggest that even keeping m equal for all species, communities with nonsymmetric memory effects may behave similarly to the symmetric case, or very dissimilarly, with the possibility for limit cycles and stability dependent on the magnitude of m. To better understand which outcomes might be typical, we sampled nonsymmetric P matrices and integrated the model dynamics for a range of m values (equal for all species) up to $m_{\max}$ for each model community. Specifically, we sampled P matrices for 3-species communities with $p_{ij} \sim U[0,1]$ i.i.d. and discarded matrices which were not potentially feasible (i.e., $P^{-1}\mathbf{1}$ not all positive). To save computing time, we checked whether each matrix had a locally stable equilibrium for m small ($m = \frac{1}{100}m_{\max}$); if not, it was discarded. This procedure was motivated by the hypothesis that if a P matrix is compatible with stability for some choice of m, say m', then we will find stability for any $m < m'$. This hypothesis is suggested by the case of cyclic P, and supported by the simulation results. However, to ensure the observed pattern was a not a consequence of selecting communities stable at low m, we also repeated the simulations with P drawn as before, but checking local stability for m large ($m = \frac{99}{100}m_{\max}$). For both sets of simulations, we collected 200 matrices meeting the stated criteria, and then simulated the model dynamics for 50 values of m evenly spaced between 0 and $m_{\max}$. Each community was initialized at a random point near the coexistence equilibrium, to avoid long transients. We integrated the dynamics for 5000 time steps, and then

checked if (i) species frequencies had converged to the coexistence equilibrium, (ii) one or more species had gone extinct, or (iii) the dynamics had converged to a stable limit cycle (using the criterion that the final frequencies had been visited at least 5 times independently through the dynamics). If none of these criteria were met, we integrated another 5000 time steps and checked again. This was repeated up to 10 times, until an outcome could be classified.

The results of these simulations are shown in Fig. 4.9. We find that a progression from stability, to limit cycles, to instability as m increases is a common outcome (47% of the communities lose stability). Thus, the qualitative behavior shown analytically for cyclic P seems to be a fairly general feature of the dynamics when P is nonsymmetric. However, many communities exhibited a stable equilibrium for all values of m, consistent with the symmetric and symmetrizable cases. When we required P to produce a stable equilibrium at high m (Figure 4.9, right), the only observed outcome was stability for all values of m. Together, these results strongly support our hypothesis that stability can only be lost, not gained, as m increases.

4.5.5 Waning memory effects

Modified model

To relax the assumption that patches remain in state i indefinitely after occupation by species i, we extended our model to include an additional "naïve" state. The dynamics of this extended model are given by:

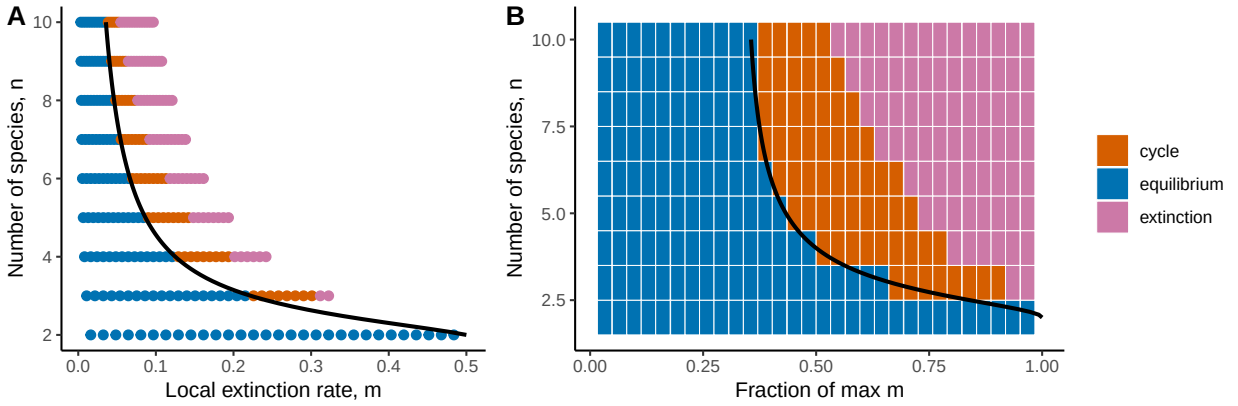

Figure 4.7: Long-term dynamics for cyclic memory effects. When P is proportional to a cyclic permutation matrix, all species may coexist stably, cycle, or go extinct, depending on the magnitude of m. (A) Each point represents the outcome of simulated dynamics with n species and local extinction rate m. Coexistence (blue) occurs for sufficiently small values of m. Above a threshold given by Eq. 4.61 (black curve), stability is lost, leading to limit cycles (orange) and eventually extinction of all species (pink). For each n, we simulated communities at 30 values of m evenly space between 0 and $m_{\max}$. Beyond $m_{\max}$, there is no feasible equilibrium. Notice that the feasibility threshold declines sharply with n. (B) As in (A), except the x-axis shows m values normalized by $m_{\max}$, for each n (rows).

$$\begin{aligned}
\frac{dx_i(t)}{dt} &= -m_i x_i(t) + c_i x_i(t) z(t) + x_i(t) \sum_{j=1}^{n} p_{ij} y_j(t) \\
\frac{dy_i(t)}{dt} &= m_i x_i(t) - d_i y_i(t) - y_i(t) \sum_{j=1}^{n} p_{ji} x_j(t) \\
\frac{dz(t)}{dt} &= \sum_{j=1}^{n} d_j y_j(t) - z(t) \sum_{j=1}^{n} c_j x_j(t)
\end{aligned} \tag{4.62}$$

where $z(t)$ is the frequency of naïve patches. All parameters are interpreted as before, with the addition of decay rates d_i (the rate at which patches in state i transition into the naïve state) and parameters c_i, which encode the rate at which species i colonizes naïve patches. While this model easily accommodates differences in the durability of memory effects or baseline colonization rates across species, we will assume all species have equal demographic

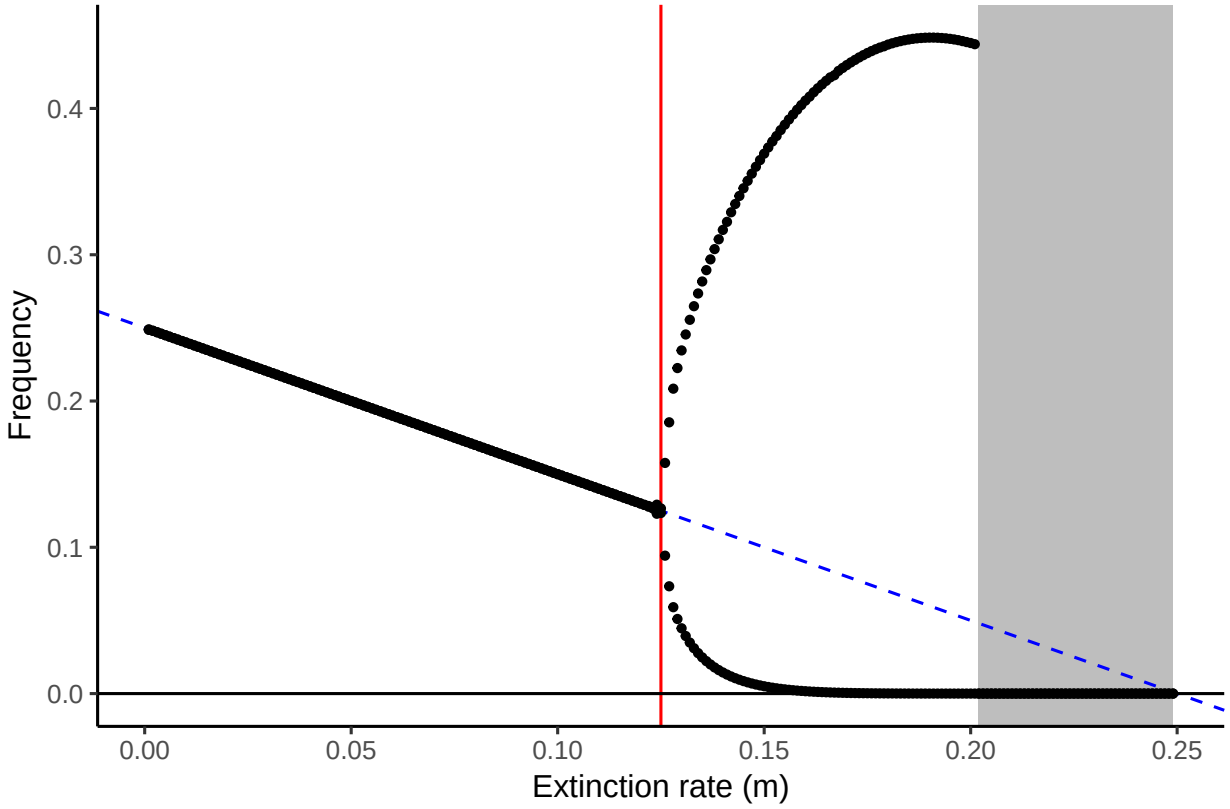

Figure 4.8: Bifurcation diagram for cyclic P. As m increases, the (common) equilibrium abundance of all species decreases linearly. At a threshold indicated in red (m_c), there is a bifurcation point where the dynamics begin to cycle (minimum and maximum points shown). The amplitude of these cycles increases rapidly, leading to the extinction of all species before the feasibility threshold is reached at $m_{\max} = 0.25$ (gray shaded area). In a community experiencing gradually increasing m (e.g. increasing disturbance), predicting future equilibrium frequencies based on the rate of decline at small m (dashed blue line) fails suddenly at $m = m_c$. These simulations used $n = 4$ and $c = 1$, but qualitatively identical behavior is observed for any $n \geq 3$ and any c.

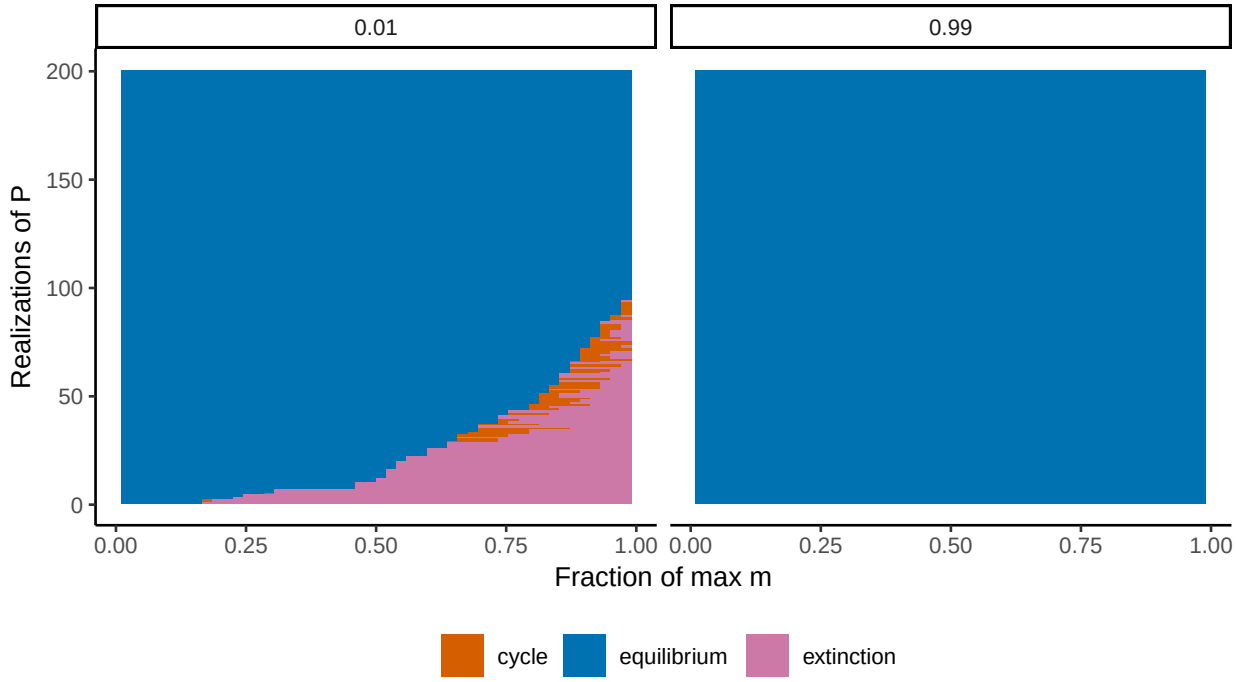

Figure 4.9: Long-term dynamics for nonsymmetric P. Each row shows the long-term dynamics for a different 3-species community with randomly-distributed P, along a gradient of m values. Communities were selected to be stable at either low ($m = \frac{1}{100}m_{\max}$; left) or high ($m = \frac{99}{100}m_{\max}$; right) values of m. For the latter, stability may be lost as m increases (this occurs in 47% of cases shown). As suggested by the analysis of cyclic P, there is often a narrow region where limit cycles are observed between loss of stability of the equilibrium and the extinction of some species. When P is selected for stability at high m (right), stability is never lost. In the left panel, communities are ordered along the y-axis by the point at which they lose stability.

rates m, c, and d for simplicity. We also focus on the case where P is symmetric. In this section, we show that the stability condition derived for symmetric P without memory extends straightforwardly to the modified model.

For the coexistence equilibrium of the modified model one finds

$$\begin{aligned} \boldsymbol{y}^\star &= (m - \frac{d}{k})\, P^{-1}\mathbf{1} \\ \boldsymbol{x}^\star &= k\, \boldsymbol{y}^\star \\ z^\star &= \frac{d}{c\, k}. \end{aligned} \tag{4.63}$$

Just as before, $\boldsymbol{x}^\star$ is proportional to $\boldsymbol{y}^\star$, with constant of proportionality k. Now, however, we have the modified zero-sum condition $\mathbf{1}^T(\boldsymbol{x}^\star + \boldsymbol{y}^\star + z^\star) = 1$, so k satisfies the quadratic equation

$$(m - \frac{d}{k})\frac{1}{q} + (k\, m - d)\frac{1}{q} + \frac{d}{c\, k} = 1 \tag{4.64}$$

or

$$k^2 + (1 - \frac{d}{m} - \frac{q}{m})\, k + \frac{d}{m}(\frac{q}{c} - 1) = 0 \tag{4.65}$$

where $q = (\mathbf{1}^T P^{-1}\mathbf{1})^{-1}$. The value q can be seen as a statistic summarizing the effective whole-community colonization rate, in the following sense: If matrix P has summary statistic q, then the associated system behaves identically – with respect to its "demographic" features, such as k values and demographic eigenvalues (see below) – to a single-species metapopulation with colonization rate q.

From Eq. 4.65, there are two solutions for k (and possibly two distinct equilibria), given

by

$$k = \frac{\frac{d}{m} + \frac{q}{m} - 1 \pm \sqrt{(1 - \frac{d}{m} - \frac{q}{m})^2 - 4\frac{d}{m}(\frac{q}{c} - 1)}}{2}. \tag{4.66}$$

An examination of Eq. 4.63 shows that for feasibility, we must have all entries of $P^{-1}\mathbf{1} > 0$, as before, and also $k > \frac{d}{m}$. The latter inequality might be satisfied by 0, 1 or 2 values of k. When $c > m$, there will be exactly one such k. On the other hand, when $d+m < q$, there will be no k compatible with feasibility. These conditions are found by substituting $k = k' + \frac{d}{m}$ into Eq. 4.65 and applying Descartes' rule of signs. In cases where $c < m$ and $d + m > q$, there may be 0 or 2 feasible values of k, depending on the sign of the discriminant in Eq. 4.66. The condition $c < m$ implies that the zero-biomass equilibrium, $z^\star = 1$, is attractive, and we will see that the second equilibrium, corresponding to the smaller value of k, is always unstable when feasible. These properties signal the presence of a strong Allee effect. If the coexistence equilibrium corresponding to the larger value of k is locally stable in this case, there will be bistability, with trajectories attracted to the zero-biomass equilibrium or the coexistence equilibrium depending on the initial condition.

When is the coexistence equilibrium stable in this extended model? Evaluating the Jacobian at the equilibrium corresponding to either k (and assuming feasibility), we find

$$J^\star = \begin{pmatrix} 0 & D(\boldsymbol{x}^\star)P & c\,\boldsymbol{x}^\star \\ D(\boldsymbol{m}) - D(\boldsymbol{y}^\star)P & -D(P\boldsymbol{x}^\star) - d\,I & 0 \\ -c\,z^\star\,\mathbf{1}^T & d\,\mathbf{1}^T & -c\,(\mathbf{1}^T\boldsymbol{x}^\star) \end{pmatrix} \tag{4.67}$$

with appropriate $\boldsymbol{x}^\star, \boldsymbol{y}^\star$, and $z^\star$.

As in Supporting Information 4.5.3, we can use an equilibrium relationship $D(\boldsymbol{m})\boldsymbol{x}^\star =$

$D(\boldsymbol{y}^\star)(P\boldsymbol{x}^\star - dI)$ to re-write this matrix slightly:

$$J^\star = \begin{pmatrix} 0 & D(\boldsymbol{x}^\star)P & c\,\boldsymbol{x}^\star \\ D(\boldsymbol{m}) - D(\boldsymbol{y}^\star)P & -kmI & 0 \\ -c\,z^\star\,\mathbf{1}^T & d\,\mathbf{1}^T & -c\,(\mathbf{1}^T\boldsymbol{x}^\star) \end{pmatrix}. \tag{4.68}$$

Let us denote the upper-left $2n \times 2n$ block of $J^\star$ by Q. Notice that Q is of exactly the same form as Eq. 4.36. We will see that $2n-2$ of the eigenvalues of J are also eigenvalues of Q, governed by the same stability criterion as in the case without waning memory. In other words, the condition *P has exactly one positive eigenvalue* is now a necessary condition for local stability of the coexistence equilibrium. In fact, we will see that it is also sufficient.

But first we will consider the eigenvalues of $J^\star$ corresponding to those of Q more carefully. Any eigenvectors of Q, written with components of length n as $(\boldsymbol{u}, \boldsymbol{v})^T$, must satisfy the system

$$\begin{aligned} D(\boldsymbol{x}^\star)P\boldsymbol{v} &= \lambda\boldsymbol{u} \\ m\boldsymbol{u} - D(\boldsymbol{y}^\star)P\boldsymbol{u} - km\boldsymbol{v} &= \lambda\boldsymbol{v}. \end{aligned} \tag{4.69}$$

Multiplying both equations by $\mathbf{1}^T$, we obtain

$$\begin{aligned} (km-d)(\mathbf{1}^T\boldsymbol{v}) &= \lambda(\mathbf{1}^T\boldsymbol{u}) \\ m(\mathbf{1}^T\boldsymbol{u}) - (m - \frac{d}{k})(\mathbf{1}^T\boldsymbol{u}) - km(\mathbf{1}^T\boldsymbol{v}) &= \lambda(\mathbf{1}^T\boldsymbol{v}) \end{aligned} \tag{4.70}$$

and so

$$km(\mathbf{1}^T\boldsymbol{v}) = \frac{d}{k}(\mathbf{1}^T\boldsymbol{u}) - \lambda(\mathbf{1}^T\boldsymbol{v}) = \lambda(\mathbf{1}^T\boldsymbol{u}) + d(\mathbf{1}^T\boldsymbol{v}). \tag{4.71}$$

This last set of equalities can be satisfied by $(\mathbf{1}^T\boldsymbol{u}) = (\mathbf{1}^T\boldsymbol{v}) = 0$, or when $(\mathbf{1}^T\boldsymbol{u}), (\mathbf{1}^T\boldsymbol{v}) \neq 0$. In the latter case, one can divide by $(\mathbf{1}^T\boldsymbol{u})$ to obtain the system

$$\begin{aligned} (d - km)w^2 - kmw + \frac{d}{k} &= 0 \\ \lambda = \frac{d}{k}\frac{1}{w} - km & \end{aligned} \tag{4.72}$$

for $w = (\mathbf{1}^T\boldsymbol{v})/(\mathbf{1}^T\boldsymbol{u})$ and the eigenvalue, λ. Two eigenvalues of Q are associated with Eq. 4.72, and the remaining $2n-2$ must be associated with eigenvectors that satisfy $(\mathbf{1}^T\boldsymbol{u}) = (\mathbf{1}^T\boldsymbol{v}) = 0$. The latter eigenpairs of Q generate eigenpairs of $J^\star$ with the same eigenvalues and augmented eigenvectors $(\boldsymbol{u}\,, \boldsymbol{v},\, 0)^T$. This is easy to verify:

$$\begin{aligned} J^\star\,(\boldsymbol{u}\,, \boldsymbol{v}\,, 0)^T &= \begin{pmatrix} Q & \dots & c\,\boldsymbol{x}^\star \\ \vdots & \ddots & 0 \\ -c\,\boldsymbol{z}^\star\,\mathbf{1}^T & d\,\mathbf{1}^T & -c\,(\mathbf{1}^T\boldsymbol{x}^\star) \end{pmatrix} (\boldsymbol{u}\,, \boldsymbol{v}\,, 0)^T \\ &= \begin{pmatrix} \lambda\,(\boldsymbol{u}\,, \boldsymbol{v})^T + 0 \\ -c\,\boldsymbol{z}^\star\,\mathbf{1}^T\boldsymbol{u} + d\,\mathbf{1}^T\boldsymbol{u} + 0 \end{pmatrix} = \begin{pmatrix} \lambda\,(\boldsymbol{u}\,, \boldsymbol{v})^T \\ 0 \end{pmatrix} = \lambda\,(\boldsymbol{u}\,, \boldsymbol{v}\,0)^T. \end{aligned} \tag{4.73}$$

Since Q is of the same form as Eq. 4.36, its eigenvalues (all $2n$) are related to the eigenvalues of $S = D(\boldsymbol{y}^\star)^{1/2} P D(\boldsymbol{y}^\star)^{1/2}$ according to Eq. 4.43. The Perron eigenvector of S is non-negative, and therefore must violate $(\mathbf{1}^T\boldsymbol{u}) = (\mathbf{1}^T\boldsymbol{v}) = 0$, so the two eigenvalues of Q that are not also eigenvalues of $J^\star$ are those associated with the Perron eigenvalue of S. This eigenvalue is equal to $m - \frac{d}{k}$, which bounds the spectral radius of S below m, and following the logic developed in the unmodified case, the remaining $2n - 2$ eigenvalues of Q will be negative if and only if P has exactly exactly one positive eigenvalue.

Finally we consider the remaining three eigenvalues of $J^\star$. One of these must be zero, because the dynamics are confined to the simplex. We call the final two eigenvalues of $J^\star$ its

"demographic" eigenvalues, as they depend only on c, m, q, and d – and not on the structure of P. Each of these three eigenvalues correspond to eigenvectors of the form $(\boldsymbol{x}^\star, a_1\boldsymbol{x}^\star, a_2)^T$ for undetermined constants a_1 and a_2. Assuming this structure and multiplying by $J^\star$ yields the nonlinear scalar system

$$\begin{aligned} a_1\, k\, (m - \frac{d}{k}) + a_2\, c &= \lambda \\ \frac{d}{k} - a_1\, k\, m &= a_1\, \lambda \\ (\frac{-d}{k} + a_1\, d - a_2\, c)(k\, m - d)\frac{1}{q} &= a_2\, \lambda. \end{aligned} \tag{4.74}$$

We solved this system using Wolfram Mathematica (12.2) (scripts available on GitHub [165]). One solution is $\lambda = 0$, as expected. The two demographic eigenvalues are given by

$$\frac{rd - km(r+1) \pm \sqrt{(rd - km(r-1))^2 + 4d(\frac{d}{k} - m)(r-1)}}{2}. \tag{4.75}$$

using the shorthand $r = \frac{c}{q}$. We used Mathematica to verify that these eigenvalues are always negative for the unique feasible coexistence equilibrium (when $c > m$). When two equilibria are feasible, we verified that one or both eigenvalues are always positive for the equilibrium corresponding to smaller k. Although we are unable to prove it analytically, extensive numerical simulations suggest that the other equilibrium is always stable in this case, as well.

Altogether, this analysis suggests that if the equilibrium corresponding to larger k is feasible, it will always be locally stable provided P has exactly one positive eigenvalue. If the second equilibrium is also feasible, the model exhibits bistability. The possible outcomes across parameter space are illustrated graphically in Fig. 4.5 in the main text.

CHAPTER 5

CONCLUSION

The extent to which environmental feedbacks can drive community dynamics has, in many ecosystems, become clear only quite recently. The *ecosystem engineer* concept, which centers the role of biotic drivers of environmental heterogeneity – and, ultimately, biodiversity – was proposed less than 30 years ago [120]. Most of the other research programs surveyed in the Introduction – the study of microbial cross-feeding, plant-soil feedbacks, and immune-mediated pathogen competition – are even younger. This pattern is evident across ecology, where interest in "top-down" control of environmental heterogeneity, ranging from predator effects on spatial biogeochemistry [38, 208, 170] to forest effects on atmospheric flows and rainfall regimes [33, 216, 228], has surged in the last two decades. The only exception among our examples, Janzen-Connell effects, serve to prove the rule: While hypothesized more than 50 years ago [118, 54], research on this mechanism has matured and advanced rapidly in just the last few years [30, 238].

As we have discussed, a central role for environmental feedbacks challenges ecology's historical focus on explaining biological diversity within the fixed constraints of abiotic variation. This has undoubtedly contributed to their late arrival in the mainstream of the discipline. But aside from intellectual inertia, recognizing these processes is inherently challenging, because it requires a holistic view of ecosystems. Understanding the dynamics of microbial cross-feeding has required community ecologists to contemplate the details of intracellular metabolism and biochemistry. An appreciation of plant-soil feedbacks requires forest ecologists to consider the interactions between trees and soil microbes, organisms that can differ by eight orders of magnitude in size, and six or more orders of magnitude in lifespan. These processes cut across physical scales and disciplinary boundaries, and unraveling them has demanded new tools and new perspectives.

The same features that complicate the identification of environmental feedbacks pose

challenges for modeling them. To account for these processes, it is necessary to couple dynamics across multiple spatial and temporal scales. Feedbacks also open the door to complex dynamics, such as long transients, limit cycles, and historical contingency, that can be difficult to analyze. In this thesis, we developed and studied simple models for these processes, using minimal implementations of distinct spatial and temporal scales to capture the essential features of environmental feedback dynamics, while preserving analytical tractability. This simplicity made it possible to identify precise criteria for community coexistence, as well as new insights into the emergence of ecologically-relevant phenomena, such as the potential for instability at high rates of disturbance, episodic dynamics when environmental change is much slower than population dynamics, and a generic relationship between diversity and robustness when feedbacks take a symmetric form. In the second chapter, however, we analyzed a canonical model for plant-soil feedbacks and demonstrated that simplification can go too far, making it impossible to account for the coexistence of diverse communities. Striking an appropriate balance between simplicity and biological veracity is a recurring theme in this work, and an important ongoing challenge for developing a comprehensive theory of environmental feedbacks.

Minimal models are not only desirable because they permit analysis, but also because they lay bare the basic structure of environmental feedback dynamics. This facilitates comparison and synthesis across ecosystems, and across distinct strands of theory. The recent recognition of many kinds of environmental feedbacks means that these strands of theory have developed unevenly and not yet coalesced; there is surely much to gain simply by sharing insights, methods, and models between them. In this thesis, we have emphasized connections between models: the equivalence of the Bever model for plant-soil feedbacks and bimatrix game dynamics from evolutionary game theory, the essential similarity of metapopulation dynamics in heterogeneous landscapes and classical consumer-resource dynamics, the close relationship between our "fast" feedback model and recent models for microbial cross-feeding. These

connections are not mere curiosities, but powerful tools to leverage knowledge from one area to another. For example, we used the well-developed theory of bimatrix games to characterize the dynamics of the extended Bever model, and the theory of consumer-resource dynamics to conclude that our metapopulation model with exogenous heterogeneity is globally stable.

Our analysis sheds new light on the potential for environmental feedbacks to maintain coexistence of many species, but leaves many questions only dimly illuminated. We conclude by briefly discussing some of these questions, and the challenges and opportunities they hold for future study. These open directions can be roughly grouped into three categories: (i) questions regarding further analysis of our models, which will likely demand new mathematical insights or analytical tools, (ii) questions regarding extensions or generalizations of the model framework, which will demand a mix of careful biology to distill the necessary components and creative mathematical implementation to preserve model tractability, and finally (iii) some questions regarding experimental validation and application of these models, which only nature can answer.

5.1 Open questions for analysis

Our analysis of the Bever model in the second chapter leaves little open, aside from the already long-standing rescaled zero-sum games conjecture [103], which is of more mathematical than biological relevance, in any case. However, there is a great deal of room for deeper analysis of the models introduced in our third and fourth chapters. One especially intriguing phenomenon is the transition to instability sometimes observed as the rate of disturbance increases. We were able to characterize this transition in a special case, but our simulation results suggest that such bifurcations are a much more general feature of nonsymmetric environmental feedbacks. Indeed, the same type of behavior has recently received attention in models for microbial cross-feeding [156, 41, 73]. The existence of such transitions in our mathematical models raises the possibility that real-world ecosystems could collapse

suddenly under deteriorating environmental conditions. In general, it is unclear when the model will possess such a transition point – we observe this feature in the limiting case of fast feedbacks, but prove that it is precluded in the opposite limit of slow feedbacks. Is it a generic feature of the dynamics in between? Can we predict quantitatively where a transition will occur, as function of the colonization rate matrix P?

Aside from the practical relevance of this phenomenon, it seems a promising entry point for further analysis of the nonsymmetric model. Many of our results hold only under certain symmetries; for example, we can give a complete account of the local stability of the coexistence equilibrium only in the limit where feedbacks are very slow. Even in this case, the stability condition we derive lacks an intuitive interpretation comparable to what we can establish when the matrix P is symmetric. We rely on other symmetries, such as the assumptions that local extinction rates and environmental modification rates are the same for all species and patch types. Relaxing these assumptions would greatly extend the scope of the model analysis, and in particular make it possible to account for the obvious biological reality that some species are much more impactful "ecosystem engineers" than others. For the fast feedback model in our fourth chapter, we presented some evidence that variation in local extinction rates has little effect on the qualitative model dynamics, at least when P is symmetric. However, once these rates are allowed to vary, the model reduction that we employ in the third chapter becomes impossible. Progress here will likely come from studying the full model directly.

Finally, we note that while our analysis focused almost exclusively on establishing conditions for coexistence, our model framework could be used to investigate other aspects of ecosystem dynamics, such as invasions and community assembly, or aspects of community structure, composition, and function. Exploring these questions would require little or no modification to the model itself, but necessitate new approaches to the analysis.

5.2 Open questions for extension

As we have emphasized, our intention in this thesis is to develop theory of a minimal character, so there are many ways our model framework could be amended or extended. Here, we mention a few of particular interest.

Our model is grounded in the metapopulation framework, and treats space implicitly. Incorporating explicit spatial structure in our analysis, by considering the configuration of patches and limitations to dispersal, has the potential to refine or alter our conclusions. The distribution of species in space is considered an important aspect of some environmental feedback paradigms, such as Janzen-Connell effects, but it remains unclear how much the details of spatial structure and dispersal affect the essential dynamics [231]. Some theoretical studies have suggested that accounting for these factors can significantly modify the conditions for coexistence by, for example, reducing dispersal between habitat types [226], dampening or distributing oscillations over space [127, 198], or concentrating and strengthening feedbacks that maintain coexistence [232, 223]. Modern extensions of the metapopulation framework offer a variety of tools to account for explicit landscape structure and spatial distribution of habitat quality [91, 178, 173, 101, 147], but adapting these approaches to include multiple species and habitat modification poses significant challenges.

Another limitation of our framework is the assumption that patches can be characterized by one of n discrete states at any time. In many systems, especially those where environmental modification plays out on longer timescales than population dynamics, it is likely that local conditions will reflect the modifications of many species, which accumulate in some way over time. However, tracking the full history of patches becomes intractable using naïve approaches, because even simply accounting for the presence or absence of each species within some window of "memory" leads to an exponential blow-up in the number of model variables [11, 132]. Epidemiological strain theory offers some strategies to attack this problem [76, 77, 132, 13]. One promising possibility is to explicitly model only pairwise

associations between species, and use a low-order closure approach to approximate the full distribution of patch histories. However, one still needs to consider how the modifications of different species interact with one another. In epidemiological models, it is often reasonable to assume that specific immunity accumulates in an additive way, or to avoid this issue by assuming polarized immunity, but in other contexts, such as chemical habitat modification by microbes, the mechanics of such interactions may be non-trivial. As an alternative to our state-based framework, one could deal with this issue by explicitly modeling the internal processes and variables that mediate local patch conditions, but this would sacrifice the main virtues of our approach, which makes it possible to model dynamics without detailed knowledge of these internal details. It is worth noting that a solution to this problem of accumulated modification effects would open the door to allowing co-occupancy of patches – another desirable extension of the model, bringing the framework closer to true metacommunity models [139] – by resolving the associated ambiguity in how to combine modification effects.

A final generalization of the model is perhaps the most approachable, requiring only the integration of pieces already present in our framework. In our third chapter, we constructed and compared models for exogenous or endogenous environmental heterogeneity, but any natural landscape will contain some of both sources. While for the purposes of developing theoretical expectations it is useful to contrast the two cases, for accurately modeling ecosystems of interest, it may be important to combine the two mechanisms within a single model. This could be easily done by including additional patch types in our feedback model with fixed frequencies and no associated species. However, analysis of the model becomes more complicated because the number of environmental variables exceeds the number of species. For this scenario, it may be useful to draw on recent research in consumer-resource theory, where approaches from statistical physics have been applied to study equilibrium coexistence in the generic case where the number of species is less than the number of resources

[241, 5, 60]. This extension is also closely related to the problem of allowing variation in environmental modification rates, discussed above. A more general approach to that problem would likely translate into progress here.

5.3 Open questions for application

The ultimate goal of any theory is to help make sense of real-world ecosystems. Throughout this thesis, we have discussed the implications of our models and analysis for studying and managing natural systems. Like most "strategic" models, our approach is primarily meant as a platform to explore the essential features and qualitative behaviors of a general class of dynamics, and not as an attempt to accurately model any particular ecosystem. Our analysis suggests several qualitative hypotheses that should be robust to system specifics or quantitative details, such as general features of feedbacks that promote coexistence, a diversity-robustness relationship that should emerge when these conditions are met, and long-term qualitative differences between landscapes dominated by exogenous or endogenous heterogeneity. However, there are cases where our framework may be put to the test, and ultimately to work, more directly. Plant-soil feedbacks, in particular, represent a promising system for the application of our models. Experiments of the kind needed to parameterize our feedback model are routinely conducted in plant-soil feedback research, usually with the goal of conducting inference using the Bever model [31, 186]. While we showed in our second chapter that such inference may be spurious, it would be straightforward to use these data, and this kind of experimental design, to instead parameterize our model and attempt to predict plant community dynamics or outcomes such as community coexistence. This experimental paradigm could also be used to test specific model assumptions or approximations, such as the dependence of patch states on the most recent resident species, as we assume in our fourth chapter. This approximation could easily be assessed using a fully factorial experiment with two stages of soil conditioning.

We have also discussed the possibility of inferring model parameters from static associations between species and patch states in natural landscapes. Plant communities offer a suitable context for this kind of approach, because these associations persist on timescales long enough to measure without difficulty. Indeed, for trees and other long-lived species, these associations persist so long that manipulative approaches to parameter estimation are impractical. While validation of the model would be more challenging in these systems, our framework represents a promising tool for inferring coexistence mechanisms and long-term dynamics. For these applications, a combined framework integrating exogenous and endogenous sources of heterogeneity, as discussed above, would be most useful.

One specific application of considerable interest is clarifying the degree and structure of host specialization needed for natural enemies to maintain coexistence via Janzen-Connell effects or plant-soil feedbacks. This question has been a matter of significant debate as different modeling approaches have suggested conflicting requirements, in some cases casting doubt on the capacity of these mechanisms to maintain high levels of diversity [174, 211, 22, 49, 158, 227]. The tractability of our framework makes it a promising tool to help resolve this kind of ambiguity.

In general, our phenomenological modeling approach represents a practical way forward for studying environmental feedbacks. For applications where one is interested in emergent dynamics at the community level, suppression of the mechanistic details that underlie feedbacks may be a convenient and potentially more robust alternative to more granular modeling (see, for example, [187, 160]). However, the flexibility of this kind of approach can create other challenges. Combining estimates for many free model parameters can lead to inconsistent or unbiological predictions and inference, even in situations where very small changes in the parameter estimates would yield qualitative improvement [161, 160]. Such situations often arise when some model parameters are not strongly constrained and the mapping between model parameters and predictions is complex [87]. In diverse communi-

ties, this is the generic case. We view this issue as a fundamental challenge not only for modeling environmental feedbacks, but for all of community ecology. Robust inference for whole-community dynamics and outcomes will require a strong focus on the unique features of high-dimensional models [10, 230, 242]; emphasis on model prediction rather than parameterization [87, 160]; and creative strategies to constrain model fitting, such as ecologically-inspired low-dimensional structures [214, 221], biologically-informed penalization [161, 160], and other forms of statistical regularization [43, 255].

REFERENCES

[1] K. C. Abbott, M. B. Eppinga, J. Umbanhowar, M. Baudena, and J. D. Bever. Microbiome influence on host community dynamics: Conceptual integration of microbiome feedback with classical host–microbe theory. *Ecology Letters*, 24(12):2796–2811, 2021.

[2] P. A. Abrams and W. G. Wilson. Coexistence of competitors in metacommunities due to spatial variation in resource growth rates: does R* predict the outcome of competition? *Ecology Letters*, 7(10):929–940, 2004.

[3] C. I. Abreu, J. Friedman, V. L. A. Woltz, and J. Gore. Mortality causes universal changes in microbial community composition. *Nature communications*, 10(1):1–9, 2019.

[4] P. B. Adler, J. HilleRisLambers, and J. M. Levine. A niche for neutrality. *Ecology letters*, 10(2):95–104, 2007.

[5] M. Advani, G. Bunin, and P. Mehta. Statistical physics of community ecology: a cavity solution to Macarthur's consumer resource model. *Journal of Statistical Mechanics: Theory and Experiment*, 2018(3):033406, 2018.

[6] S. Allesina and J. M. Levine. A competitive network theory of species diversity. *Proceedings of the National Academy of Sciences*, 108(14):5638–5642, 2011.

[7] P. Amarasekare. Competitive coexistence in spatially structured environments: a synthesis. *Ecology letters*, 6(12):1109–1122, 2003.

[8] P. Amarasekare and H. Possingham. Patch dynamics and metapopulation theory: the case of successional species. *Journal of Theoretical Biology*, 209(3):333–344, 2001.

[9] D. R. Amor, C. Ratzke, and J. Gore. Transient invaders can induce shifts between alternative stable states of microbial communities. *Science Advances*, 6(8):eaay8676, 2020.

[10] P. W. Anderson. More is different. *Science*, 177(4047):393–396, 1972.

[11] V. Andreasen, J. Lin, and S. A. Levin. The dynamics of cocirculating influenza strains conferring partial cross-immunity. *Journal of mathematical biology*, 35(7):825–842, 1997.

[12] H. G. Andrewartha and L. C. Birch. *The distribution and abundance of animals*. University of Chicago Press, 1954.

[13] T. Aquino, D. Bolster, and A. Nunes. Characterization of the endemic equilibrium and response to mutant injection in a multi-strain disease model. *Journal of Theoretical Biology*, 368:27–36, 2015.

[14] G. Arfken. *Mathematical methods for physicists*. Academic Press, 1985.

[15] R. A. Armstrong. Competition, seed predation, and species coexistence. *Journal of Theoretical Biology*, 141(2):191–195, 1989.

[16] R. Bagchi, P. A. Henrys, P. E. Brown, D. F. P. Burslem, P. J. Diggle, C. S. Gunatilleke, I. N. Gunatilleke, A. R. Kassim, R. Law, S. Noor, et al. Spatial patterns reveal negative density dependence and habitat associations in tropical trees. *Ecology*, 92(9):1723–1729, 2011.

[17] C. A. Baldeck, K. E. Harms, J. B. Yavitt, R. John, B. L. Turner, R. Valencia, H. Navarrete, S. Bunyavejchewin, S. Kiratiprayoon, A. Yaacob, et al. Habitat filtering across tree life stages in tropical forest communities. *Proceedings of the Royal Society B: Biological Sciences*, 280(1766):20130548, 2013.

[18] R. B. Bapat, R. B. Bapat, T. Raghavan, et al. *Nonnegative matrices and applications*. Cambridge University Press, 1997.

[19] G. Barabás, M. J. Michalska-Smith, and S. Allesina. The effect of intra-and interspecific competition on coexistence in multispecies communities. *The American Naturalist*, 188(1):E1–E12, 2016.

[20] R. A. Bartel, N. M. Haddad, and J. P. Wright. Ecosystem engineers maintain a rare species of butterfly and increase plant diversity. *Oikos*, 119(5):883–890, 2010.

[21] J. T. Bauer, N. Blumenthal, A. J. Miller, J. K. Ferguson, and H. L. Reynolds. Effects of between-site variation in soil microbial communities and plant-soil feedbacks on the productivity and composition of plant communities. *Journal of Applied Ecology*, 54(4):1028–1039, 2017.

[22] M.-S. Benítez, M. H. Hersh, R. Vilgalys, and J. S. Clark. Pathogen regulation of plant diversity via effective specialization. *Trends in Ecology & Evolution*, 28(12):705–711, 2013.

[23] J. A. Bennett and J. Klironomos. Mechanisms of plant–soil feedback: interactions among biotic and abiotic drivers. *New Phytologist*, 222(1):91–96, 2019.

[24] J. Bever. Dynamics within mutualism and the maintenance of diversity: inference from a model of interguild frequency dependence. *Ecology Letters*, 2(1):52–61, 1999.

[25] J. D. Bever. *Ecological and evolutionary dynamics between plants and their soil community*. Duke University, 1992.

[26] J. D. Bever. Feedback between plants and their soil communities in an old field community. *Ecology*, 75(7):1965–1977, 1994.

[27] J. D. Bever. Host-specificity of am fungal population growth rates can generate feedback on plant growth. *Plant and Soil*, 244(1):281–290, 2002.

[28] J. D. Bever. Soil community feedback and the coexistence of competitors: conceptual frameworks and empirical tests. *New phytologist*, 157(3):465–473, 2003.

[29] J. D. Bever, I. A. Dickie, E. Facelli, J. M. Facelli, J. Klironomos, M. Moora, M. C. Rillig, W. D. Stock, M. Tibbett, and M. Zobel. Rooting theories of plant community ecology in microbial interactions. *Trends in ecology & evolution*, 25(8):468–478, 2010.

[30] J. D. Bever, S. A. Mangan, and H. M. Alexander. Maintenance of plant species diversity by pathogens. *Annual review of ecology, evolution, and systematics*, 46:305–325, 2015.

[31] J. D. Bever, K. M. Westover, and J. Antonovics. Incorporating the soil community into plant population dynamics: the utility of the feedback approach. *Journal of Ecology*, pages 561–573, 1997.

[32] B. M. Bolker. Combining endogenous and exogenous spatial variability in analytical population models. *Theoretical Population Biology*, 64(3):255–270, 2003.

[33] G. B. Bonan. Forests and climate change: forcings, feedbacks, and the climate benefits of forests. *science*, 320(5882):1444–1449, 2008.

[34] G. Bonanomi, F. Giannino, and S. Mazzoleni. Negative plant–soil feedback and species coexistence. *Oikos*, 111(2):311–321, 2005.

[35] W. E. Boyce, R. C. DiPrima, and D. B. Meade. *Elementary differential equations*. John Wiley & Sons, 2017.

[36] L. Brenig. Complete factorisation and analytic solutions of generalized lotka-volterra equations. *Physics Letters A*, 133(7-8):378–382, 1988.

[37] J. H. Brown. Two decades of homage to Santa Rosalia: toward a general theory of diversity. *American Zoologist*, 21(4):877–888, 1981.

[38] J. K. Bump, R. O. Peterson, and J. A. Vucetich. Wolves modulate soil nutrient heterogeneity and foliar nitrogen by configuring the distribution of ungulate carcasses. *Ecology*, 90(11):3159–3167, 2009.

[39] C. C. Buser, R. D. Newcomb, A. C. Gaskett, and M. R. Goddard. Niche construction initiates the evolution of mutualistic interactions. *Ecology Letters*, 17(10):1257–1264, 2014.

[40] S. Butler and J. P. O'Dwyer. Stability criteria for complex microbial communities. *Nature communications*, 9(1):1–10, 2018.

[41] S. Butler and J. P. O'Dwyer. Cooperation and stability for complex systems in resource-limited environments. *Theoretical Ecology*, 13(2):239–250, 2020.

[42] B. B. Casper and J. P. Castelli. Evaluating plant–soil feedback together with competition in a serpentine grassland. *Ecology letters*, 10(5):394–400, 2007.

[43] S. Cenci, G. Sugihara, and S. Saavedra. Regularized S-map for inference and forecasting with noisy ecological time series. *Methods in Ecology and Evolution*, 10(5):650–660, 2019.

[44] J. M. Chase and M. A. Leibold. *Ecological Niches: Linking Classical and Contemporary Approaches*. University of Chicago Press, 2003.

[45] X. Chen and J. E. Cohen. Global stability, local stability and permanence in model food webs. *Journal of Theoretical Biology*, 212(2):223–235, 2001.

[46] P. Chesson. Macarthur's consumer-resource model. *Theoretical Population Biology*, 37(1):26–38, 1990.

[47] P. Chesson. General theory of competitive coexistence in spatially-varying environments. *Theoretical population biology*, 58(3):211–237, 2000.

[48] P. L. Chesson. Coexistence of competitors in spatially and temporally varying environments: a look at the combined effects of different sorts of variability. *Theoretical Population Biology*, 28(3):263–287, 1985.

[49] R. A. Chisholm and T. Fung. Janzen-Connell effects are a weak impediment to competitive exclusion. *The American Naturalist*, 196(5):649–661, 2020.

[50] S. Cobey. Pathogen evolution and the immunological niche. *Annals of the New York Academy of Sciences*, 1320(1):1, 2014.

[51] C. Codeco and J. Grover. Competition along a spatial gradient of resource supply: a microbial experimental model. *The American Naturalist*, 157(3):300–315, 2001.

[52] M. L. Cody. *Competition and the Structure of Bird Communities*. Princeton University Press, 1974.

[53] C. D. Collins, J. D. Bever, and M. H. Hersh. Community context for mechanisms of disease dilution: insights from linking epidemiology and plant–soil feedback theory. *Annals of the New York Academy of Sciences*, 1469(1):65, 2020.

[54] J. H. Connell. On the role of natural enemies in preventing competitive exclusion in some marine animals and in rain forest trees. *Dynamics of populations*, 298:312, 1971.

[55] K. M. Crawford, J. T. Bauer, L. S. Comita, M. B. Eppinga, D. J. Johnson, S. A. Mangan, S. A. Queenborough, A. E. Strand, K. N. Suding, J. Umbanhowar, et al. When and where plant-soil feedback may promote plant coexistence: a meta-analysis. *Ecology Letters*, 22(8):1274–1284, 2019.

[56] R. Cressman and Y. Tao. The replicator equation and other game dynamics. *Proceedings of the National Academy of Sciences*, 111(Supplement 3):10810–10817, 2014.

[57] J. A. Crooks. Characterizing ecosystem-level consequences of biological invasions: the role of ecosystem engineers. *Oikos*, 97(2):153–166, 2002.

[58] F. Crotty, R. Fychan, R. Sanderson, J. Rhymes, F. Bourdin, J. Scullion, and C. Marley. Understanding the legacy effect of previous forage crop and tillage management on soil biology, after conversion to an arable crop rotation. *Soil Biology and Biochemistry*, 103:241–252, 2016.

[59] K. Cuddington, W. G. Wilson, and A. Hastings. Ecosystem engineers: feedback and population dynamics. *The American Naturalist*, 173(4):488–498, 2009.

[60] W. Cui, R. Marsland III, and P. Mehta. Effect of resource dynamics on species packing in diverse ecosystems. *Physical Review Letters*, 125(4):048101, 2020.

[61] M. Dal Bello, H. Lee, A. Goyal, and J. Gore. Resource–diversity relationships in bacterial communities reflect the network structure of microbial metabolism. *Nature Ecology & Evolution*, 5(10):1424–1434, 2021.

[62] T. Daufresne and L. O. Hedin. Plant coexistence depends on ecosystem nutrient cycles: extension of the resource-ratio theory. *Proceedings of the National Academy of Sciences*, 102(26):9212–9217, 2005.

[63] O. Diekmann and J. A. P. Heesterbeek. *Mathematical epidemiology of infectious diseases: model building, analysis and interpretation*, volume 5. John Wiley & Sons, 2000.

[64] M. B. Eppinga, M. Baudena, D. J. Johnson, J. Jiang, K. M. Mack, A. E. Strand, and J. D. Bever. Frequency-dependent feedback constrains plant community coexistence. *Nature Ecology & Evolution*, 2(9):1403–1407, 2018.

[65] M. B. Eppinga, M. Rietkerk, S. C. Dekker, P. C. De Ruiter, and W. H. Van der Putten. Accumulation of local pathogens: a new hypothesis to explain exotic plant invasions. *Oikos*, 114(1):168–176, 2006.

[66] M. J. Eppstein and J. Molofsky. Invasiveness in plant communities with feedbacks. *Ecology Letters*, 10(4):253–263, 2007.

[67] I. Eshel, E. Akin, et al. Coevolutionary instability of mixed nash solutions. *J. Math. Biol*, 18(2):123–133, 1983.

[68] M. S. Fitzsimons and R. M. Miller. The importance of soil microorganisms for maintaining diverse plant communities in tallgrass prairie. *American Journal of Botany*, 97(12):1937–1943, 2010.

[69] R. P. Freckleton and O. T. Lewis. Pathogens, density dependence and the coexistence of tropical trees. *Proceedings of the Royal Society B: Biological Sciences*, 273(1604):2909–2916, 2006.

[70] D. Friedman. Evolutionary games in economics. *Econometrica: Journal of the Econometric Society*, pages 637–666, 1991.

[71] G. F. Gause. *The struggle for existence: a classic of mathematical biology and ecology*. Courier Dover Publications, 2019.

[72] T. Gibbs, J. Grilli, T. Rogers, and S. Allesina. Effect of population abundances on the stability of large random ecosystems. *Physical Review E*, 98(2):022410, 2018.

[73] T. Gibbs, Y. Zhang, Z. R. Miller, and J. P. O'Dwyer. Stability criteria for the consumption and exchange of essential resources. *bioRxiv*, 2021.

[74] E. Gilad, J. von Hardenberg, A. Provenzale, M. Shachak, and E. Meron. A mathematical model of plants as ecosystem engineers. *Journal of Theoretical Biology*, 244(4):680–691, 2007.

[75] G. S. Gilbert and C. O. Webb. Phylogenetic signal in plant pathogen–host range. *Proceedings of the National Academy of Sciences*, 104(12):4979–4983, 2007.

[76] J. R. Gog and B. T. Grenfell. Dynamics and selection of many-strain pathogens. *Proceedings of the National Academy of Sciences*, 99(26):17209–17214, 2002.

[77] J. R. Gog and J. Swinton. A status-based approach to multiple strain dynamics. *Journal of mathematical biology*, 44(2):169–184, 2002.

[78] B. S. Goh. Global stability in many-species systems. *The American Naturalist*, 111(977):135–143, 1977.

[79] J. E. Goldford, N. Lu, D. Bajić, S. Estrela, M. Tikhonov, A. Sanchez-Gorostiaga, D. Segrè, P. Mehta, and A. Sanchez. Emergent simplicity in microbial community assembly. *Science*, 361(6401):469–474, 2018.

[80] B. T. Grenfell, O. G. Pybus, J. R. Gog, J. L. Wood, J. M. Daly, J. A. Mumford, and E. C. Holmes. Unifying the epidemiological and evolutionary dynamics of pathogens. *science*, 303(5656):327–332, 2004.

[81] J. Grilli, G. Barabás, M. J. Michalska-Smith, and S. Allesina. Higher-order interactions stabilize dynamics in competitive network models. *Nature*, 548(7666):210–213, 2017.

[82] T. Gross, K. T. Allhoff, B. Blasius, U. Brose, B. Drossel, A. K. Fahimipour, C. Guill, J. D. Yeakel, and F. Zeng. Modern models of trophic meta-communities. *Philosophical Transactions of the Royal Society B*, 375(1814):20190455, 2020.

[83] J. P. Grover. Resource storage and competition with spatial and temporal variation in resource availability. *The American Naturalist*, 178(5):E124–E148, 2011.

[84] P. J. Grubb. The maintenance of species-richness in plant communities: the importance of the regeneration niche. *Biological review*, 52:107–145, 1977.

[85] S. Gupta, N. Ferguson, and R. Anderson. Chaos, persistence, and evolution of strain structure in antigenically diverse infectious agents. *Science*, 280(5365):912–915, 1998.

[86] W. Gurney and J. Lawton. The population dynamics of ecosystem engineers. *Oikos*, 76(2):273–283, 1996.

[87] R. N. Gutenkunst, J. J. Waterfall, F. P. Casey, K. S. Brown, C. R. Myers, and J. P. Sethna. Universally sloppy parameter sensitivities in systems biology models. *PLoS computational biology*, 3(10):e189, 2007.

[88] J. L. Gutiérrez, C. G. Jones, D. L. Strayer, and O. O. Iribarne. Mollusks as ecosystem engineers: the role of shell production in aquatic habitats. *Oikos*, 101(1):79–90, 2003.

[89] W. Hahn, H. H. Hosenthien, and H. Lehnigk. *Theory and application of Liapunov's direct method*, volume 3. Prentice-Hall Englewood Cliffs, NJ, 1963.

[90] S. R. Hall. Stoichiometrically explicit food webs: feedbacks between resource supply, elemental constraints, and species diversity. *Annual Review of Ecology, Evolution, and Systematics*, 40:503–528, 2009.

[91] I. Hanski and O. Ovaskainen. The metapopulation capacity of a fragmented landscape. *Nature*, 404(6779):755–758, 2000.

[92] I. A. Hanski, M. E. Gilpin, and D. E. McCauley. *Metapopulation biology*, volume 454. Elsevier, 1997.

[93] G. Hardin. The competitive exclusion principle: An idea that took a century to be born has implications in ecology, economics, and genetics. *science*, 131(3409):1292–1297, 1960.

[94] K. E. Harms, R. Condit, S. P. Hubbell, and R. B. Foster. Habitat associations of trees and shrubs in a 50-ha neotropical forest plot. *Journal of ecology*, 89(6):947–959, 2001.

[95] A. Hastings, K. C. Abbott, K. Cuddington, T. Francis, G. Gellner, Y.-C. Lai, A. Morozov, S. Petrovskii, K. Scranton, and M. L. Zeeman. Transient phenomena in ecology. *Science*, 361(6406):eaat6412, 2018.

[96] A. Hastings, J. E. Byers, J. A. Crooks, K. Cuddington, C. G. Jones, J. G. Lambrinos, T. S. Talley, and W. G. Wilson. Ecosystem engineering in space and time. *Ecology letters*, 10(2):153–164, 2007.

[97] Q. He, S. Pilosof, K. E. Tiedje, K. P. Day, and M. Pascual. Frequency-dependent competition between strains imparts persistence to perturbations in a model of plasmodium falciparum malaria transmission. *Frontiers in Ecology and Evolution*, 9:633263, 2021.

[98] A. Hector and R. Hooper. Darwin and the first ecological experiment. *Science*, 295(5555):639–640, 2002.

[99] A. Hector, B. Schmid, C. Beierkuhnlein, M. Caldeira, M. Diemer, P. G. Dimitrakopoulos, J. Finn, H. Freitas, P. Giller, J. Good, et al. Plant diversity and productivity experiments in european grasslands. *Science*, 286(5442):1123–1127, 1999.

[100] B. Hernández-Bermejo, V. Fairén, and L. Brenig. Algebraic recasting of nonlinear systems of ODEs into universal formats. *Journal of Physics A: Mathematical and General*, 31(10):2415, 1998.

[101] D. E. Hiebeler, I. J. Michaud, B. A. Wasserman, and T. D. Buchak. Habitat association in populations on landscapes with continuous-valued heterogeneous habitat quality. *Journal of theoretical biology*, 317:47–54, 2013.

[102] A. Hodge and A. H. Fitter. Microbial mediation of plant competition and community structure. *Functional Ecology*, 27(4):865–875, 2013.

[103] J. Hofbauer. Evolutionary dynamics for bimatrix games: A hamiltonian system? *Journal of mathematical biology*, 34(5):675–688, 1996.

[104] J. Hofbauer. Deterministic evolutionary game dynamics. In *Evolutionary Game Dynamics*, volume 69, pages 61–79. American Mathematical Society Providence, RI, 2011.

[105] J. Hofbauer and K. Sigmund. *Evolutionary games and population dynamics*. Cambridge University Press, 1998.

[106] R. D. Holt. From metapopulation dynamics to community structure: some consequences of spatial heterogeneity. In *Metapopulation biology*, pages 149–164. Elsevier, 1997.

[107] D. U. Hooper, F. Chapin Iii, J. J. Ewel, A. Hector, P. Inchausti, S. Lavorel, J. H. Lawton, D. Lodge, M. Loreau, S. Naeem, et al. Effects of biodiversity on ecosystem functioning: a consensus of current knowledge. *Ecological monographs*, 75(1):3–35, 2005.

[108] H. S. Horn and R. H. MacArthur. Competition among fugitive species in a harlequin environment. *Ecology*, 53(4):749–752, 1972.

[109] R. A. Horn and C. R. Johnson. *Matrix analysis*. Cambridge University Press, 2012.

[110] P. Hughes and E. Seneta. Selection equilibria in a multiallele single-locus setting. *Heredity*, 35(2):185–194, 1975.

[111] C. Hui, Z. Li, and D.-x. Yue. Metapopulation dynamics and distribution, and environmental heterogeneity induced by niche construction. *Ecological Modelling*, 177(1-2):107–118, 2004.

[112] G. E. Hutchinson. Homage to Santa Rosalia or why are there so many kinds of animals? *The American Naturalist*, 93(870):145–159, 1959.

[113] G. E. Hutchinson. The paradox of the plankton. *The American Naturalist*, 95(882):137–145, 1961.

[114] V. Hutson. The existence of an equilibrium for permanent systems. *The Rocky Mountain Journal of Mathematics*, pages 1033–1040, 1990.

[115] V. Hutson and K. Schmitt. Permanence and the dynamics of biological systems. *Mathematical biosciences*, 111(1):1–71, 1992.

[116] Y. Iwasa and J. Roughgarden. Interspecific competition among metapopulations with space-limited subpopulations. *Theoretical Population Biology*, 30(2):194–214, 1986.

[117] S. T. Jackson. Alexander von Humboldt and the general physics of the earth. *Science*, 324(5927):596–597, 2009.

[118] D. H. Janzen. Herbivores and the number of tree species in tropical forests. *The American Naturalist*, 104(940):501–528, 1970.

[119] C. G. Jones, J. L. Gutiérrez, J. E. Byers, J. A. Crooks, J. G. Lambrinos, and T. S. Talley. A framework for understanding physical ecosystem engineering by organisms. *Oikos*, 119(12):1862–1869, 2010.

[120] C. G. Jones, J. H. Lawton, and M. Shachak. Organisms as ecosystem engineers. In *Ecosystem management*, pages 130–147. Springer, 1994.

[121] E. Juárez-Ruiz, R. Cortés-Maldonado, and F. Pérez-Rodríguez. Relationship between the inverses of a matrix and a submatrix. *Computación y Sistemas*, 20(2):251–262, 2016.

[122] G. S. Kandlikar, C. A. Johnson, X. Yan, N. J. Kraft, and J. M. Levine. Winning and losing with microbes: how microbially mediated fitness differences influence plant diversity. *Ecology letters*, 22(8):1178–1191, 2019.

[123] S. Karlin. Levels of multiallelic overdominance fitness, heterozygote excess and heterozygote deficiency. *Theoretical population biology*, 37(1):129–149, 1990.

[124] P.-J. Ke and T. Miki. Incorporating the soil environment and microbial community into plant competition theory. *Frontiers in microbiology*, 6:1066, 2015.

[125] P.-J. Ke and J. Wan. Effects of soil microbes on plant competition: A perspective from modern coexistence theory. *Ecological Monographs*, 90(1):e01391, 2020.

[126] E. D. Kelsic, J. Zhao, K. Vetsigian, and R. Kishony. Counteraction of antibiotic production and degradation stabilizes microbial communities. *Nature*, 521(7553):516–519, 2015.

[127] B. Kerr, M. A. Riley, M. W. Feldman, and B. J. Bohannan. Local dispersal promotes biodiversity in a real-life game of rock–paper–scissors. *Nature*, 418(6894):171–174, 2002.

[128] J. F. Kingman. A mathematical problem in population genetics. In *Mathematical Proceedings of the Cambridge Philosophical Society*, volume 57, pages 574–582. Cambridge University Press, 1961.

[129] J. N. Klironomos. Feedback with soil biota contributes to plant rarity and invasiveness in communities. *Nature*, 417(6884):67–70, 2002.

[130] T. Koffel, T. Daufresne, and C. A. Klausmeier. From competition to facilitation and mutualism: a general theory of the niche. *Ecological Monographs*, 91(3):e01458, 2021.

[131] D. C. Krakauer, K. M. Page, and D. H. Erwin. Diversity, dilemmas, and monopolies of niche construction. *The American Naturalist*, 173(1):26–40, 2009.

[132] S. Kryazhimskiy, U. Dieckmann, S. A. Levin, and J. Dushoff. On state-space reduction in multi-strain pathogen models, with an application to antigenic drift in influenza a. *PLoS computational biology*, 3(8):e159, 2007.

[133] A. J. Kucharski, V. Andreasen, and J. R. Gog. Capturing the dynamics of pathogens with many strains. *Journal of mathematical biology*, 72(1):1–24, 2016.

[134] S. E. Kuebbing, A. T. Classen, J. J. Call, J. A. Henning, and D. Simberloff. Plant–soil interactions promote co-occurrence of three nonnative woody shrubs. *Ecology*, 96(8):2289–2299, 2015.

[135] A. Kulmatiski, K. H. Beard, J. R. Stevens, and S. M. Cobbold. Plant–soil feedbacks: a meta-analytical review. *Ecology letters*, 11(9):980–992, 2008.

[136] A. Kulmatiski, J. Heavilin, and K. H. Beard. Testing predictions of a three-species plant–soil feedback model. *Journal of Ecology*, 99(2):542–550, 2011.

[137] G. Kylafis and M. Loreau. Niche construction in the light of niche theory. *Ecology Letters*, 14(2):82–90, 2011.

[138] K. N. Laland, J. Odling-Smee, and M. W. Feldman. Niche construction, biological evolution, and cultural change. *Behavioral and brain sciences*, 23(1):131–146, 2000.

[139] M. A. Leibold, M. Holyoak, N. Mouquet, P. Amarasekare, J. M. Chase, M. F. Hoopes, R. D. Holt, J. B. Shurin, R. Law, D. Tilman, et al. The metacommunity concept: a framework for multi-scale community ecology. *Ecology letters*, 7(7):601–613, 2004.

[140] Y. Lekberg, J. D. Bever, R. A. Bunn, R. M. Callaway, M. M. Hart, S. N. Kivlin, J. Klironomos, B. G. Larkin, J. L. Maron, K. O. Reinhart, et al. Relative importance of competition and plant–soil feedback, their synergy, context dependency and implications for coexistence. *Ecology Letters*, 21(8):1268–1281, 2018.

[141] S. A. Levin. Community equilibria and stability, and an extension of the competitive exclusion principle. *The American Naturalist*, 104(939):413–423, 1970.

[142] S. A. Levin. Population dynamic models in heterogeneous environments. *Annual review of ecology and systematics*, 7(1):287–310, 1976.

[143] J. M. Levine, E. Pachepsky, B. E. Kendall, S. G. Yelenik, and J. H. R. Lambers. Plant–soil feedbacks and invasive spread. *Ecology letters*, 9(9):1005–1014, 2006.

[144] R. Levins. Some demographic and genetic consequences of environmental heterogeneity for biological control. *American Entomologist*, 15(3):237–240, 1969.

[145] J. Levinton. Bioturbators as ecosystem engineers: control of the sediment fabric, inter-individual interactions, and material fluxes. In *Linking species & ecosystems*, pages 29–36. Springer, 1995.

[146] C. Liao, T. Wang, S. Maslov, and J. B. Xavier. Modeling microbial cross-feeding at intermediate scale portrays community dynamics and species coexistence. *PLoS computational biology*, 16(8):e1008135, 2020.

[147] J. Liao, Z. Li, D. E. Hiebeler, Y. Iwasa, J. Bogaert, and I. Nijs. Species persistence in landscapes with spatial variation in habitat quality: a pair approximation model. *Journal of Theoretical Biology*, 335:22–30, 2013.

[148] E. J. Lundgren, D. Ramp, J. C. Stromberg, J. Wu, N. C. Nieto, M. Sluk, K. T. Moeller, and A. D. Wallach. Equids engineer desert water availability. *Science*, 372(6541):491–495, 2021.

[149] R. MacArthur. Species packing and competitive equilibrium for many species. *Theoretical population biology*, 1(1):1–11, 1970.

[150] R. MacArthur and R. Levins. The limiting similarity, convergence, and divergence of coexisting species. *The american naturalist*, 101(921):377–385, 1967.

[151] R. MacArthur, H. Recher, and M. Cody. On the relation between habitat selection and species diversity. *The American Naturalist*, 100(913):319–332, 1966.

[152] R. H. MacArthur. Population ecology of some warblers of northeastern coniferous forests. *Ecology*, 39(4):599–619, 1958.

[153] E. Mächler and F. Altermatt. Interaction of species traits and environmental disturbance predicts invasion success of aquatic microorganisms. *PLoS ONE*, 7(9), 2012.

[154] K. M. Mack, M. B. Eppinga, and J. D. Bever. Plant-soil feedbacks promote coexistence and resilience in multi-species communities. *Plos one*, 14(2):e0211572, 2019.

[155] S. A. Mangan, S. A. Schnitzer, E. A. Herre, K. M. Mack, M. C. Valencia, E. I. Sanchez, and J. D. Bever. Negative plant–soil feedback predicts tree-species relative abundance in a tropical forest. *Nature*, 466(7307):752–755, 2010.

[156] R. Marsland III, W. Cui, J. Goldford, A. Sanchez, K. Korolev, and P. Mehta. Available energy fluxes drive a transition in the diversity, stability, and functional structure of microbial communities. *PLoS computational biology*, 15(2):e1006793, 2019.

[157] R. Marsland III, W. Cui, and P. Mehta. The minimum environmental perturbation principle: A new perspective on niche theory. *The American Naturalist*, 196(3):291–305, 2020.

[158] F. May, T. Wiegand, A. Huth, and J. M. Chase. Scale-dependent effects of conspecific negative density dependence and immigration on biodiversity maintenance. *Oikos*, 129(7):1072–1083, 2020.

[159] R. M. May. On the theory of niche overlap. *Theoretical population biology*, 5(3):297–332, 1974.

[160] D. S. Maynard, Z. R. Miller, and S. Allesina. Predicting coexistence in experimental ecological communities. *Nature ecology & evolution*, 4(1):91–100, 2020.

[161] D. S. Maynard, J. T. Wootton, C. A. Serván, and S. Allesina. Reconciling empirical interactions and species coexistence. *Ecology letters*, 22(6):1028–1037, 2019.

[162] E. J. McIntire and A. Fajardo. Facilitation as a ubiquitous driver of biodiversity. *New phytologist*, 201(2):403–416, 2014.

[163] G. Meszéna, M. Gyllenberg, L. Pásztor, and J. A. Metz. Competitive exclusion and limiting similarity: a unified theory. *Theoretical population biology*, 69(1):68–87, 2006.

[164] Z. R. Miller and S. Allesina. Metapopulations with habitat modification. *Proceedings of the National Academy of Sciences*, 118(49), 2021.

[165] Z. R. Miller and S. Allesina. Metapopulations with habitat modification. `https://github.com/zacharyrmiller/metapopulations_with_habitat_modification`, 2021.

[166] Z. R. Miller and S. Allesina. Habitat heterogeneity, environmental feedbacks, and species coexistence across timescales. `https://github.com/zacharyrmiller/heterogeneity_and_coexistence`, 2022.

[167] Z. R. Miller, P. Lechón-Alonso, and S. Allesina. No robust multispecies coexistence in a canonical model of plant–soil feedbacks. *Ecology Letters*, 2022.

[168] J. Molofsky, J. D. Bever, J. Antonovics, and T. J. Newman. Negative frequency dependence and the importance of spatial scale. *Ecology*, 83(1):21–27, 2002.

[169] B. Momeni, L. Xie, and W. Shou. Lotka-volterra pairwise modeling fails to capture diverse pairwise microbial interactions. *Elife*, 6:e25051, 2017.

[170] J. D. Monk and O. J. Schmitz. Landscapes shaped from the top down: predicting cascading predator effects on spatial biogeochemistry. *Oikos*, 2021.

[171] M. Nicolson. Alexander von Humboldt, Humboldtian science and the origins of the study of vegetation. *History of science*, 25(2):167–194, 1987.

[172] L. Niehaus, I. Boland, M. Liu, K. Chen, D. Fu, C. Henckel, K. Chaung, S. E. Miranda, S. Dyckman, M. Crum, et al. Microbial coexistence through chemical-mediated interactions. *Nature communications*, 10(1):1–12, 2019.

[173] A. North and O. Ovaskainen. Interactions between dispersal, competition, and landscape heterogeneity. *Oikos*, 116(7):1106–1119, 2007.

[174] V. Novotny, Y. Basset, S. E. Miller, G. D. Weiblen, B. Bremer, L. Cizek, and P. Drozd. Low host specificity of herbivorous insects in a tropical forest. *Nature*, 416(6883):841–844, 2002.

[175] F. J. Odling-Smee, K. N. Laland, and M. W. Feldman. Niche construction. In *Niche Construction*. Princeton University Press, 2013.

[176] R. J. Oidtman, P. Arevalo, Q. Bi, L. McGough, C. J. Russo, D. V. Cruz, M. C. Vieira, and K. M. Gostic. Influenza immune escape under heterogeneous host immune histories. *Trends in Microbiology*, 29(12):1072–1082, 2021.

[177] T. Oliver, D. B. Roy, J. K. Hill, T. Brereton, and C. D. Thomas. Heterogeneous landscapes promote population stability. *Ecology letters*, 13(4):473–484, 2010.

[178] O. Ovaskainen, K. Sato, J. Bascompte, and I. Hanski. Metapopulation models for extinction threshold in spatially correlated landscapes. *Journal of theoretical Biology*, 215(1):95–108, 2002.

[179] J. P. O'Dwyer. Whence Lotka-Volterra? *Theoretical Ecology*, 11(4):441–452, 2018.

[180] S. W. Pacala and D. Tilman. Limiting similarity in mechanistic and spatial models of plant competition in heterogeneous environments. *The American Naturalist*, 143(2):222–257, 1994.

[181] J. Pastor. Thoughts on the generation and importance of spatial heterogeneity in ecosystems and landscapes. In *Ecosystem function in heterogeneous landscapes*, pages 49–66. Springer, 2005.

[182] T. Peller, J. N. Marleau, and F. Guichard. Traits affecting nutrient recycling by mobile consumers can explain coexistence and spatially heterogeneous trophic regulation across a meta-ecosystem. *Ecology letters*, 25(2):440–452, 2022.

[183] J. Pena. Positive symmetric matrices with exactly one positive eigenvalue. *Linear algebra and its applications*, 430(5-6):1566–1573, 2009.

[184] J. M. Peña. Exclusion and inclusion intervals for the real eigenvalues of positive matrices. *SIAM journal on matrix analysis and applications*, 26(4):908–917, 2005.

[185] T. H. Pendergast IV, D. J. Burke, and W. P. Carson. Belowground biotic complexity drives aboveground dynamics: a test of the soil community feedback model. *New Phytologist*, 197(4):1300–1310, 2013.

[186] E. Pernilla Brinkman, W. H. Van der Putten, E.-J. Bakker, and K. J. Verhoeven. Plant–soil feedback: experimental approaches, statistical analyses and ecological interpretations. *Journal of Ecology*, 98(5):1063–1073, 2010.

[187] C. T. Perretti, S. B. Munch, and G. Sugihara. Model-free forecasting outperforms the correct mechanistic model for simulated and experimental data. *Proceedings of the National Academy of Sciences*, 110(13):5253–5257, 2013.

[188] J. S. Petermann, A. J. Fergus, L. A. Turnbull, and B. Schmid. Janzen-Connell effects are widespread and strong enough to maintain diversity in grasslands. *Ecology*, 89(9):2399–2406, 2008.

[189] P. S. Petraitis and R. E. Latham. The importance of scale in testing the origins of alternative community states. *Ecology*, 80(2):429–442, 1999.

[190] S. Pettersson, V. M. Savage, and M. N. Jacobi. Stability of ecosystems enhanced by species-interaction constraints. *Physical Review E*, 102(6):062405, 2020.

[191] L. Philippot, J. M. Raaijmakers, P. Lemanceau, and W. H. Van Der Putten. Going back to the roots: the microbial ecology of the rhizosphere. *Nature Reviews Microbiology*, 11(11):789–799, 2013.

[192] O. L. Phillips, P. N. Vargas, A. L. Monteagudo, A. P. Cruz, M.-E. C. Zans, W. G. Sánchez, M. Yli-Halla, and S. Rose. Habitat association among Amazonian tree species: a landscape-scale approach. *Journal of ecology*, 91(5):757–775, 2003.

[193] E. R. Pianka. Niche overlap and diffuse competition. *Proceedings of the National Academy of Sciences*, 71(5):2141–2145, 1974.

[194] P. Piccardi, B. Vessman, and S. Mitri. Toxicity drives facilitation between 4 bacterial species. *Proceedings of the National Academy of Sciences*, 116(32):15979–15984, 2019.

[195] C. Pizano, K. Kitajima, J. H. Graham, and S. A. Mangan. Negative plant–soil feedbacks are stronger in agricultural habitats than in forest fragments in the tropical andes. *Ecology*, 100(12):e02850, 2019.

[196] C. Ratzke and J. Gore. Modifying and reacting to the environmental ph can drive bacterial interactions. *PLoS biology*, 16(3):e2004248, 2018.

[197] X. Raynaud, C. G. Jones, and S. Barot. Ecosystem engineering, environmental decay and environmental states of landscapes. *Oikos*, 122(4):591–600, 2013.

[198] T. A. Revilla, G. C. Veen, M. B. Eppinga, and F. J. Weissing. Plant–soil feedbacks and the coexistence of competing plants. *Theoretical Ecology*, 6(2):99–113, 2013.

[199] T. M. Rocha Filho, I. M. Gléria, A. Figueiredo, and L. Brenig. The lotka–volterra canonical format. *Ecological modelling*, 183(1):95–106, 2005.

[200] R. P. Rohr, S. Saavedra, G. Peralta, C. M. Frost, L.-F. Bersier, J. Bascompte, and J. M. Tylianakis. Persist or produce: a community trade-off tuned by species evenness. *The American Naturalist*, 188(4):411–422, 2016.

[201] G. Q. Romero, T. Gonçalves-Souza, C. Vieira, and J. Koricheva. Ecosystem engineering effects on species diversity across ecosystems: a meta-analysis. *Biological Reviews*, 90(3):877–890, 2015.

[202] R. F. Rosenzweig, R. Sharp, D. S. Treves, and J. Adams. Microbial evolution in a simple unstructured environment: genetic differentiation in Escherichia coli. *Genetics*, 137(4):903–917, 1994.

[203] J. Roughgarden. Influence of competition on patchiness in a random environment. *Theoretical Population Biology*, 14(2):185–203, 1978.

[204] S. Saavedra and M. AlAdwani. Feasibility conditions of ecological models: Unfolding links between model parameters. *bioRxiv*, 2021.

[205] S. Saavedra, R. P. Rohr, J. Bascompte, O. Godoy, N. J. Kraft, and J. M. Levine. A structural approach for understanding multispecies coexistence. *Ecological Monographs*, 87(3):470–486, 2017.

[206] P. F. Sale. Maintenance of high diversity in coral reef fish communities. *The American Naturalist*, 111(978):337–359, 1977.

[207] C. Sarmiento, P.-C. Zalamea, J. W. Dalling, A. S. Davis, S. M. Stump, J. M. U'Ren, and A. E. Arnold. Soilborne fungi have host affinity and host-specific effects on seed germination and survival in a lowland tropical forest. *Proceedings of the National Academy of Sciences*, 114(43):11458–11463, 2017.

[208] O. J. Schmitz, D. Hawlena, and G. C. Trussell. Predator control of ecosystem nutrient dynamics. *Ecology letters*, 13(10):1199–1209, 2010.

[209] T. W. Schoener. Resource partitioning in ecological communities: Research on how similar species divide resources helps reveal the natural regulation of species diversity. *Science*, 185(4145):27–39, 1974.

[210] J. A. Schweitzer, J. K. Bailey, D. G. Fischer, C. J. LeRoy, E. V. Lonsdorf, T. G. Whitham, and S. C. Hart. Plant–soil–microorganism interactions: heritable relationship between plant genotype and associated soil microorganisms. *Ecology*, 89(3):773–781, 2008.

[211] B. E. Sedio and A. M. Ostling. How specialised must natural enemies be to facilitate coexistence among plants? *Ecology Letters*, 16(8):995–1003, 2013.

[212] R. Selten. A note on evolutionarily stable strategies in asymmetric animal conflicts. In *Models of Strategic Rationality*, pages 67–75. Springer, 1988.

[213] C. A. Serván, J. A. Capitán, J. Grilli, K. E. Morrison, and S. Allesina. Coexistence of many species in random ecosystems. *Nature ecology & evolution*, 2(8):1237–1242, 2018.

[214] C. A. Serván, J. A. Capitán, Z. R. Miller, and S. Allesina. Effects of phylogeny on coexistence in model communities. *bioRxiv*, 10.1101/2020.09.04.283507, 2020.

[215] C. A. Serván and S. Allesina. Tractable models of ecological assembly. *Ecology Letters*, 24(5):1029–1037, 2021.

[216] D. Sheil and D. Murdiyarso. How forests attract rain: an examination of a new hypothesis. *Bioscience*, 59(4):341–347, 2009.

[217] L. G. Shoemaker and B. A. Melbourne. Linking metacommunity paradigms to spatial coexistence mechanisms. *Ecology*, 97(9):2436–2446, 2016.

[218] J. B. Shurin, P. Amarasekare, J. M. Chase, R. D. Holt, M. F. Hoopes, and M. A. Leibold. Alternative stable states and regional community structure. *Journal of Theoretical Biology*, 227(3):359–368, 2004.

[219] J. Silvertown, M. E. Dodd, D. J. Gowing, and J. O. Mountford. Hydrologically defined niches reveal a basis for species richness in plant communities. *Nature*, 400(6739):61–63, 1999.

[220] G. Sinclair. *Hortus Gramineus Woburnensis: Or, An Account of the Results of Experiments on the Produce and Nutritive Qualities of Different Grasses and Other Plants: Used as the Food of the More Valuable Domestic Animals: Instituted by John, Duke of Bedford*. James Ridgway, 1826.

[221] A. Skwara, P. Lemos-Costa, Z. R. Miller, and S. Allesina. Modeling ecological communities when composition is manipulated experimentally. *bioRxiv*, 2022.

[222] S. Smale. On the differential equations of species in competition. *Journal of Mathematical Biology*, 3(1):5–7, 1976.

[223] D. J. Smith. On the interaction between Janzen-Connell effects and habitat partitioning in spatially structured environments. *bioRxiv*, 2022.

[224] D. J. Smith, A. S. Lapedes, J. C. De Jong, T. M. Bestebroer, G. F. Rimmelzwaan, A. D. Osterhaus, and R. A. Fouchier. Mapping the antigenic and genetic evolution of influenza virus. *science*, 305(5682):371–376, 2004.

[225] L. M. Smith and H. L. Reynolds. Plant–soil feedbacks shift from negative to positive with decreasing light in forest understory species. *Ecology*, 96(9):2523–2532, 2015.

[226] R. E. Snyder and P. Chesson. Local dispersal can facilitate coexistence in the presence of permanent spatial heterogeneity. *Ecology letters*, 6(4):301–309, 2003.

[227] X. Song, J. Y. Lim, J. Yang, and M. S. Luskin. When do Janzen–Connell effects matter? a phylogenetic meta-analysis of conspecific negative distance and density dependence experiments. *Ecology Letters*, 24(3):608–620, 2021.

[228] D. Spracklen, J. Baker, L. Garcia-Carreras, J. Marsham, et al. The effects of tropical vegetation on rainfall. *Annual Review of Environment and Resources*, 43(1):193–218, 2018.

[229] D. B. Stouffer, O. Godoy, G. V. Dalla Riva, and M. M. Mayfield. The dimensionality of plant–plant competition. *bioRxiv*, 2021.

[230] C. Strobeck. N species competition. *Ecology*, 54(3):650–654, 1973.

[231] S. M. Stump and P. Chesson. Distance-responsive predation is not necessary for the Janzen–Connell hypothesis. *Theoretical Population Biology*, 106:60–70, 2015.

[232] S. M. Stump, E. C. Johnson, and C. A. Klausmeier. Local interactions and self-organized spatial patterns stabilize microbial cross-feeding against cheaters. *Journal of the Royal Society Interface*, 15(140):20170822, 2018.

[233] K. N. Suding, W. Stanley Harpole, T. Fukami, A. Kulmatiski, A. S. MacDougall, C. Stein, and W. H. van der Putten. Consequences of plant–soil feedbacks in invasion. *Journal of Ecology*, 101(2):298–308, 2013.

[234] G. Szederkenyi, A. Magyar, and K. M. Hangos. *Analysis and control of polynomial dynamic models with biological applications*. Academic Press, 2018.

[235] P. D. Taylor. Evolutionarily stable strategies with two types of player. *Journal of applied probability*, 16(1):76–83, 1979.

[236] L. Tedersoo, M. Bahram, and M. Zobel. How mycorrhizal associations drive plant population and community biology. *Science*, 367(6480), 2020.

[237] J. Terborgh. Enemies maintain hyperdiverse tropical forests. *The American Naturalist*, 179(3):303–314, 2012.

[238] J. Terborgh. At 50, Janzen–Connell has come of age. *BioScience*, 70(12):1082–1092, 2020.

[239] M. S. Thomsen, T. Wernberg, A. Altieri, F. Tuya, D. Gulbransen, K. J. McGlathery, M. Holmer, and B. R. Silliman. Habitat cascades: the conceptual context and global relevance of facilitation cascades via habitat formation and modification. *Integrative and Comparative Biology*, 50(2):158–175, 2010.

[240] A. N. Tikhonov. Systems of differential equations containing small parameters in the derivatives. *Matematicheskii sbornik*, 73(3):575–586, 1952.

[241] M. Tikhonov and R. Monasson. Collective phase in resource competition in a highly diverse ecosystem. *Physical review letters*, 118(4):048103, 2017.

[242] M. Tikhonov and R. Monasson. Innovation rather than improvement: A solvable high-dimensional model highlights the limitations of scalar fitness. *Journal of Statistical Physics*, 172(1):74–104, 2018.

[243] D. Tilman. Resources: a graphical-mechanistic approach to competition and predation. *The American Naturalist*, 116(3):362–393, 1980.

[244] D. Tilman. *Resource Competition and Community Structure*. Princeton University Press, 1982.

[245] D. Tilman. Competition and biodiversity in spatially structured habitats. *Ecology*, 75(1):2–16, 1994.

[246] D. Tilman, P. B. Reich, J. Knops, D. Wedin, T. Mielke, and C. Lehman. Diversity and productivity in a long-term grassland experiment. *Science*, 294(5543):843–845, 2001.

[247] J. Umbanhowar and K. McCann. Simple rules for the coexistence and competitive dominance of plants mediated by mycorrhizal fungi. *Ecology Letters*, 8(3):247–252, 2005.

[248] F. S. Valdovinos and R. Marsland III. Niche theory for mutualism: A graphical approach to plant-pollinator network dynamics. *The American Naturalist*, 197(4):393–404, 2021.

[249] E. van der Maarel. Vegetation dynamics: patterns in time and space. In *Temporal and Spatial Patterns of Vegetation Dynamics*, pages 7–19. Springer, 1988.

[250] W. H. Van der Putten, R. D. Bardgett, J. D. Bever, T. M. Bezemer, B. B. Casper, T. Fukami, P. Kardol, J. N. Klironomos, A. Kulmatiski, J. A. Schweitzer, et al. Plant–soil feedbacks: the past, the present and future challenges. *Journal of Ecology*, 101(2):265–276, 2013.

[251] W. H. Van der Putten, R. D. Bardgett, P. De Ruiter, W. Hol, K. Meyer, T. Bezemer, M. Bradford, S. Christensen, M. Eppinga, T. Fukami, et al. Empirical and theoretical challenges in aboveground–belowground ecology. *Oecologia*, 161(1):1–14, 2009.

[252] W. H. Van der Putten, C. Van Dijk, and B. Peters. Plant-specific soil-borne diseases contribute to succession in foredune vegetation. *Nature*, 362(6415):53–56, 1993.

[253] O. S. Venturelli, A. V. Carr, G. Fisher, R. H. Hsu, R. Lau, B. P. Bowen, S. Hromada, T. Northen, and A. P. Arkin. Deciphering microbial interactions in synthetic human gut microbiome communities. *Molecular systems biology*, 14(6):e8157, 2018.

[254] V. Volterra. Variazioni e fluttuazioni del numero d'individui in specie animali conviventi. *Memorie della Regia Accademia Nazionale dei Lincei*, 2:31–113, 1926.

[255] C. P. Weiss-Lehman, C. M. Werner, C. H. Bowler, L. M. Hallett, M. M. Mayfield, O. Godoy, L. Aoyama, G. Barabás, C. Chu, E. Ladouceur, et al. Disentangling key species interactions in diverse and heterogeneous communities: A Bayesian sparse modelling approach. *Ecology Letters*, 25(5):1263–1276, 2022.

[256] R. H. Whittaker. Gradient analysis of vegetation. *Biological reviews*, 42(2):207–264, 1967.

[257] P. S. Wikramaratna, A. Kucharski, S. Gupta, V. Andreasen, A. R. McLean, and J. R. Gog. Five challenges in modelling interacting strain dynamics. *Epidemics*, 10:31–34, 2015.

[258] B. E. Wolfe and J. N. Klironomos. Breaking new ground: soil communities and exotic plant invasion. *Bioscience*, 55(6):477–487, 2005.

[259] J. P. Wright, W. S. Gurney, and C. G. Jones. Patch dynamics in a landscape modified by ecosystem engineers. *Oikos*, 105(2):336–348, 2004.

[260] J. P. Wright, C. G. Jones, and A. S. Flecker. An ecosystem engineer, the beaver, increases species richness at the landscape scale. *Oecologia*, 132(1):96–101, 2002.

[261] D. W. Yu and H. B. Wilson. The competition-colonization trade-off is dead; long live the competition-colonization trade-off. *The American Naturalist*, 158(1):49–63, 2001.

[262] A. Zelezniak, S. Andrejev, O. Ponomarova, D. R. Mende, P. Bork, and K. R. Patil. Metabolic dependencies drive species co-occurrence in diverse microbial communities. *Proceedings of the National Academy of Sciences*, 112(20):6449–6454, 2015.